CARNEGIE INSTITUTE OF TECHNOLOGY
Department of Electrical Engineering
Pittsburgh 13, Pennsylvania

SILICON CONTROLLED RECTIFIERS: LATERAL TURN-ON VELOCITY, LATERAL FIELD DISTRIBUTION, AND LATERAL SKIP PHENOMENON

by

William H. Dodson

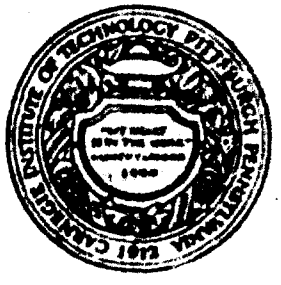

June, 1965

This work has been supported in part by an Office of Naval Research Contract Nonr 760 (00) NR 375-272/11-12-64

(R. L. Longini, Advisor)

(6) SILICON CONTROLLED RECTIFIERS:
LATERAL TURN-ON VELOCITY, LATERAL FIELD
DISTRIBUTION, AND LATERAL SKIP PHENOMENON,

(9) Final technical rept. 1 Sep 64 - 30 Jun 65,

(10) by

William H. Dodson,

(15) [redacted] Contract Nonr 760(09),

(16) Proj. NR 375-272 [redacted]

(5) Carnegie Inst[redacted] of Tech[redacted]
Pittsburgh, [redacted] P[redacted]a.

(11) Jun[redacted]65,

(12) IV.

Professor R. L. Longini, Advisor

TABLE OF CONTENTS

PAGE

LIST OF FIGURES

LIST OF FIGURES

ACKNOWLEDGEMENTS

The guidance and many suggestions of Professor R. L. Longini are gratefully acknowledged. The suggestions and encouragement of other faculty members were greatly appreciated.

Thanks are extended to fellow graduate students, especially Joseph M. Brown and Jerrold L. Wagener, whose assistance and suggestions helped solve many of the device fabrication problems.

Thanks also to Westinghouse Semiconductor Division who generously supplied the silicon from which most of the devices were made.

ABSTRACT

The silicon controlled rectifier (SCR) is essentially an "area" device whereas the transistor is a "periphery" device. In the application of SCRs some trouble arises in making use of this large area because of the slow spreading of turn-on from the gate region. SCRs were specially constructed to permit the direct observation of the lateral spread of turn-on within the device. The effects on the spread of turn-on of load current, base widths, temperature, anode-cathode voltage, the gate signal, and a large inhomogeneity were observed.

The spreading velocity of the on-state and the load current are related approximately by the expression $V^n \propto I$ at high load currents. The spreading velocity is higher in devices with narrower base widths and increases with temperature. Neither the anode-cathode voltage before turn-on nor the gate control pulse affect the spreading velocity of the on-state. Measurements on end gate devices and center gate linear devices show that triggering at the center enables an equivalent area of the SCR to turn on in less time than occurs when triggering at the end. A large gap in the emitter layer will delay the spread of the on-state but will not necessarily stop the spreading.

An analysis of a linear and of a cylindrical transistor with lateral currents in both the emitter and the base layers is included. The results are written in a general form and can be applied to many specific cases including those that have a lateral current only in the

base layer or only in the emitter layer. They may also be useful in the analysis of other multijunction devices in addition to transistors.

A lateral current in an emitter layer of an SCR is shown to vary the lateral field in the base layers and also to change the distribution of the current density injected from the emitter to the base. A method of using lateral emitter layer currents in an SCR to increase the spreading velocity of the on-region and, at higher currents, to turn on quickly areas of the SCR remote from the gate contact is demonstrated experimentally.

Details of device fabrication and the measuring circuitry are included in appendices.

INTRODUCTION

The silicon controlled rectifier (SCR) is potentially capable of handling much greater power than the transistor. This power handling ability arises from the nearly uniform conduction over an extended area present in the SCR in the steady state. Thus the power dissipation is nearly uniform over the entire area. In the high power transistor, on the other hand, conduction is restricted to the emitter periphery so the power dissipation is concentrated at the periphery. As a result of this, and also because the voltage withstanding ability of the SCR is much larger, the power handling ability of the SCR is many times as great as that of the transistor.

The advantages of the SCR over the transistor are a result of the inherent principles of operation. A base current must be supplied to the transistor to maintain it in the on-state. This base current, which flows laterally in the transistor, causes the injected emitter current to be crowded towards the base connection. As a result, conduction in the transistor is limited mainly to the periphery of the emitter. The SCR, however, does not require any external base current to maintain it in the on-state. In steady state no large lateral base currents are present to produce crowding and therefore the SCR conducts nearly uniformly over its entire area. To increase the current handling capability, only the emitter area of the SCR need be enlarged whereas the emitter periphery of the transistor must be increased, involving more elaborate techniques.

In the period following the gated turn-on the current in the SCR, which is initially crowded toward the gate electrode, spreads across the entire area and becomes uniformly distributed. Thus the conduction is nonuniform for a period of each cycle. In the off-state the gate current flows laterally in a base of the SCR and causes emitter crowding analogous to that in the transistor. The injected emitter current is greatest near the gate connection so the alphas, which are current dependent, are highest near the gate connection. As a result the turn-on criterion for the SCR, $\alpha_1 + \alpha_2 = 1$, will first occur near the gate. When the region next to the gate begins conducting, the entire load current is initially limited to this small area of the SCR. The initial current must be limited by external means to a fraction of the maximum current the SCR is capable of handling since the effective area of the SCR is only a fraction of the total area during the turn-on period.

After the initial region of the SCR is conducting, this conducting region spreads laterally throughout the SCR until the entire area is conducting. The application of large area SCRs is severely limited by this spreading phenomenon since the spread of turn-on within the SCR is a relatively slow process requiring tens or hundreds of microseconds.

The earliest theories of operation of the SCR were one-dimensional and did not consider the lateral phenomenon present after gate triggering. Although these analyses satisfactorily explain the operation of small area SCRs, their application to large area SCRs is limited to the initial turn-on of the small region next to the gate.

After the initial region is conducting the usual one-dimensional analyses offer little insight to understanding the lateral spread of the on-region within the SCR.

A more recent analysis by Longini and Melngailis[1] considers the lateral spread of turn-on within the SCR. Although this paper offers considerable insight into the mechanism of spreading and the factors influencing it, a number of assumptions were necessary to make the problem tractable. For example, both bases are assumed equal, the effect of any lateral fields in the bases is neglected, and the change of the diffusion coefficient with carrier concentration is neglected. These and other assumptions limit the direct application of this analysis to actual rectifiers. Experimental measurements are needed to clarify some of the aspects of turn-on.

In spite of the importance of the spread of turn-on in SCRs, experimental measurements of the spreading have been very limited. This may be partly due to the difficulty of direct measurement since the spreading of the on-state is wholly within the device. Mapham[2] has measured the mean spreading velocity in a two-gated SCR. Although the magnitude of the mean spreading velocity is obtained, no measurements were taken to determine the effect of various parameters such as the base widths, lifetime, load current, or temperature. Such measurements are needed to gain greater physical insight into the factors controlling the spread of the on-state.

This thesis reports the results of an investigation of the lateral spread of turn-on within SCRs. Special SCRs were constructed which permitted the direct observation of the spread of turn-on. The thesis consists of three chapters. The first shows experimentally how the spreading is affected by the load current, base widths, temperature, anode-cathode voltage, gate signal and a large inhomogeneity. Comparison of experiment and theory is included. The second is an analysis of a transistor with lateral currents in both the base and emitter layers. The results of this analysis are written in a general form and can be applied to many specific cases including SCRs under special conditions. The third uses the results of chapter two to explain a method of triggering SCRs which can increase the spreading velocity of turn-on and can also initially turn on areas of the SCR remote from the gate connection. Experimental results are included which illustrate this method of triggering.

REFERENCES

1. R. L. Longini and J. Melngailis. "Gated Turn-On of Four Layer Switch." IEEE Trans. on Electron Devices, ED-10, 178-185. (May, 1963).

2. N. Mapham. "Overcoming Turn-On Effects in Silicon Controlled Rectifiers." Electronics, 35, 50-51. (Aug. 17, 1962).

CHAPTER ONE

PROBED DETERMINATION OF TURN-ON SPREAD OF LARGE AREA GATED SILICON CONTROLLED RECTIFIERS

ABSTRACT

Silicon controlled rectifiers (SCRs) were specially constructed to permit the direct observation of the lateral spread of turn-on within the device. The effects on the spread of turn-on of the load current, base widths, temperature, anode-cathode voltage, gate control pulse, and a large inhomogeneity were observed.

The spreading velocity of the on-state and the load current are related approximately by the expression $V^n \simeq I$ at high load currents. The spreading velocity is higher in devices with narrower base widths and increases with temperature. Neither the anode-cathode voltage before turn-on nor the gate control pulse affect the spreading velocity of the on-state. Measurements on end gate devices and center gate linear devices show that triggering at the center enables an equivalent area of the SCR to turn on in less time than occurs when triggering at the end. A large gap in the emitter layer will delay the spread of the on-state but will not necessarily stop the spreading.

1. INTRODUCTION

When a silicon controlled rectifier (SCR) is initially turned on with a gate, only a small area next to the gate contact becomes on. This is followed by a spreading of the on-condition throughout the total area of the SCR. The gate current causes the emitter current to crowd towards the gate connection just as the base current causes emitter crowding in a transistor. Since α increases with increasing emitter current density, the turn-on criterion, $\alpha_1 + \alpha_2 = 1$, occurs first in the region next to the gate contact. As a result the gate current turns on only the area next to the gate contact. After the initial area is conducting, the external gate current loses control. Gate current is supplied to the remaining off-portion of the device by the flow of carriers from the adjacent on-region, permitting the on-region to spread throughout the device.(1)

Although the turn-on of the initial area of the SCR may be quite rapid--in the order of a microsecond or less--the spread of the on-condition over the entire area is relatively slow--in the order of tens or even hundreds of microseconds, depending upon the area and other design features of the SCR. Because of this slow spreading of the on-state the initial current through a large area SCR must be limited. If the load current, being restricted to the on-region, is allowed to rise very rapidly to a high value the resulting concentrated power dissipation may damage the device even though the voltage across the entire device falls to a relatively low value when initially turned on. After the entire area is on, very high currents may be safely carried since

the current would then be distributed nearly uniformly over the device. A knowledge of the factors controlling the spread of the on-region is of major importance, especially in the design of large area SCRs.

Exact studies of the spread of the on-condition are difficult for two reasons. First, theoretical work is complicated because the spread of the on-region is a lateral phenomenon so the usual one-dimensional analyses of PNPN structures are no longer sufficient. Longini and Melngailis (L&M)[1] have made an analytical study of the spreading of the on-region based on first order approximations. Second, experimental work is complicated because the spread of the on-region is wholly within the device and not amenable to direct outside observation. Mapham[2] has measured the time necessary for the total area of a two-gated SCR to turn on by triggering one gate and observing the voltages on both gates. Attempts to obtain information on the lateral spreading by observing the turn-on current transient have been made but without success.

This paper presents the results of experiments made on specially constructed SCRs which permitted the measurement of the spread of turn-on. Observations are made on the effect of load current, base widths, temperature, anode-cathode voltage, the gate signal, and a large inhomogeneity. Comparisons of the experimental results with current theories are included.

2. EXPERIMENTAL PROCEDURE

2.1 Device Fabrication

The rectifiers were made by diffusing boron and then phosphorus into 15 Ω-cm N-type silicon. Gate contacts were made by etching through the N emitter and evaporating and alloying aluminum to the inner P layer. Contacts were made to the N emitter layer by electroless nickel plating followed by annealing and to the P-emitter layer by evaporating and alloying aluminum.

The wafers were cut into long bar-shaped samples approximately 1.5 mm by 15 to 20 mm. Small circular grooves were etched through the N-emitter layer to the inner P layer in order to isolate small islands in the N-emitter layer. The purpose of these islands will be explained subsequently. These circular grooves were made small, approximately 0.125 mm inner diameter and 0.25 mm outer diameter, so that their presence would not greatly disturb the operation of the SCR. Five islands were spaced approximately uniformly down the length of each bar. Fig. 1 shows the final device configuration.

2.2 Measurement Technique

No leads were soldered to the devices. Instead, connections to the anode and cathode were made by placing the anode against a flat aluminum bar and then bringing four phosphor-bronze spring fingers down on the cathode between the islands. Fig. 2 shows the basic arrangement. A eutectic mixture of indium and gallium

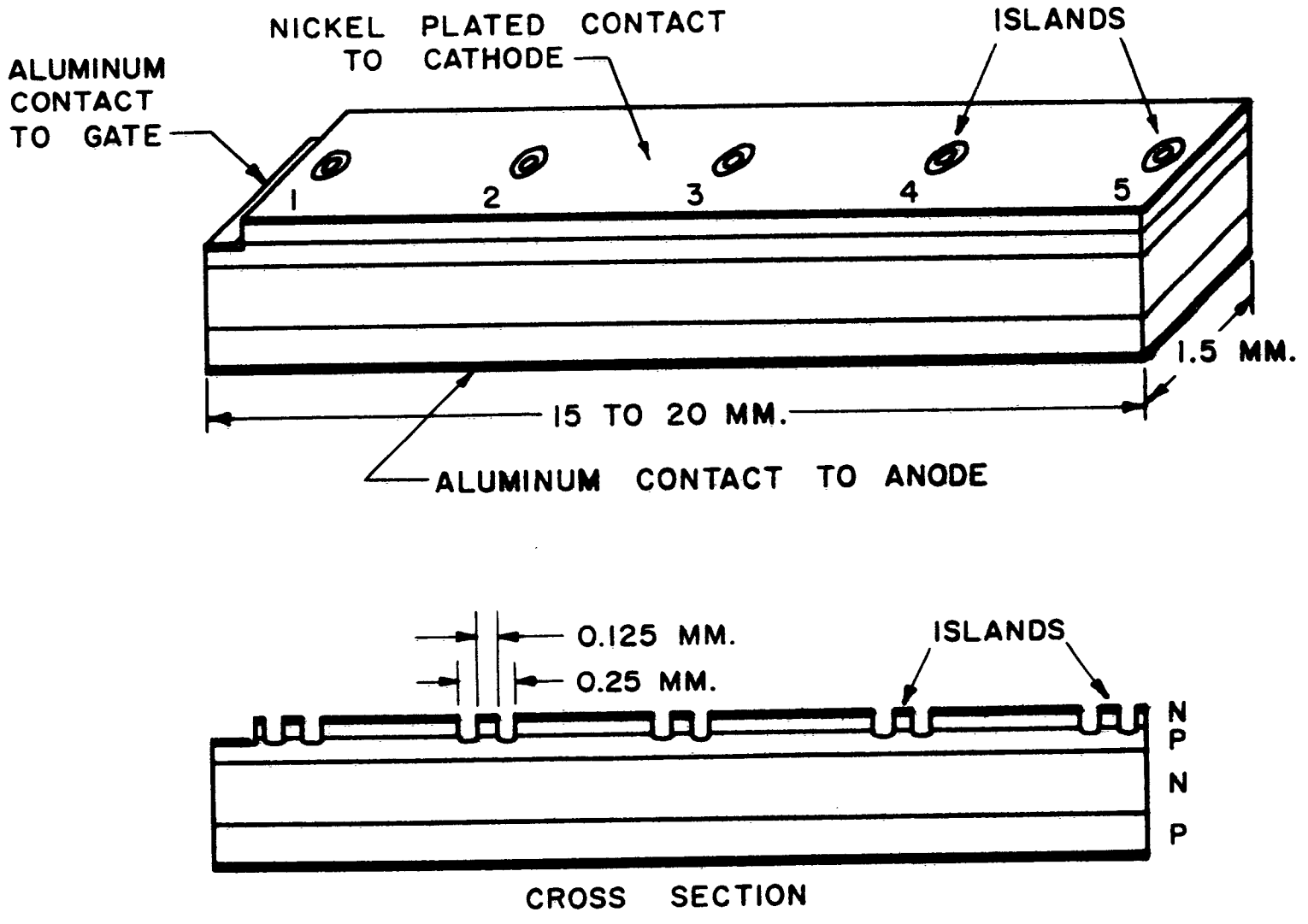

Fig. 1. Device configuration. The islands permitted the observation of the spread of the on-state.

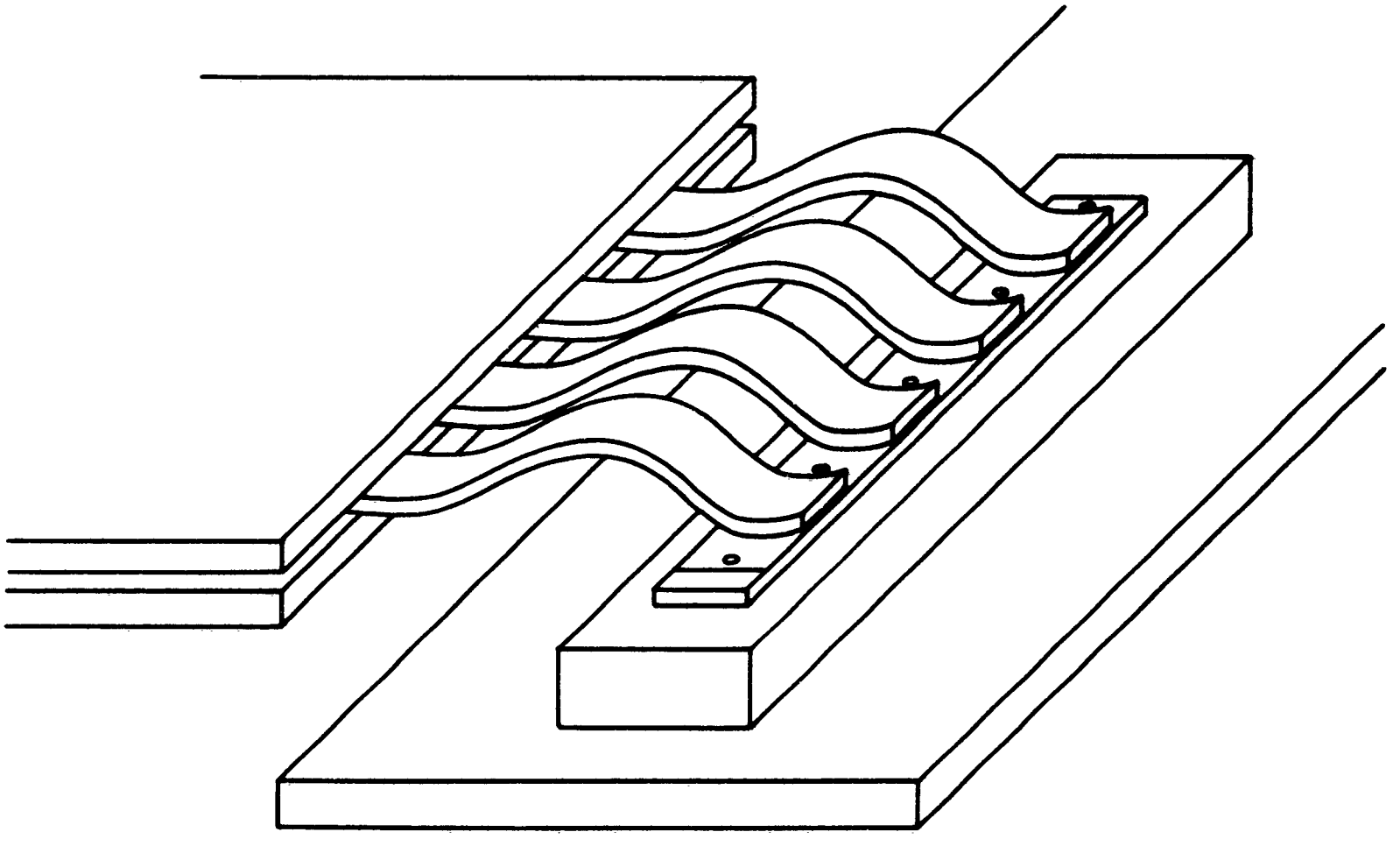

Fig. 2. Method of contacting the anode and cathode layers of the SCR.

was spread over the surface of the nickel plated cathode to insure intimate electrical contact between the spring fingers and the nickel. Connection to the gate contact was made by positioning a tungsten probe against the aluminum contact.

In order to control the temperature of the device, the aluminum bar upon which the device rested was attached to a heavy copper plate the temperature of which was controllable. The entire device was kept under a layer of mineral oil throughout the tests to help keep the temperature of the device uniform and to maintain stable ambient conditions. A thermocouple inserted in the mineral oil served to monitor the temperature of the device.

The islands in the emitter layer of the device permitted the observation of the spread of turn-on within the device. When an SCR is fully turned on, the inner base layers are flooded with injected minority carriers. If only a part of the device is turned on, then only the base layers in the on-region are flooded with minority carriers. The presence of minority carriers within a small region of the device was detected by reverse biasing the island in that region and observing the reverse-bias current. Connection to each island was made by positioning a fine tungsten probe on the island with a micromanipulator. When the region of the device next to an island turns on, the reverse-bias current of the island increases due to the presence of injected minority carriers. Hence, by triggering the SCR with a gate pulse and

observing the reverse-bias current of each individual island, the propagation of the on-state across the device was directly observed.

The basic test circuit consisted of a fixed d-c supply voltage with a resistive load in series with the SCR. The resistive load allowed the load current rise time to be in the order of a very few microseconds in most cases. However, at the highest load current, 70 amperes, the low load resistance in combination with distributed circuit inductance increased the rise time to about 20 microseconds. Still the load current rise time was always only a fraction of the total time required for the on-region to spread across the entire device.

Internal heating of the SCR during the tests was minimized by applying power to it just long enough to permit the total area to become conducting and by triggering at a repetition rate of 2.5 cps.

3. RESULTS AND DISCUSSION

3.1 Determining the Spreading Velocity

The data for this experiment were obtained from oscilloscope traces such as those shown in Fig. 3. The top trace shows the rise of the load current through the device. The second trace shows the trailing end of the fall of the voltage across the device. The voltage across the SCR is originally at a high value out of the range of the figure, falls rapidly to an initial low value when triggered, and then falls more slowly as the on-region spreads throughout the device.

The remaining five traces show the reverse-bias current of each island. When the area next to the individual island turns on, the reverse-bias current of islands 1 through 4 increases, reaches a maximum, and then decreases to a steady state value. The decrease after the increase occurs because the anode-cathode current density within the device decreases as more area turns on and the injected carrier density near the islands decreases. Island 5 does not show this decrease since this island is at the end of the bar farthest from the gate connection and will receive minority carriers only after the on-region has spread practically across the entire device and the anode-cathode current density is at its final minimum value. As is expected, the arrival of minority carriers at island 5 coincide with the time when the voltage across the SCR reaches its final minimum value.

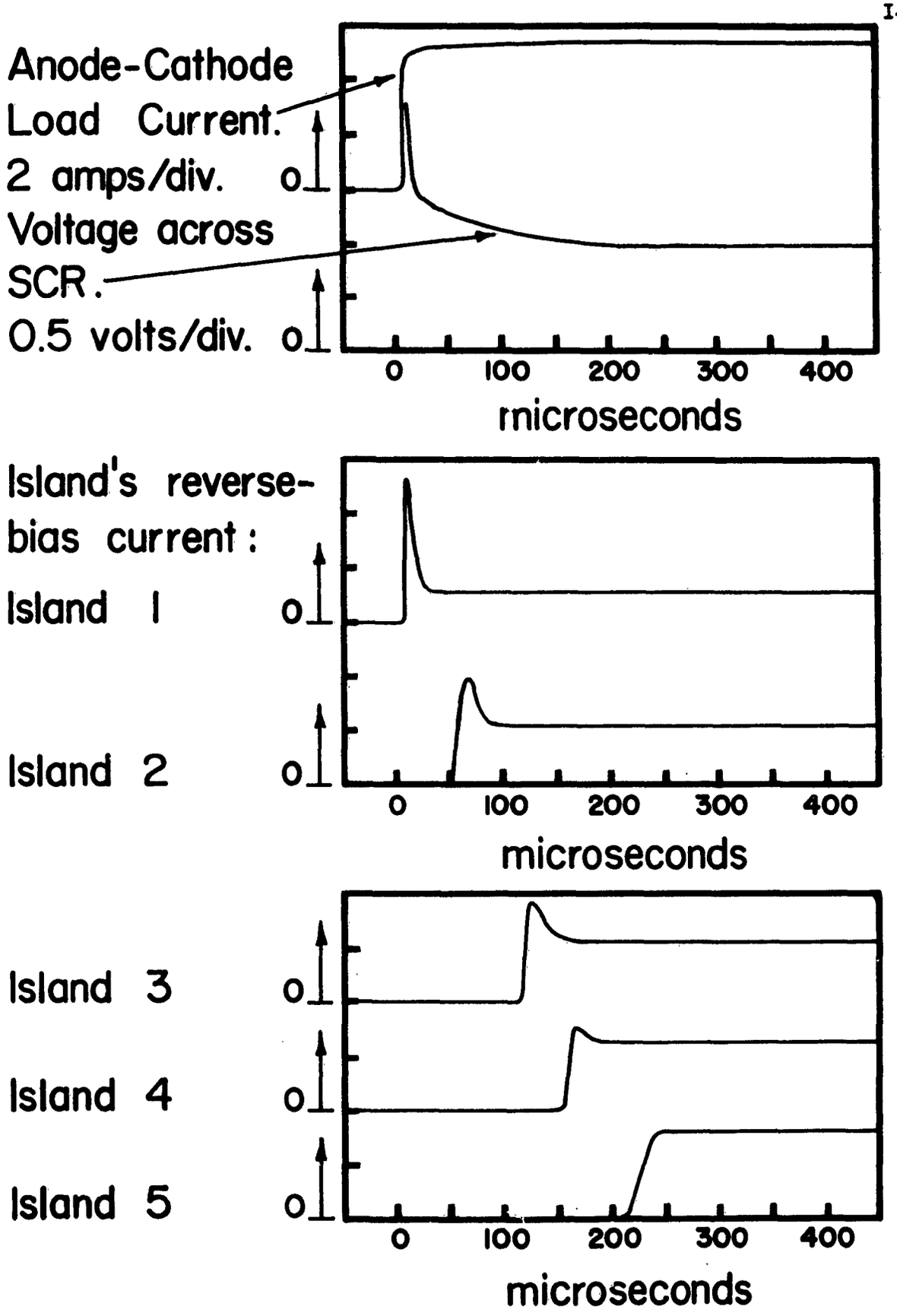

Fig. 3. Typical oscilloscope traces. (Device A5, T = 363°K)

In order to obtain a measure of the spreading velocity it is necessary to select a point on the trace of an island's reverse-bias current which designates the time when the area next to the island changes from off to on. As the traces of Fig. 3 show, the reverse-bias current of an island is not a step function but has a finite rise time. Furthermore, the rise time depends to some extent upon the size of the island and the detection circuitry. Consequently, the time when the reverse-bias current of an island just begins to increase has been selected as the time to denote when a region goes from off to on. This selection is somewhat arbitrary but since these times are subtracted to calculate velocities, the consistency of the method seems more important.

The same time scale for each island has been used in Fig. 3 in order to show better the sequence of arrival of the on-region. The actual data were taken with the time scale of each island's trace expanded the greatest extent possible in order to obtain the most accuracy.

Fig. 4 shows the times when the on-region reaches the individual islands of device A3 as a function of the final load current and is typical of the many plots obtained. Time on this graph is measured from the application of the gate pulse. The spreading of the on-state is a relatively slow process requiring tens or hundreds of microseconds and increases quite rapidly at low load currents. Times as long as a few milliseconds have been

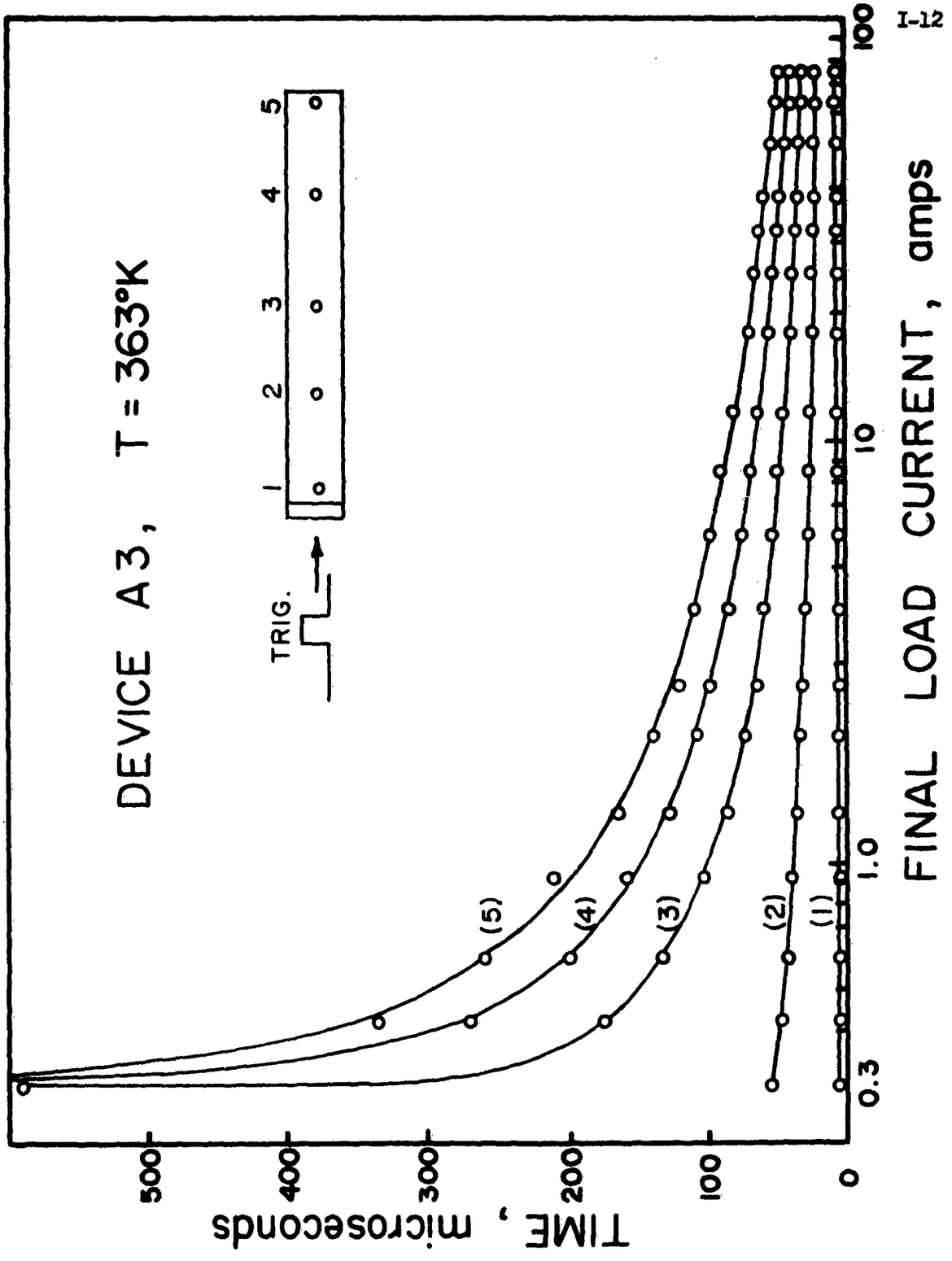

Fig. 4. The arrival time of the on-state at the individual islands vs the final load current.

observed in some devices. At still lower load currents, below about 0.3 amperes in Fig. 4, no increase in the reverse-bias current of the islands away from the gate was observed. This is because, at the lowest currents, the device does not turn on throughout its area. The holding current for device A3, and for most of the other devices used in this experiment, was about 10 to 20 ma at room temperature.

A measure of the velocity of propagation of the on-state can be obtained by dividing the distance between two islands by the time necessary for the on-state to travel from one island to the next. If the velocity is varying with time, which it probably is, the velocities so calculated will be the average velocity over the distance from one island to the next. The velocity of propagation as a function of load current is plotted for device A3 in Figs. 5. The velocity of propagation from island 1 to island 2 is indicated by the notation V_{12}, etc.

3.2 The effect of the Load Current

The propagation of the on-state in an SCR has been analyzed by L & M.[1] In their analysis they have considered the primary mechanism for the spread of the on-state to be the diffusion of excess carriers from the on-region to the off-region in the bases of the SCR. As the off-region adjacent to the on-region receives sufficient carriers and therefore excess charge from the on-region, this off-region will turn on and in turn contribute carriers to

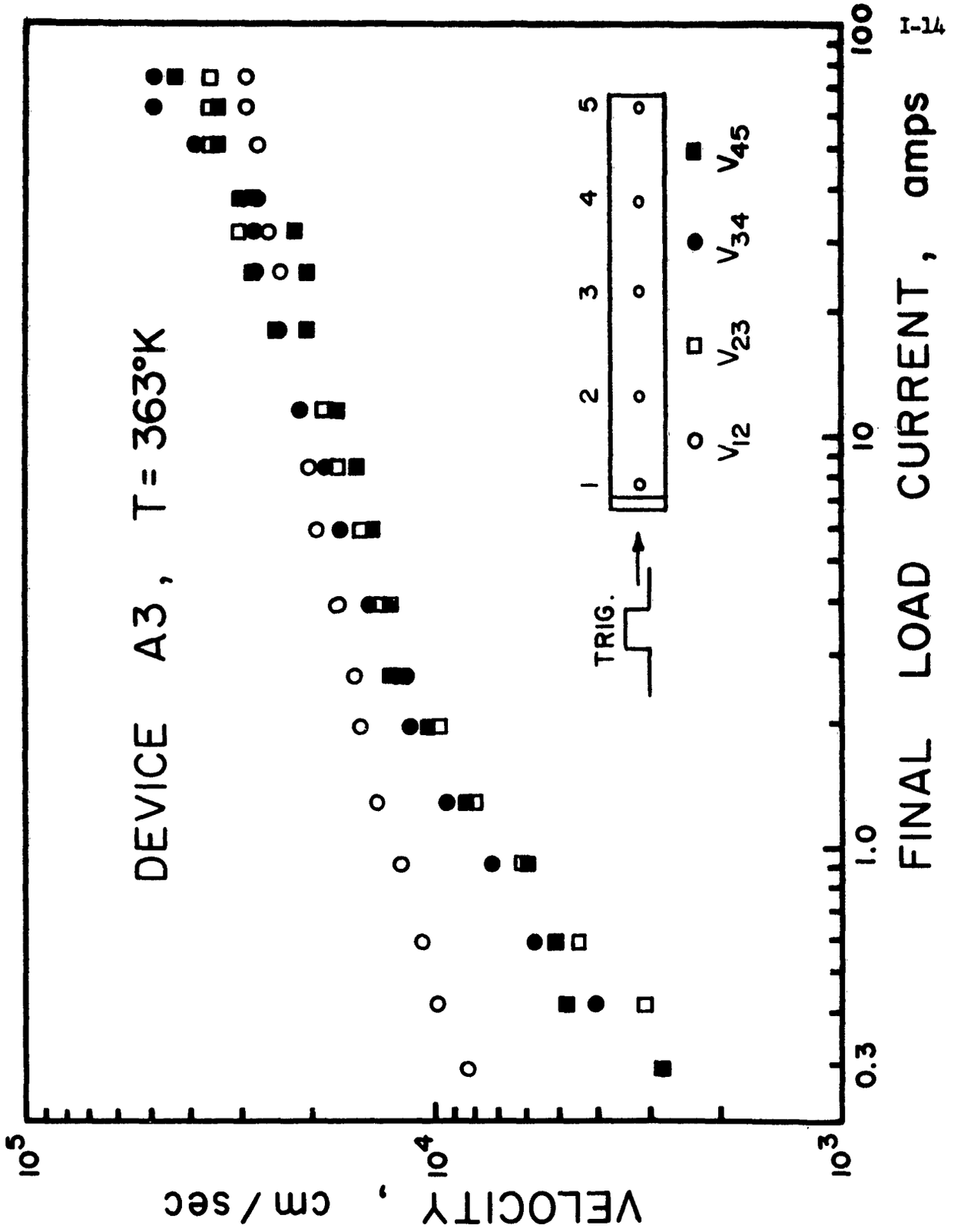

Fig. 5. The velocity of propagation of the on-state vs the final load current.

the next adjacent off-region. As long as the carrier loss from the on-region to the adjacent off-region is sufficiently great, the on-state will continue to propagate throughout the device. The expression derived in reference (1) for the velocity of propagation of the on-state is

$$V = \frac{F}{N_0} - \frac{N_0}{F}\left[\frac{D}{\tau} + \frac{\pi^2 D^2}{a^2}\right] \qquad (1)$$

where $\frac{2F}{\pi}$ = flux of carriers to the off-region per unit base thickness per unit length of periphery of the on-region,

N_0 = maximum carrier density at the periphery of the on region,

D = diffusion coefficient,

τ = the base lifetime,

and a = the base thickness (both bases assumed equal).

In a given device D, τ, and a may be assumed to be constant. The density N_0 may also be considered constant since N_0 essentially defines the boundary between the on- and off-regions. The velocity will now depend only on the lateral flux of carriers, $2F/\pi$. The lateral flux of carriers was related to the device parameters by the expression,

$$\frac{4}{\pi} Fsa = (\alpha_1 + \alpha_2 - 1)\frac{I}{q} \qquad (2)$$

where S is the peripheral length of the on-region, I is the load current and α_1 and α_2 are the alphas in the on-region of each base. This expression was derived from a conservation of charge argument.

Expression (2) says that F is approximately proportional to (I/S) in a given device. The alphas are also functions of the load current but since the alphas in expression (2) are the alphas in the on-region, their change with load current is small compared to the load current change itself. Therefore, the velocity of propagation will be given by

$$V = C_1(I/s) - C_2(s/I) \qquad (3)$$

where C_1 and C_2 are independent of current but C_2 is temperature dependent as will be discussed. The peripheral length S increases as the on-region spreads throughout the device but this change can be kept small by observing the velocity while the on-region spreads but a short distance. At higher load currents the first term of eq. (3) dominates and the velocity should be proportional to the load current.

Examination of Fig. 5 reveals that the measured velocity increases with load current but the relation is not a direct proportionality except perhaps for a small range at low currents.

At higher currents the velocity approximately follows the relation

$$V^n \propto I \qquad (4)$$

where n is a number greater than one. This relation has been observed to be generally true for all the devices tested. The exponent n varies from device to device but is usually between 2 and 6. Although the observed relation between load current and spreading velocity does not correspond closely with the theory of L & M, close correspondence should not be expected because of the approximations used in the derivation.

A more unexpected observation, however, is that the relation $V_{12} > V_{23} > V_{34} > V_{45}$ did not always occur. Since the current density within the device decreases as more area turns on, it is expected from eq. (3) that $V_{12} > V_{23}$ etc. Fig. 5 shows that V_{12} is greater than the other velocities at lower load currents. At higher load currents V_{12} becomes less than the other velocities but this is expected since the load current has a greater rise time at high currents and will not attain its maximum until the on-region has essentially spread from island 1 to island 2. In some devices V_{12} was not always greater than all the other velocities at low load currents but the tapering off of V_{12} at high currents occurred in nearly every case.

Some of the discrepancy in the order of V_{23}, V_{34} and V_{45} may be due to experimental error. Since the velocities were calculated by subtracting two time measurements, the relative error

may be as large as $\pm$ 30 per cent at very high velocities. Usually, however, the error was much less than this. Often the discrepancy in the order of the velocities was too large and consistent to be due solely to experimental error.

One of the SCRs was constructed with a gate connection on each end of the bar in order to observe any difference as the on-state spread from left to right or from right to left along the bar. The velocity of spreading versus the load current is shown in Fig. 6 when only the first gate was triggered and in Fig. 7 when only the second gate was triggered. Examination of these figures shows that the average velocity was greater when the second gate was triggered than when the first was triggered. Furthermore, the expected order of the velocities when the second gate is triggered is $V_{54} > V_{43} > V_{32} > V_{21}$ since the current density is higher during the 5 to 4 transition, etc., but just the opposite order was observed.

Evidently the device was not perfectly symmetrical. One reason for this may be that the N-type base was not of uniform thickness across the bar. The effect of the base widths on the spreading velocity will now be considered.

3.3 The effect of the Base Widths

The base width, a, influences the velocity of spreading primarily through its effect upon the lateral flux of carriers from the on-region to the off-region. In expression (2) the

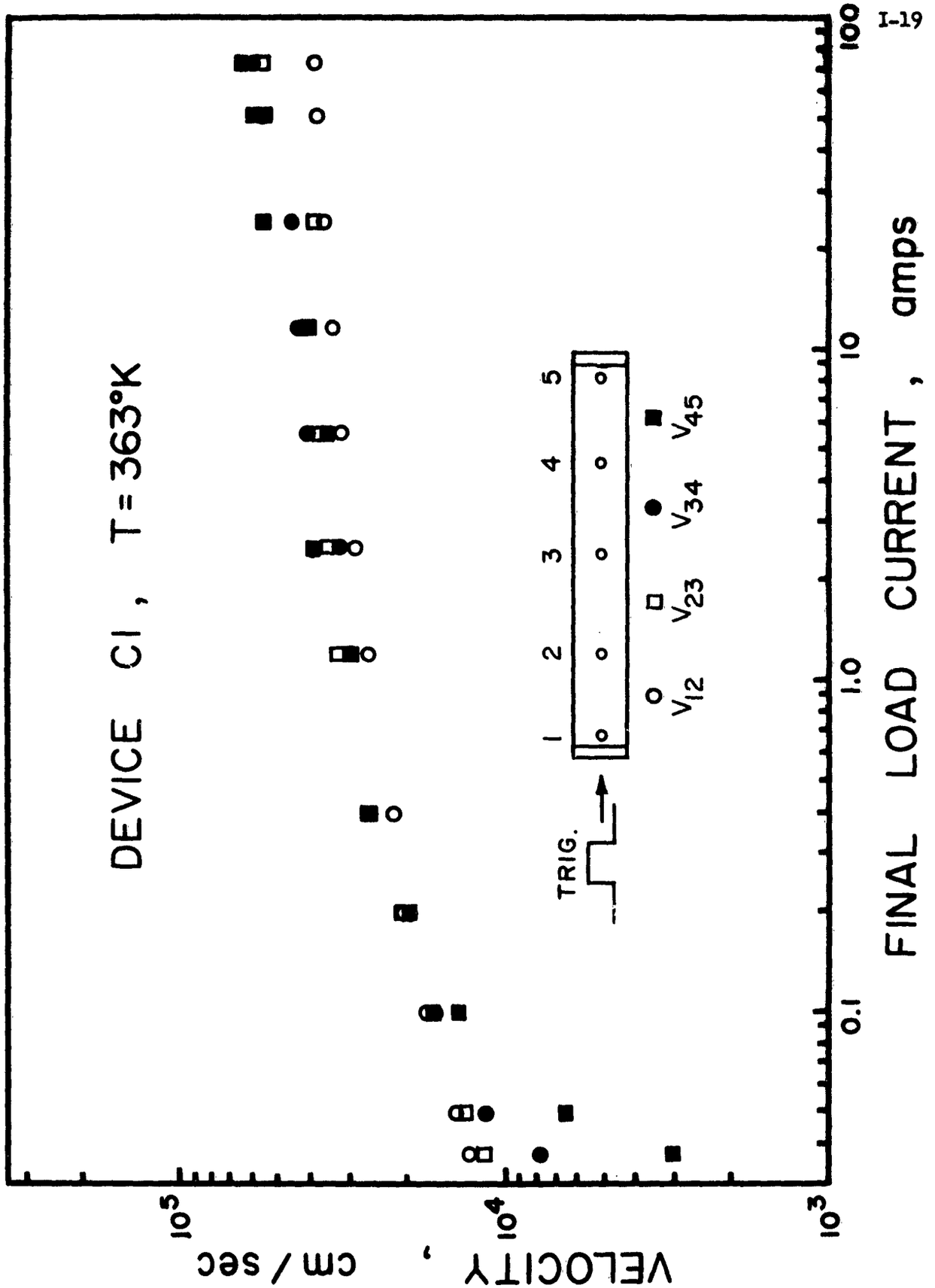

Fig. 6. The velocity of propagation of the on-state in device C1 vs the final load current when only the first gate was triggered.

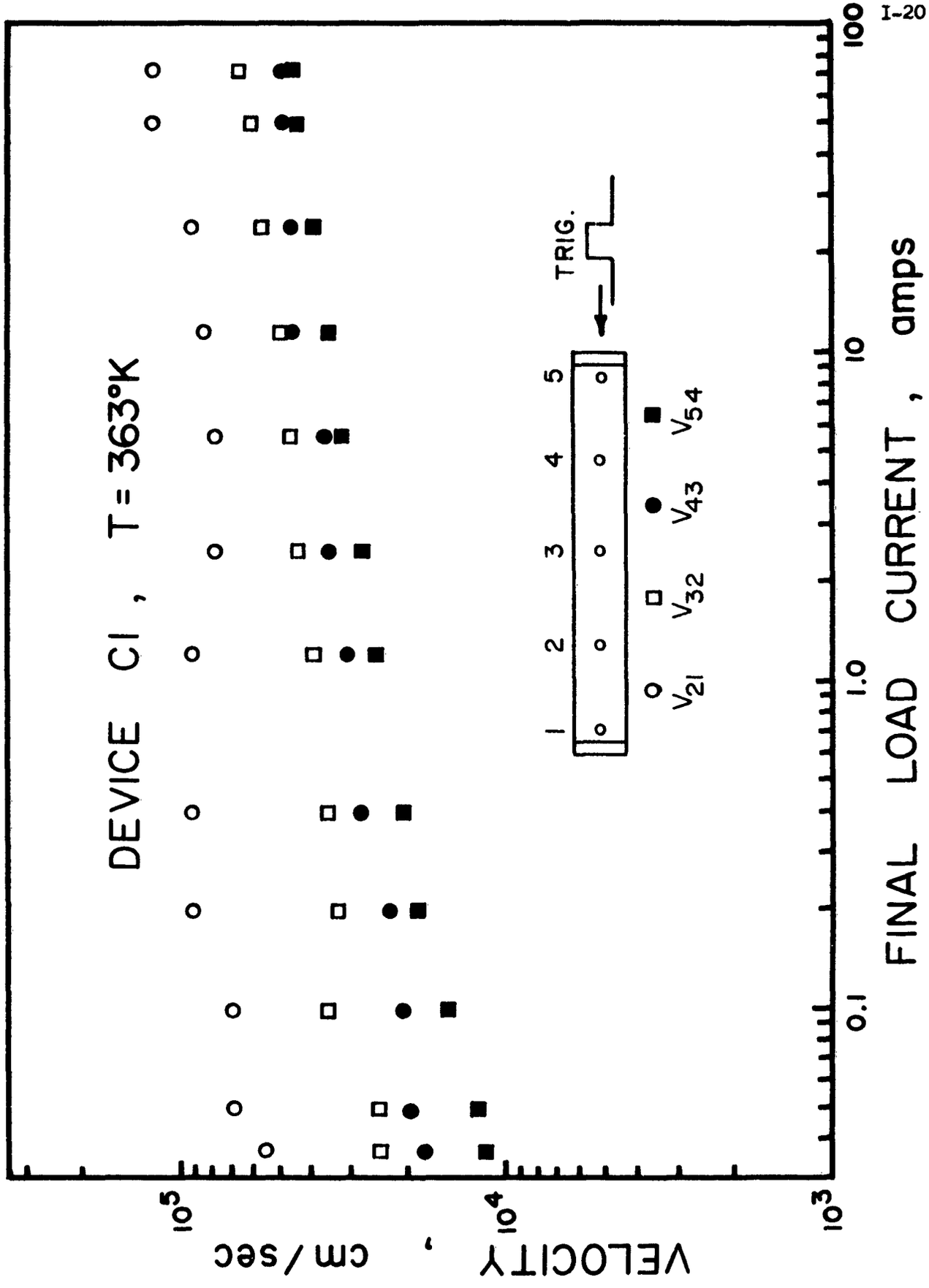

Fig. 7. The velocity of propagation of the on-state in device C1 vs the final load current when only the second gate was triggered.

flux $2F/\pi$ is inversely proportional to the sum of the base widths 2a. Since the velocity is proportional to the lateral flux at high load currents, the velocity will also be inversely proportional to the total base width. Although the base width also occurs in the denominator of the second term of expression (1), this term is negligible at high load currents. (*see footnote p. I-42)

The sum of the base widths in device A3 was about 150 microns and in device C1 about 105 microns. The velocity of spreading in C1 would be expected to be about 3/2 times the velocity in A3 and comparison of Figs. 5 and 6 shows this to be approximately true at high currents. At lower currents the velocity in C1 differs from that in A3 by a factor greater than 3/2 since the points seem to fall on a different slope, i.e., the exponent n in expression (4) is higher. Close correlation with theory is not expected, however, because of experimental and theoretical approximations.

The reason a higher average velocity was observed in device C1 when the trigger was applied to the second gate instead of the first gate may be partly due to the nonuniformity of the width of the N-type base in C1. Measurement of the base widths in C1 indicated that the wide N base narrowed from about 90 microns to about 80 microns from one end of the bar to the other. Since the narrow end of the bar was at the end with the first gate, some tendency for the velocity to increase would be expected as the on-region spread from the second gate towards the first gate. In

Fig. 7 an increase in the velocity was observed as the on-region spread from the second gate towards the first, but the observed increase is much greater than would be expected from a 10 per cent change in the base width.

3.4 The Effect of Temperature

It was noted in section 3.1 that the time for the on-region to reach the islands increased quite rapidly at low load currents. This is illustrated in Fig. 4 by the sharp upsweep which occurs at about 0.3 amperes in device A3 at 363°K. This sharp upsweep was temperature dependent. In device A3 the upsweep occurred at about 1.0 ampere at 297°K and at about 1.7 amperes at 274°K. Below these values of current the total area of the device did not stay on. At higher temperatures the total area stays on at lower load currents probably because the base α s increase with temperature. This increase in the α s is probably due to the increase of the lifetime with increasing temperature as is further evidenced by the temperature dependence of the velocity of spreading.

In eq. (2) the lateral flux of carriers has little dependence upon temperature. Most of the temperature dependence of the spreading velocity will arise from the second term of eq. (1) (or from C_2 in eq. (3)). As noted before, this term will have little influence upon the spreading velocity at high load currents and therefore we should expect temperature to have little influence at high load currents.

The temperature dependent terms of eq. (1) are $D\tau^{-1}$ and D^2. The first of these arises from the loss of carriers which recombine in the off-region. The second arises from the loss of carriers in the off-region which diffuse to the adjacent N regions in the case of the P-type base and to the adjacent P regions in the case of the N-type base. Although the diffusion coefficient, D, changes by less than a factor of two over the temperature range of this experiment, the lifetime, τ , can vary exponentially with temperature and may change by an order of magnitude over the same temperature range.[3] In any case, both $D\tau^{-1}$ and D^2 decrease as temperature increases so the second term of eq. (1) will decrease permitting the velocity of spreading to increase with temperature.

Fig. 8 is a plot of the spreading velocity versus the reciprocal temperature for device A3 and is typical of most of the devices measured. The points on this graph have been interpolated from Fig. 4 and two other sets of data. Because of the wide spread of the points in Fig. 8, a close fit with theory cannot be expected but the trend is in the proper direction. At low load currents the velocity definitely increases with temperature and at high load currents the velocity is nearly independent of temperature. This is as expected because the second term of eqs. (1) or (3), which is the temperature dependent one, is very small at high load currents.

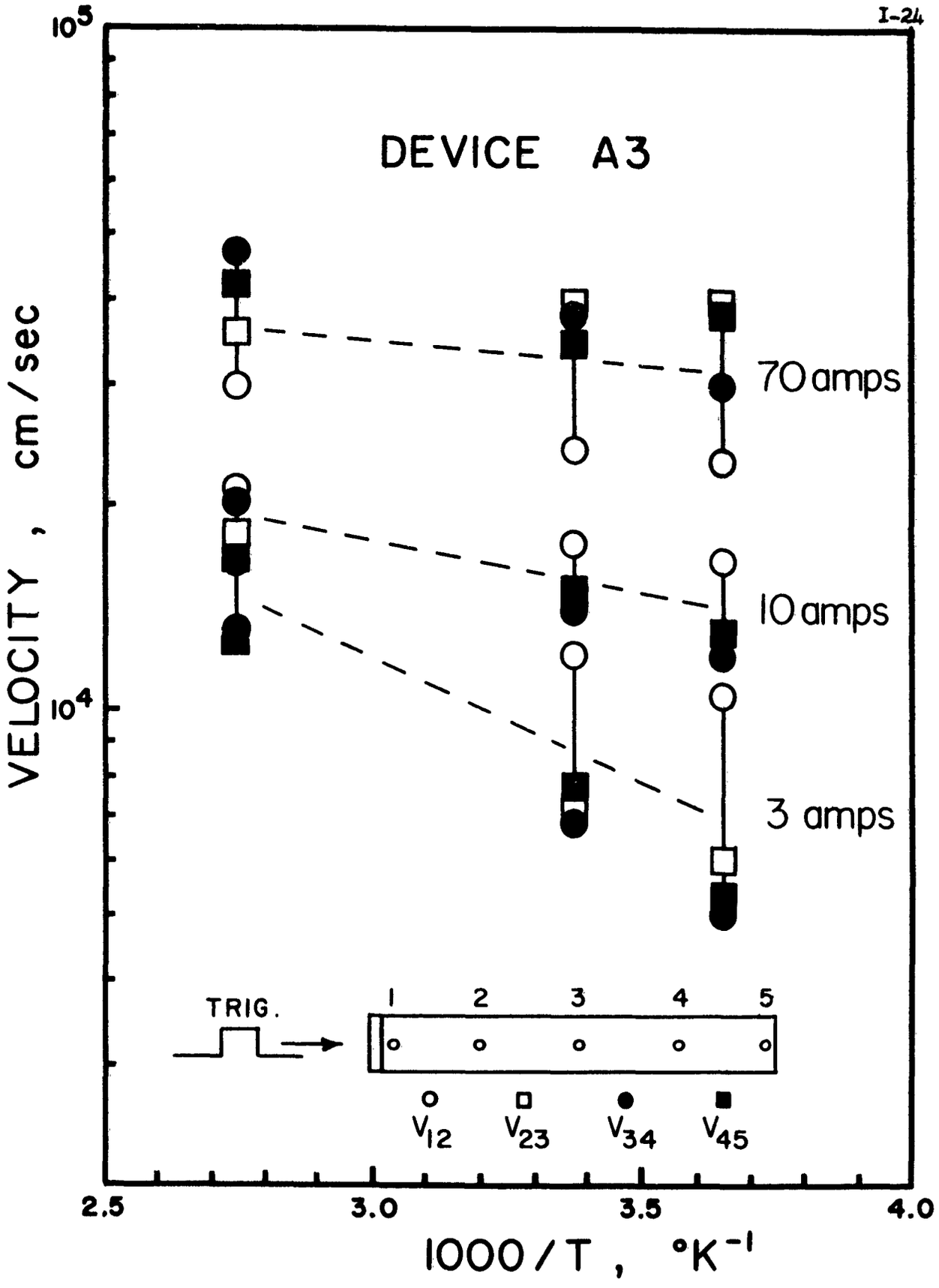

Fig. 8. The velocity of propagation of the on-state vs the reciprocal temperature for device A3.

Device C1 (Figs. 6 and 7) differed from most of the other devices in that the spreading velocity was nearly independent of temperature over the range considered. At load currents of less than 0.5 ampere the velocity showed some temperature variation. At higher load currents, however, the velocity plots for 296°K and 363°K were nearly identical when only the first gate was triggered or when only the second gate was triggered. As was noted, device C1 had a narrower N base layer than the other devices and consequently the spreading velocity in this device was determined primarily by the first term of eq. (1). Since this term is nearly temperature independent, the velocity of spreading should be temperature independent also.

If the above interpretation of the temperature dependence of the spreading velocity is correct, these temperature studies imply that the spreading velocity is higher in devices with higher base lifetime, at least at low load currents. A higher base lifetime means that a smaller fraction of the total carriers which have diffused to the off-region from the on-region will be lost by recombination in the base. More carriers will then be available to diffuse to the bordering junctions and will enable the off-region adjacent to the on-region to turn on faster. At higher load currents the lifetime in the off-region of the base has less influence upon the spreading velocity since the first term of eq. (1) dominates. The high injection-level lifetime of the on-region will then be most influential since the alphas

in equation (2) depend upon this lifetime.

Previously we showed that the spreading velocity and load current seem to obey the relation $V^n \propto I$ at high load currents. In general, the exponent n increases with temperature. For device A3, n was about 2 at 274°K and about 3 at 363°K. In device C1, which showed little temperature dependence, n was about 5.

3.5 The Effect of Anode-Cathode Voltage

The spreading velocity was observed not to be a function of the pre-triggered voltage across the SCR for constant load current. Some change in the L/R ratio occurred when the anode-cathode voltage was changed. This was due to a) the load circuit which had a constant distributed inductance, and b) the need to change the load resistance in order to maintain a constant load current when the anode-cathode voltage was changed. This affected the rise time of the load current and caused some slight changes in the spreading velocity in certain ranges of load current. It appears, however, that the spread velocity is primarily dependent upon the load current and not the voltage across the SCR prior to triggering.

3.6 The Effect of the Gate Signal

The effect of the gate trigger signal on the turn-on of silicon controlled rectifiers has been studied by Somos[4] and by Misawa[5]. They have observed that the shorter the gate pulse width, the greater must be the gate current amplitude in order to fire the SCR. Furthermore, the lower the gate current amplitude, the longer the

delay time will be. The delay time is defined as the time interval between the application of the input trigger pulse and the time when the resulting load current attains 10 per cent of its maximum amplitude.

The amplitude and pulse length of the gate signal were varied to observe the effect, if any, of the gate signal on the spreading velocity of the on-state within the SCR. Our studies have been made on three types of devices: (1) those with a single end or side gate, (2) those with two end gates and, (3) those with a center gate.

3.6.1 Single end gate structure

Most of the SCRs used throughout this investigation required a gate current of about one milliampere or less to trigger. The gate signal was a rectangular current pulse with a rise time of about one microsecond.

No spreading of the on-state was observed during the delay period. That is, the spread of the on-state appears to start when the load current through the device begins its rapid rise. When the gate current was increased from a former low value, the delay time decreased as was expected. However, the time for the on-state to reach any of the individual islands also decreased by the same amount. Thus, the gate current amplitude appears to have no effect on the velocity of propagation of the on-state. This has been observed with load currents from one-half ampere to 70 amperes and with gate currents from less than

one milliampere to one ampere.

One may have thought that extending the gate pulse length greatly beyond the delay time may enhance the spreading velocity of the on-state, but this is not observed. When the gate pulse length was reduced to much less than the delay time, the SCR was not triggered. If the gate pulse length was about equal to the delay time, the SCR would trigger but sporadically. If the gate pulse length was much greater than the delay time, the SCR would trigger regularly but greatly extending the pulse length did not affect the velocity of propagation of the on-state or change the arrival time at the first island.

3.6.2 Double end gate structure

Device C3, which had a gate on each end of the bar, permitted observing the spread of the on-region when both gates were triggered at the same time. Although no extensive quantitative measurement was made on this phenomenon, some general observations have been made.

When both gates were connected in parallel only one gate would trigger since the input impedance of the two gates was different and most of the gate current would go to one gate. A sufficiently high gate pulse may have triggered both gates simultaneously but this was not verified because of the limitations of the equipment immediately available. When the two gates were triggered separately at the same time, the gate signals could be adjusted

so that both ends of the bar switched on and the on-regions would spread from both ends towards the center. If one of the gate signals were delayed until after the first gate signal had already started the spread of the on-region from one end of the bar, the second gate signal could start a second on-region spreading from the other end of the bar provided the second gate was triggered before the first on-region had spread clear across the device.

3.6.3 Center gate structure

Although increasing the pulse length or the amplitude of the gate signal did not affect the spreading velocity in devices with an end gate, two questions arise: 1) will a long gate pulse or a high gate current help turn on a large initial area in center gate devices, and 2) is it better to initiate turn-on in the center of an SCR or at the edge?

In order to investigate these aspects of turn-on, device A7 was made with a center gate structure by etching away a section of the emitter N layer clear across the width of one of the bars as shown in Fig. 9. Contact to the inner P layer was made with a tungsten probe. Two islands were placed on either side of the center gate in addition to the other islands so that the total number of islands was six.

In general, when device A7 was triggered at the center gate the on-region would spread outward from the center in both directions along the bar. Fig. 10 shows the time of arrival of the

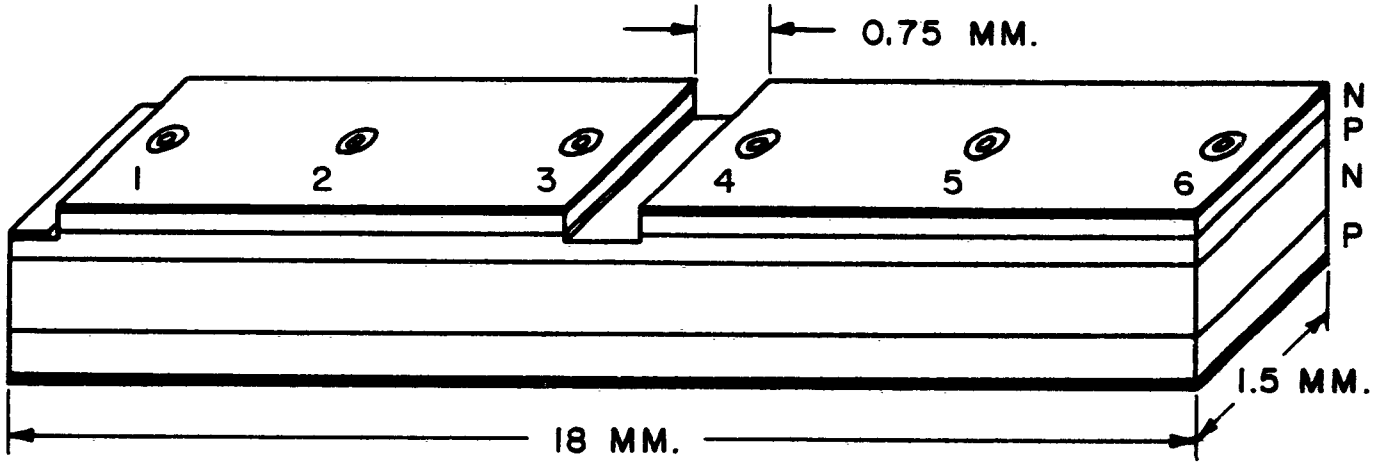

Fig. 9. Center gate device configuration. This device (A7) was used both for center gate studies and for observing the effect of the gap in the emitter layer upon the spreading of the on-state.

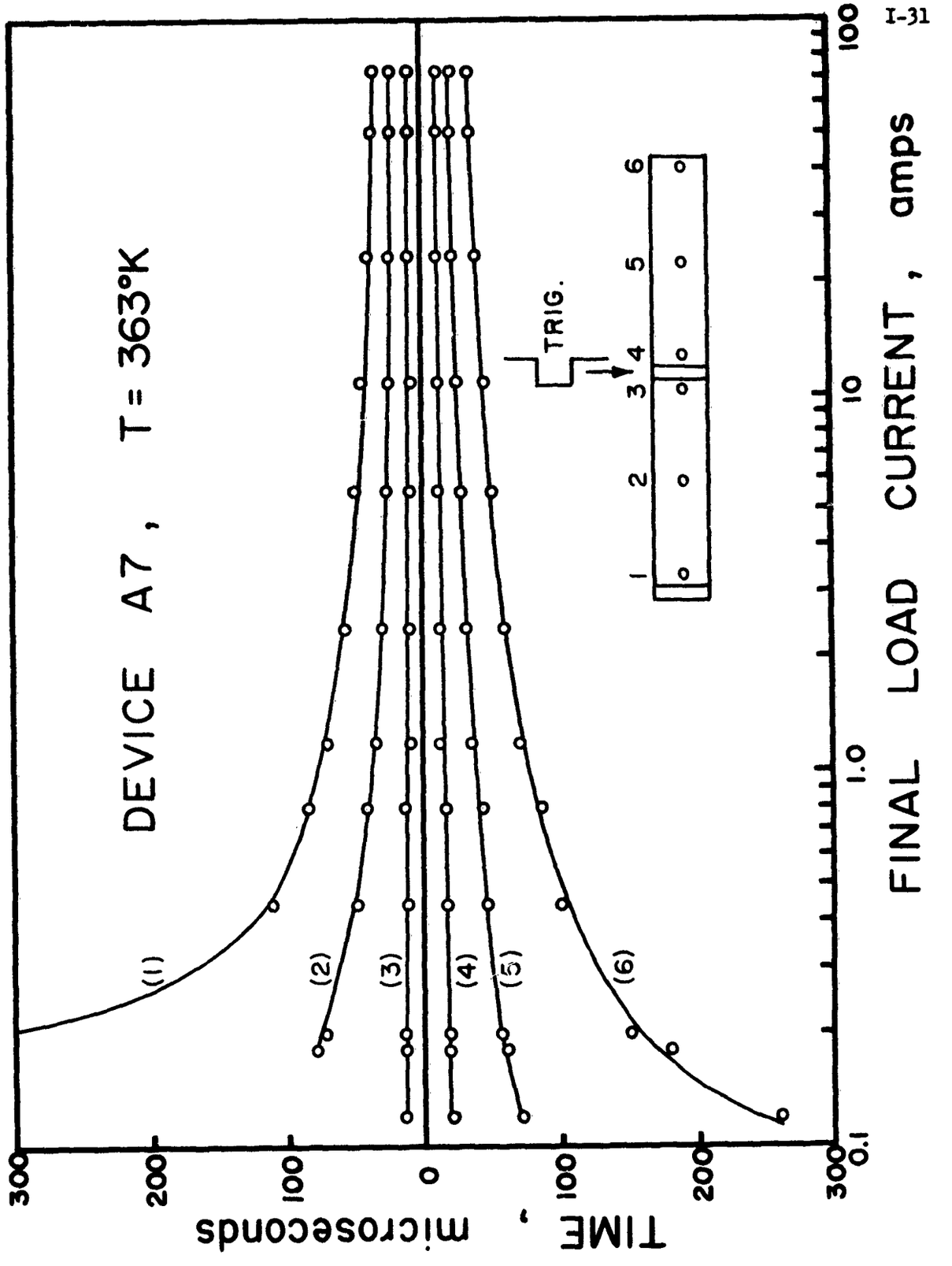

Fig. 10. The arrival time of the on-state at the individual islands of device A7 when triggered at the center gate vs the final load current.

on-region versus the load current. At very low load currents the spreading of the on-region would continue in only one direction along the bar even though both sides were obviously triggered on since minority carriers were detected at both islands next to the center gate. Increasing the gate pulse length or amplitude did not have any effect on this phenomenon. Whether one or both sides of the bar stayed on after triggering depended primarily upon the load current and temperature and the device itself.

The one exception where the gate signal did affect the turn-on region was when the gate contact probe was placed very close to the emitter N layer of one side of the bar instead of in the center of the etched P region. This purposely made the center gate asymmetrical so that more of the gate current passed through the emitter closest to the probe (the side of the bar with islands 4, 5, and 6). Under this condition and at load currents of less than 360 ma ($363^{\circ}K$), if the gate pulse length was too short only one side of the bar was triggered. If the gate pulse length was increased, both sides would be triggered but the condition for both sides staying on was the same as above. The length of the gate pulse necessary to trigger both sides of the device depended upon the gate current and the load current. If the load current was greater than 360 ma, both sides of the device triggered regardless of the gate pulse length or amplitude providing they were sufficient to trigger the device.

If the gate probe was placed near the center of the etched P region so that the center gate contact was reasonably symmetrical, both sides of the bar were always triggered on if the gate signal was sufficient to trigger the device. Furthermore, the velocity of spreading of the on-state was unaffected by the gate signal here just as with a single end gate structure.

Fig. 10 shows that the center gate structure has at least one advantage over a single end gate structure--the time necessary for the same total area to turn on is reduced by about one-half. This is because the on-region spreads in both directions from the center gate and the spreading velocity is just about the same as in the case of an end gate device. The spreading velocity of device A7 is shown in Fig. 11 as a function of the load current. It can be seen that the magnitude of the spreading velocity and its dependence on the load current is very much the same as in a device with a single end gate and similar base widths (device A3).

In summary we may state that the gate signal has little effect upon a large area SCR when the gate is adjacent to an on-region of the SCR. If the gate is adjacent to an off-region of the SCR then a proper gate signal can start an on-region spreading from the gate.

3.7 The Effect of a Large Inhomogeneity

Since device A7 had a gate connection at one end of the bar in addition to the center gate, we could trigger the end gate and

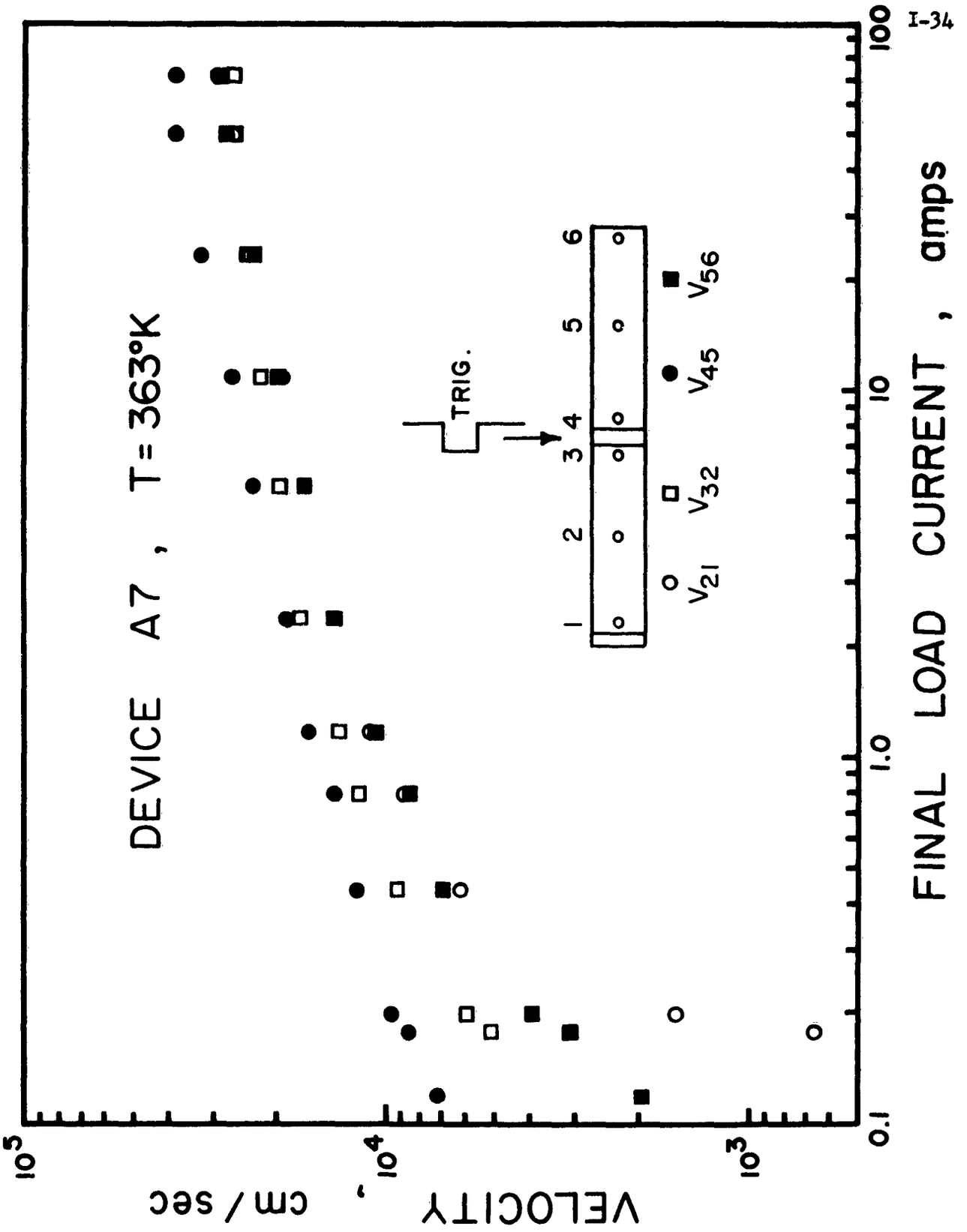

Fig. 11. The velocity of propagation of the on-state when triggered at the center gate vs the final load current.

observe the effect of the gap in the emitter layer upon the spreading of the on-region. The gap in the emitter layer was 0.75 mm wide and extended across the entire width of the device so that the emitter layer was divided into two separate portions. (Fig. 9) Although the two sections of the emitter layer were physically separated, they were connected electrically by the bronze spring fingers which contacted the N emitter layer.

A break in the emitter layer might be expected to stop the spread of the on-region so that only one-half of the device would turn on. This was not always the case, however, as Figs. 12 and 13 aptly show. Above a minimum load current the on-region continued across the gap and along the rest of the bar. The minimum load current can be seen to depend upon the temperature. At 296°K the N-region would not spread beyond the gap when the load current was less than about 17 amperes. At 363°K the on-region would not spread beyond the gap when the load current was less than about 1.1 ampere.

The basis for the on-region spread across the gap in the emitter layer can be understood if one remembers that the potential of the base P layer is a few tenths of a volt more positive in the on-region than in the off-region since the emitter is under heavy forward bias in the on-region. Consequently, when the on-region has spread up to the gap there is a lateral potential in the P layer under the gap. This potential causes the emitter in the off-region to inject carriers adjacent to the gap, thereby turning

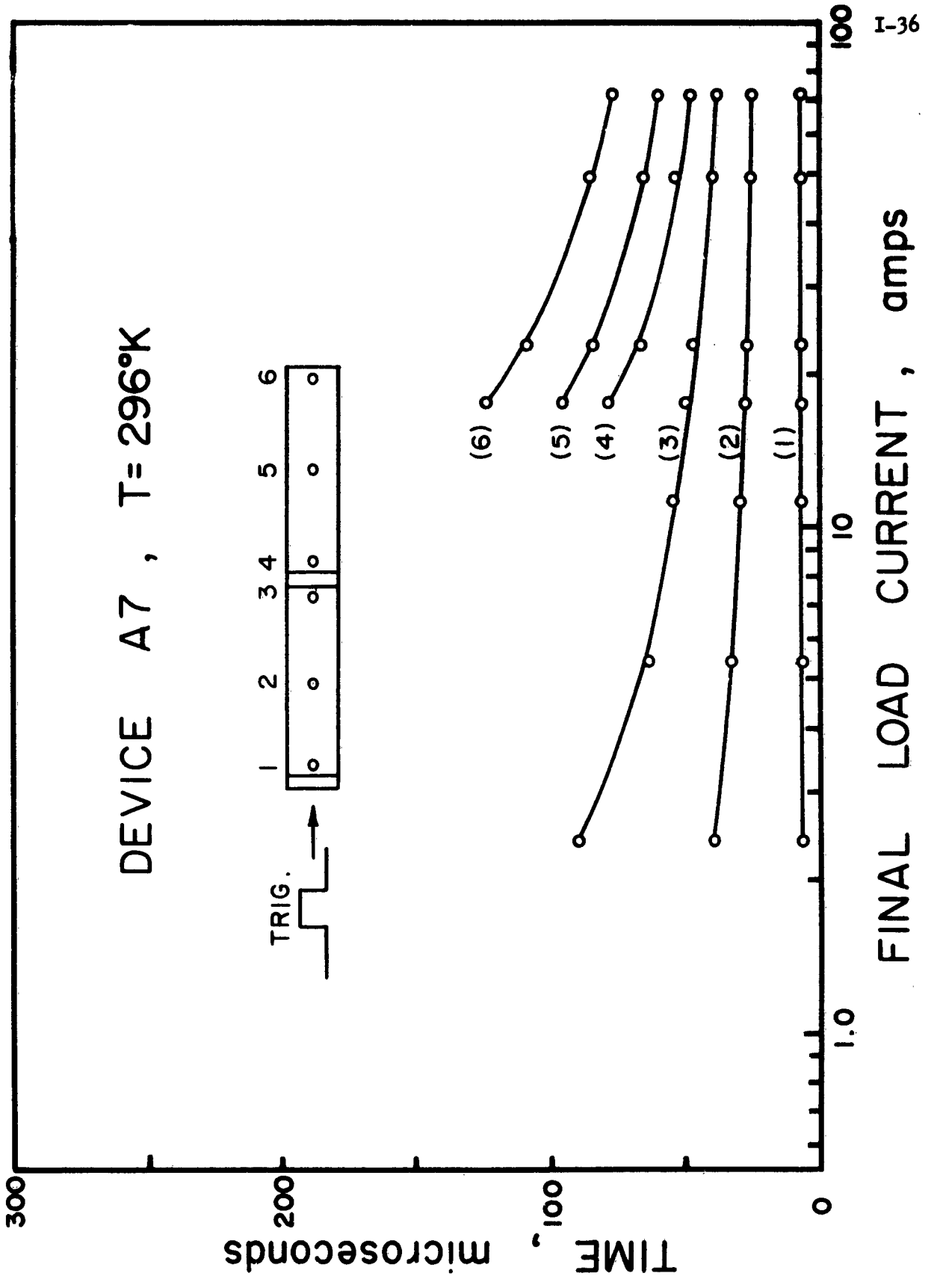

Fig. 12. The arrival time of the on-state at the idividual islands of device A7 when triggered at the end gate vs the final load current at 296°K. The on-state would not spread beyond the center gap at load currents less than about 17 amperes.

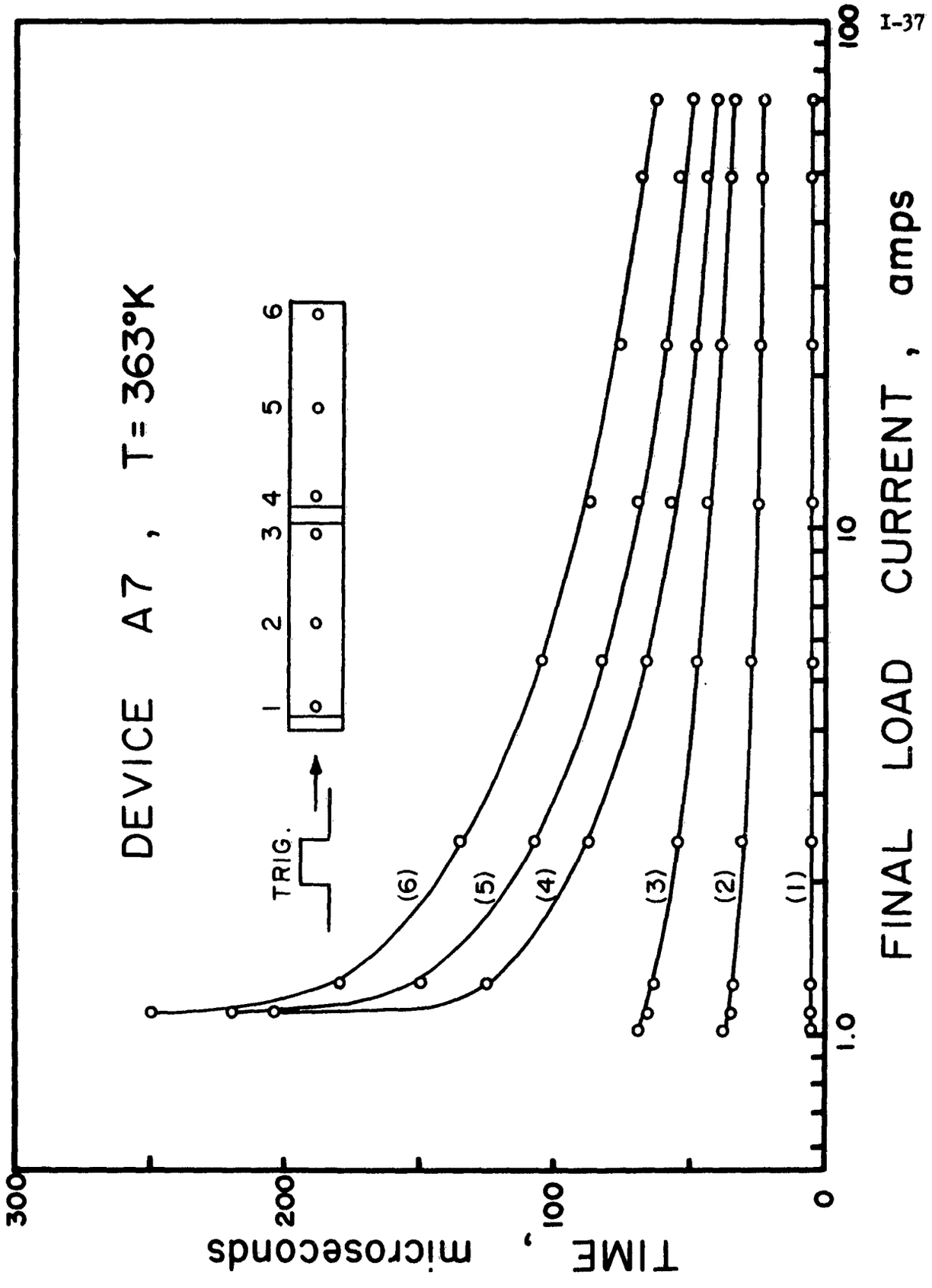

Fig. 13. The arrival time of the on-state at the individual islands of device A7 when triggered at the end gate vs the final load current at 363°K. The on-state would not spread beyond the center gap at load currents less than about 1.1 ampere.

this portion of the device on and enabling the on-region to spread the entire length of the device.

Although the on-region would spread across the gap in the emitter layer, it was delayed somewhat at low load currents. Fig. 14 shows the spreading velocity versus the load current for this situation at 363°K. The points which represent the spreading velocity across the gap show the effect of this delay. At high load currents the spreading of the on-region was delayed very little by the gap. After the on-region reached the other side of the gap it progressed across the remainder of the device at about the same velocity as before the gap regardless of the load current.

Since the on-region will spread across a large gap in the emitter layer, it stands to reason that if the SCR is triggered at the center by applying a probe to the etched P region of the gap, the on-region is certain to spread in both directions from the center regardless of the gate signal. This is in agreement with the findings of the previous section.

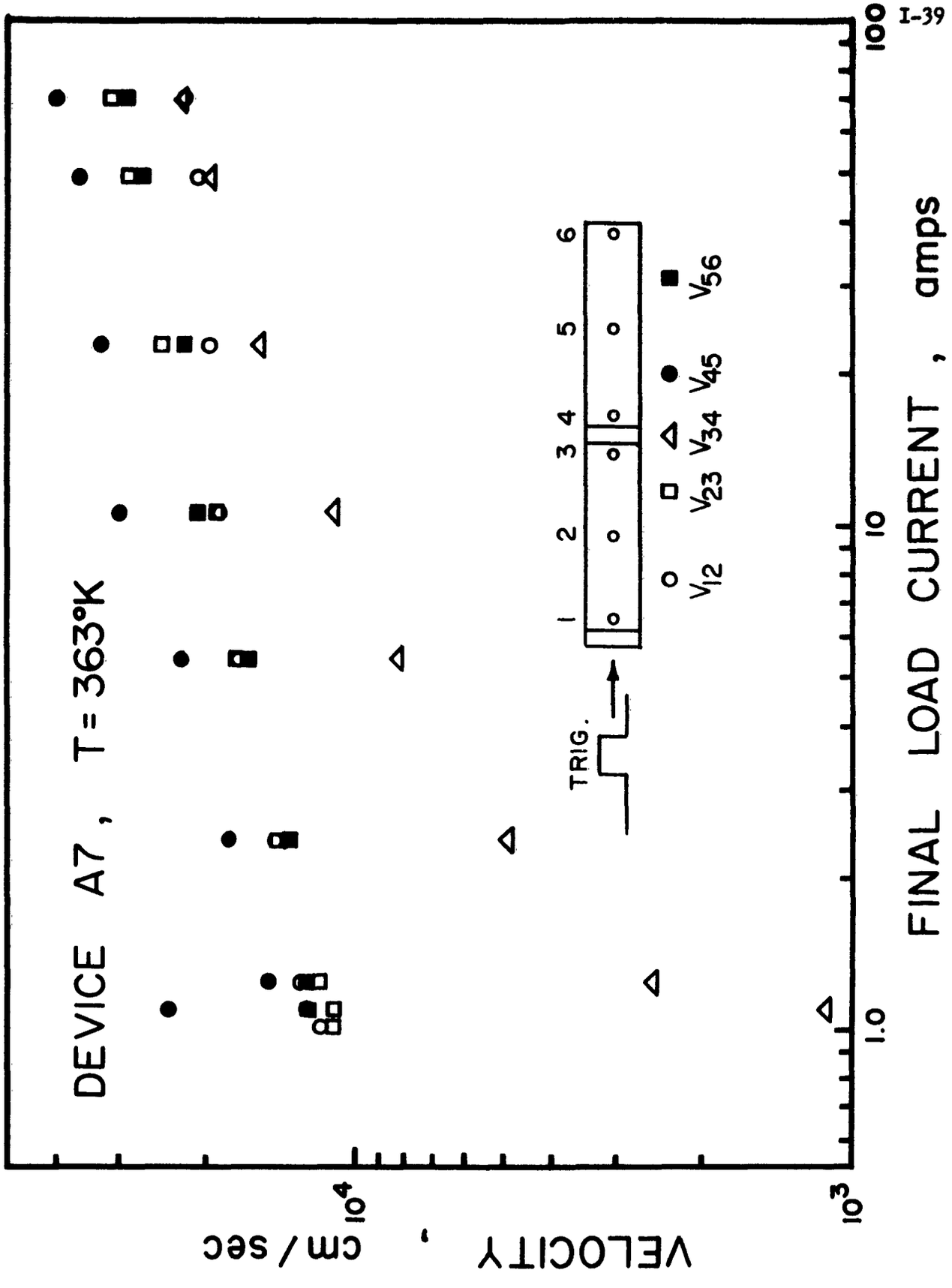

Fig. 14. The velocity of propagation of the on-state of device A7 when triggered at the end gate vs the final load current.

4. CONCLUSIONS

The velocity of propagation of the on-state within an SCR approximately follows the relation $V^n \propto I$ at high load currents. This relation between the spreading velocity and the load current is not predicted in the theory of L & M[1]. The "ideal" model used in the theoretical work did not take into account the change in the diffusion coefficient with carrier concentration in the extrinsic bases or the effect of possible lateral fields in the bases, which were assumed nearly intrinsic, upon the spreading velocity. These and other approximations may explain the differences between theory and experiment.

The observations of the effect of the base widths and temperature upon the velocity of propagation of the on-state can be interpreted in terms of the theory of reference (1). In devices with narrower base widths the spreading velocity is higher and has less temperature dependence. The temperature dependence of the velocity of propagation has been interpreted in terms of the change in lifetime with temperature. If this interpretation is correct, then the velocity of propagation of the on-state will be higher in devices with higher base lifetime, at least at low load currents.

The voltage across an SCR before turn-on is supported mainly by the center junction. The discharge of the capacitance of this junction during turn-on has little effect upon the spread of the on-state since the velocity of propagation is primarily dependent

upon the load current and is not affected by the anode-cathode voltage before turn-on.

Although the gate signal has no effect upon the velocity of propagation, the placement of the gate may be an important design feature since measurements on end gate devices show that triggering at the center enables an equivalent area of the SCR to turn on in less time than occurs when triggering at the end. Since our measurements were made on rectangular SCRs, it is not certain that the same result will occur in experiments with circular SCRs with side gates and center gates.

The experiment with the large gap in the emitter layer of an SCR indicates that inhomogeneities arising from crystal imperfections, contact alloying, or other causes may delay the spread of the on-state but is not likely to stop the spread.

All the experiments in this paper were conducted on rectangular bar-shaped SCRs. More extensive experiments with circular geometries would be needed to obtain a better understanding of the lateral spread of turn-on in "real" silicon controlled rectifiers.

REFERENCES

1. R. L. Longini and J. Melngailis, "Gated Turn-On of Four Layer Switch", IEEE Trans. on Electron Devices, Ed-10, 178-185. (May, 1963).

2. N. Mapham, "Overcoming Turn-on Effects in Silicon Controlled Rectifiers", Electronics, 35, 50-51. (August 17, 1962).

3. E. M. Pell and G. M. Roe, "Reverse Current and Carrier Lifetime as a Function of Temperature in Silicon Junction Diodes", J. of Applied Physics, 27, 768-772. (July, 1956).

4. I. Somos, "Switching Characteristics of Silicon Power-Controlled Rectifiers, I — Turn-On Action", AIEE Trans. Pt. I (Communication and Electronics), 80, 320-326. (July, 1961).

5. T. Misawa, "Turn-On Transient of p-n-p-n Triode", J. of Electronics and Control, 7, 523-533. (December 1959).

(*footnote for page I-21)

The use of the L & M analysis to interpret the velocity dependence on base widths, temperature, etc., may appear somewhat illogical since this analysis does not adequately explain the observed load current dependence of the spreading velocity. L & M, by use of a complete ambipolar model, did not include drift effects but the temperature and base widths are probably most effective in the diffusive factors. Thus the analysis probably still yields useful information on the physical operation of the device if only the general trends of the experimental data are considered.

CHAPTER TWO

BASE AND EMITTER LATERAL CURRENT ANALYSIS APPLICABLE TO MULTIJUNCTION DEVICES

ABSTRACT

This paper contains an analysis of a linear and of a cylindrical transistor with lateral currents in both the emitter and the base layers. The results are written in a general form and can be applied to many specific cases including those that have a lateral current only in the base layer or only in the emitter layer. They may also be useful in the analysis of other multijunction devices in addition to transistors.

1. INTRODUCTION

In transistors and other multijunction devices lateral currents frequently play a most important role. Edge crowding in emitters is one well known result and the spreading of the on-state in silicon controlled rectifiers is another. The effect of lateral currents is here analyzed only for the transistor because of its simplicity but it is done so in a way which is in some respects more general and more useful than has been done previously. The results are of direct use in devices of greater complexity as is shown in a subsequent paper.

Under certain conditions lateral currents may exist in both the base and the emitter layers of a transistor. The internal current distribution of a transistor with lateral currents in the emitter layer is usually analyzed by neglecting the lateral potential drop in the base due to the lateral base current.[1,2,3] In this paper analytical expressions are derived which describe the internal current and voltage distributions of a transistor with lateral currents in both the base and emitter layers and without neglecting the lateral base potential.

The equations describing the situation for a general transistor are obtained first. The general equations are then solved for two transistor models--a rectangular model and a cylindrical model. Although the transistor models are rather idealized the basic assumptions are essentially the same as those used by Fletcher[4] and later by Hauser[5] in analyzing the effect of the lateral base current on transistor operation. Basically the analysis is for low-level operation

and does not include the effects of conductivity modulation in the base as considered by Fletcher[6] and by Emeis, Herlet, and Spenke[7,8] in analyzing the effect of the lateral base current. High frequency effects as analyzed by Pritchard[9] and surface effects are not included.

2. ANALYSIS

2.1 General Model

In the transistor of Fig. 1 only the lateral variations of the voltages and currents will be considered. The lateral emitter current density $\vec{J}_e(\vec{r})$ and the lateral base current density $\vec{J}_b(\vec{r})$ are average values with respect to any Z variation that may exist in the actual current densities. The densities $\vec{J}_e(\vec{r})$ and $\vec{J}_b(\vec{r})$ are vector functions of the position vector $\vec{r}$ lying parallel to the plane of $\vec{r}$ but not necessarily in the direction of $\vec{r}$.

Let the average resistivity of the emitter and of the base layer be ρ_e and ρ_b respectively. Since the lateral currents are primarily drift currents carried by majority carriers we may write

$$\nabla V_e(\vec{r}) = -\rho_e \vec{J}_e(\vec{r}) \tag{1}$$

and

$$\nabla V_b(\vec{r}) = -\rho_b \vec{J}_b(\vec{r}) \tag{2}$$

where $V_e(\vec{r})$ and $V_b(\vec{r})$ are the lateral voltages in the emitter and base layers respectively.

The forward bias on the emitter junction is

$$V(\vec{r}) = V_b(\vec{r}) - V_e(\vec{r}) \tag{3}$$

Taking the gradient of eqn. (3) and substituting eqns. (1) and (2) yields

$$\nabla V(\vec{r}) = \rho_e \vec{J}_e(\vec{r}) - \rho_b \vec{J}_b(\vec{r}) \tag{4}$$

or

$$\nabla^2 V(\vec{r}) = \rho_e \left[\nabla \cdot \vec{J}_e(\vec{r})\right] - \rho_b \left[\nabla \cdot \vec{J}_b(\vec{r})\right] . \tag{5}$$

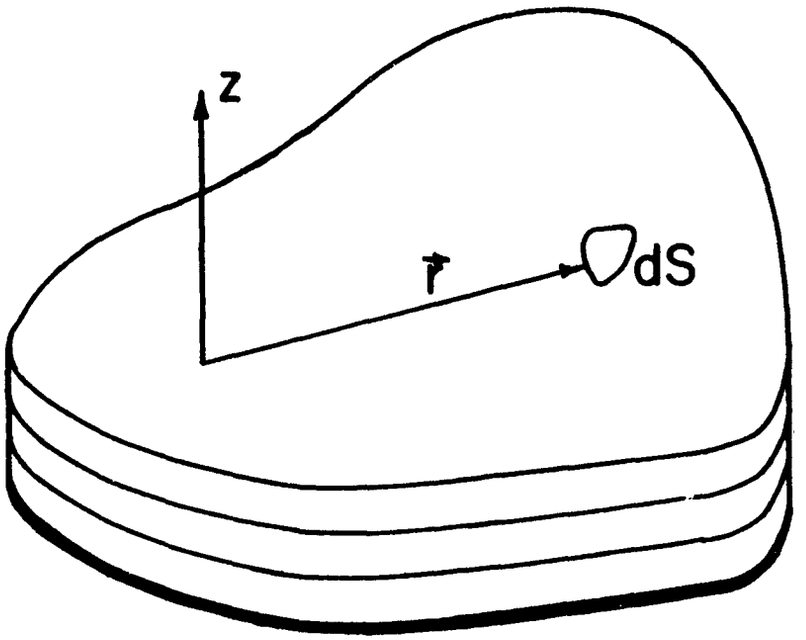

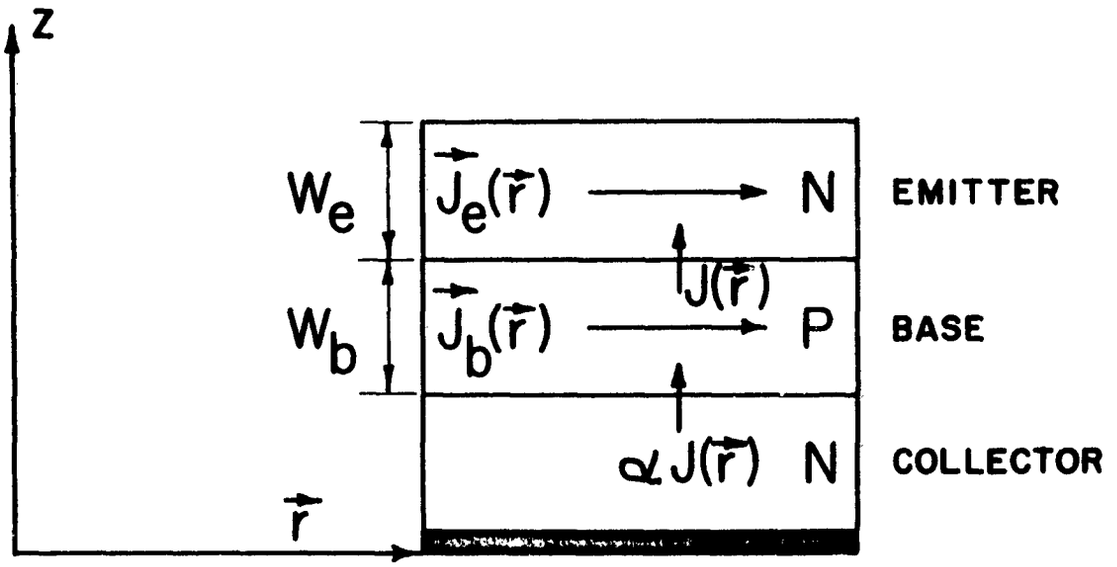

CROSS SECTION OF VOLUME ELEMENT OF TRANSISTOR AT $\vec{r}$.

Fig. 1. General transistor with lateral currents in both the emitter and base layers.

The analysis will be restricted to the case where the emitter junction current density is given by

$$J(\vec{r}) = j \exp \theta(\vec{r}) \tag{6}$$

where j is a constant and

$$\theta(\vec{r}) = \frac{qV(\vec{r})}{nkT} . \tag{7}$$

n is a constant between 1 and 2. In writing eqn. (6) we are assuming $\exp \theta(\vec{r}) \gg 1$. This is not a requirement for high injection level but rather that the injection level be high compared to equilibrium minority carriers.

The current density crossing the reverse biased collector junction is $\alpha J(\vec{r})$ where α is assumed constant. There is an implicit assumption here that carriers cross the collector junction without any lateral diffusion or drift. This is a reasonable approximation.

Applying the conservation of charge principle to the small element of emitter volume $W_e dS$ in Fig. 1 yields

$$\left[\nabla \cdot \vec{J}_e(\vec{r})\right] W_e \, dS = \vec{J}(\vec{r}) \, dS$$

or

$$\left[\nabla \cdot \vec{J}_e(\vec{r})\right] W_e = \vec{J}(\vec{r}) . \tag{8}$$

Similarly, in the base, $\left[\nabla \cdot \vec{J}_b(\vec{r})\right] W_b = -(1-\alpha) \vec{J}(\vec{r}) .$ (9)

Substituting eqns. (8) and (9) into eqn. (5) and using eqns. (6) and (7) gives

$$\nabla^2 \theta(\vec{r}) = 2Aj \exp \theta(\vec{r}) \tag{10}$$

where

$$A = \frac{q}{2nkT} \left[\frac{\rho_e}{W_e} + \frac{\rho_b}{W_b}(1-\alpha) \right]$$

is a constant of material and configuration. Eqn. (10) (Liouville's eqn.) is the basic equation since the solution $\Theta(\vec{r})$ will permit the remaining lateral currents and voltages to be obtained. Eqn. (10) and the other appropriate equations will now be solved for two specific transistor models.

2.2 Rectangular Model

In the transistor of Fig. 2 the lateral emitter and base currents are both in the x direction and functions of x only. The position vector $\vec{r}$ now has only an x component and for simplicity the vector notation will be dropped.

The form of the equations to follow will be simplified if written in terms of the dimensionless parameter

$$g = (x/x_m - 1) \tag{11}$$

where x_m is the point where $\left.\frac{d\Theta(x)}{dx}\right|_{x=x_m} = 0$.

It is not necessary for this point to be in the device but it always exists, at least mathematically. From eqn. (4) it can be seen that x_m can be defined by the equation

$$\frac{\rho_e}{W_e} I_e(x_m) = \frac{\rho_b}{W_b} I_b(x_m)$$

or

$$\frac{\rho_e}{W_e} I_{em} = \frac{\rho_b}{W_b} I_{bm} \tag{12}$$

where $I_e(x) = W_e H J_e(x)$ and $I_b(x) = W_b H J_b(x)$.

With the use of eqn. (11), eqn. (10) in rectangular coordinates becomes

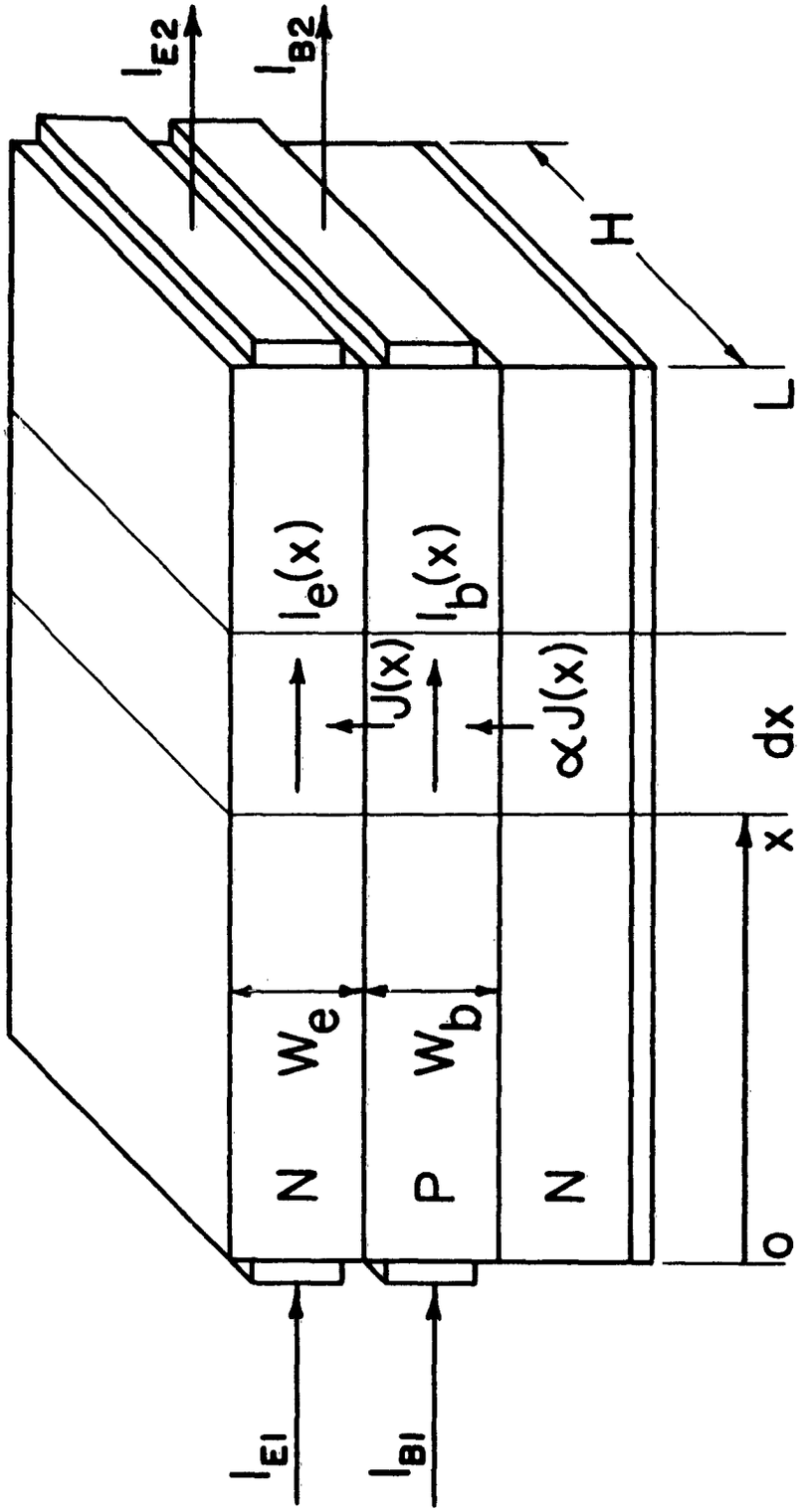

Fig. 2. Rectangular transistor.

$$\frac{d^2\theta(g)}{dg^2} = 2Ax_m^2 j \exp\theta(g) \quad . \tag{13}$$

The solution of eqn. (13) is

$$\theta(g) - \theta_m = 2 \ln \sec ag \tag{14}$$

where θ_m is the value of θ at $g = 0$ and

$$a = x_m\sqrt{AJ_m} \quad , \qquad J_m = j \exp\theta_m \quad .$$

The solution of eqn. (13) contains two arbitrary constants of integration, x_m and J_m. The equations have been written in terms of these two constants since the form of the equations to follow is thereby simplified and the two arbitrary constants have a physical significance, thereby aiding the interpretation of the resulting equations. The physical significance of x_m is already apparent and that of J_m will become so in the next equation.

The injected emitter current density can be obtained from eqns. (6) and (14).

$$J(g) = J_m \sec^2 ag \quad . \tag{15}$$

We see that J_m is the minimum emitted current density and occurs at $g = 0$, i.e., at $x = x_m$. Also, since $J(g)$ is an even function, the emitted current distribution is symmetrical about $g = 0$, at least to the limits of the device.

The lateral emitter current can be obtained by substituting eqn. (15) into eqn. (8) and integrating.

$$I_e(g) - I_{em} = \frac{Hx_mJ_m}{a} \tan ag \quad . \tag{16}$$

Similarly, integration of eqn. (9) yields

$$I_b(g) - I_{bm} = -(1-\alpha)\left[I_e(g) - I_{em}\right] \quad . \qquad (17)$$

Equations (16) and (17) have been written in terms of I_{em} and I_{bm}, the lateral emitter and base currents, respectively, at $g = 0$. I_{em} and I_{bm} are not arbitrary but are determined by x_m and J_m and they are not necessarily the minimum lateral currents but rather the lateral currents at the point where the emitted current density is minimum. This notation has been used for conciseness but since I_{em} and I_{bm} are not necessarily quantities that can be measured externally on a transistor it may be desirable to eliminate them from the expressions for $I_e(g)$ and $I_b(g)$ and later equations to be derived. This can easily be done, for example, by substituting a known boundary current $I_e(g_1)$ into eqn. (16), and using the resulting equation in conjunction with eqn. (16) to eliminate I_{em}.

The lateral voltages in the emitter and base layers can be obtained by integrating eqns. (1) and (2) with the use of eqns. (16) and (17).

$$V_e(g) - V_{em} = \frac{\rho_e}{AW_e}\left[\ln\cos ag - \left(\frac{A I_{em}}{H\sqrt{AJ_m}}\right) ag\right] \qquad (18)$$

$$V_b(g) - V_{bm} = \frac{-\rho_b(1-\alpha)}{AW_b}\left[\ln\cos ag + \left(\frac{A I_{bm}}{H\sqrt{AJ_m(1-\alpha)}}\right) ag\right] \qquad (19)$$

The voltages V_{em} and V_{bm} are the voltages which occur at $g = 0$.

A sketch of $J(g)$, $I_e(g)$, and $V_e(g)$ is shown in Fig. 3. These will be discussed in more detail after the equations applicable to the cylindrical model are derived.

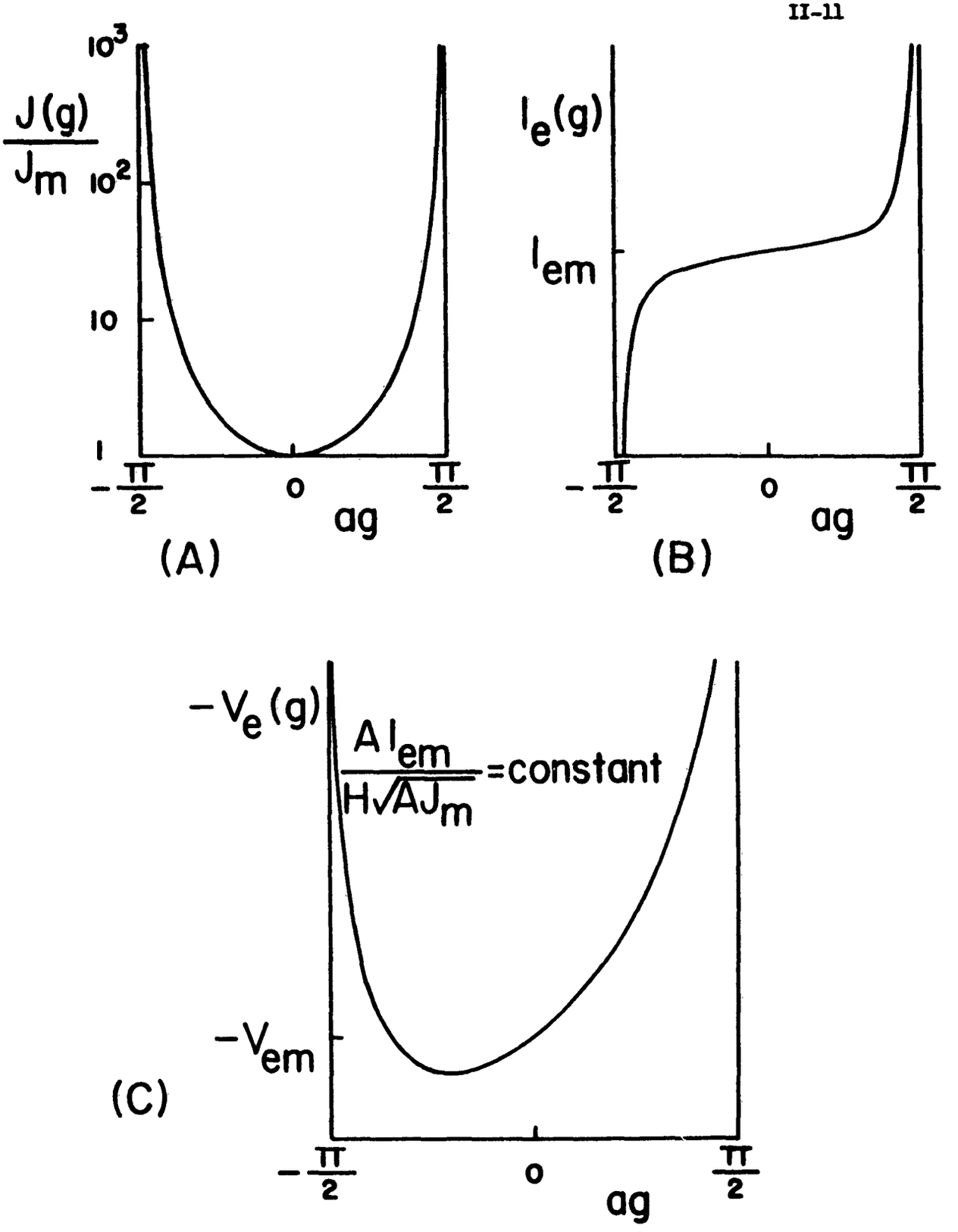

Fig. 3. Plots of (A) the emitted current density J(g), (B) the lateral emitter current $I_e(g)$, and (C) the lateral voltage in the emitter layer $V_e(g)$ of the rectangular transistor.

2.3 Cylindrically Symmetrical Model

In the transistor of Fig. 4 the lateral emitter and base currents are both in the r direction and functions of r only since we assume cylindrical symmetry.

Equation (10) becomes in our cylindrical system

$$\frac{d^2\Theta(r)}{dr^2} + \frac{1}{r}\frac{d\Theta(r)}{dr} = 2Aj \exp\Theta(r) \qquad (20)$$

The solution to eqn. (20) will be written in terms of the dimensionless parameter

$$f = \ln \frac{r}{r_m} \qquad (21)$$

where r_m is the point where

$$\left.\frac{d\Theta(r)}{dr}\right|_{r=r_m} = 0 \quad ,$$

analogous to x_m in the rectangular model. The solution to eqn. (20) is derived in the appendix. Once $\Theta(f)$ is obtained the remaining currents and voltages are then obtained by using eqn. (6) and integrating eqns. (8) and (9) and then (1) and (2). The solutions may be written in three forms according to whether $Ar_m^2 J_m > 1$, $Ar_m^2 J_m = 1$, or $Ar_m^2 J_m < 1$.

(1) $Ar_m^2 J_m > 1$. Let $b = \sqrt{Ar_m^2 J_m - 1}$.

$$J(f) = \frac{J_m}{(\exp 2f)(\cos bf - \frac{1}{b}\sin bf)^2}$$

$$I_e(f) - I_{em} = \frac{-\left[I_b(f) - I_{bm}\right]}{(1-\alpha)} = 2\pi r_m^2 J_m \left[\frac{\tan bf}{b - \tan bf}\right]$$

$$V_e(f) - V_{em} = \frac{\rho_e}{AW_e}\left[\ln(\cos bf - \frac{1}{b}\sin bf) + \left(1 - \frac{AI_{em}}{2\pi}\right) f\right]$$

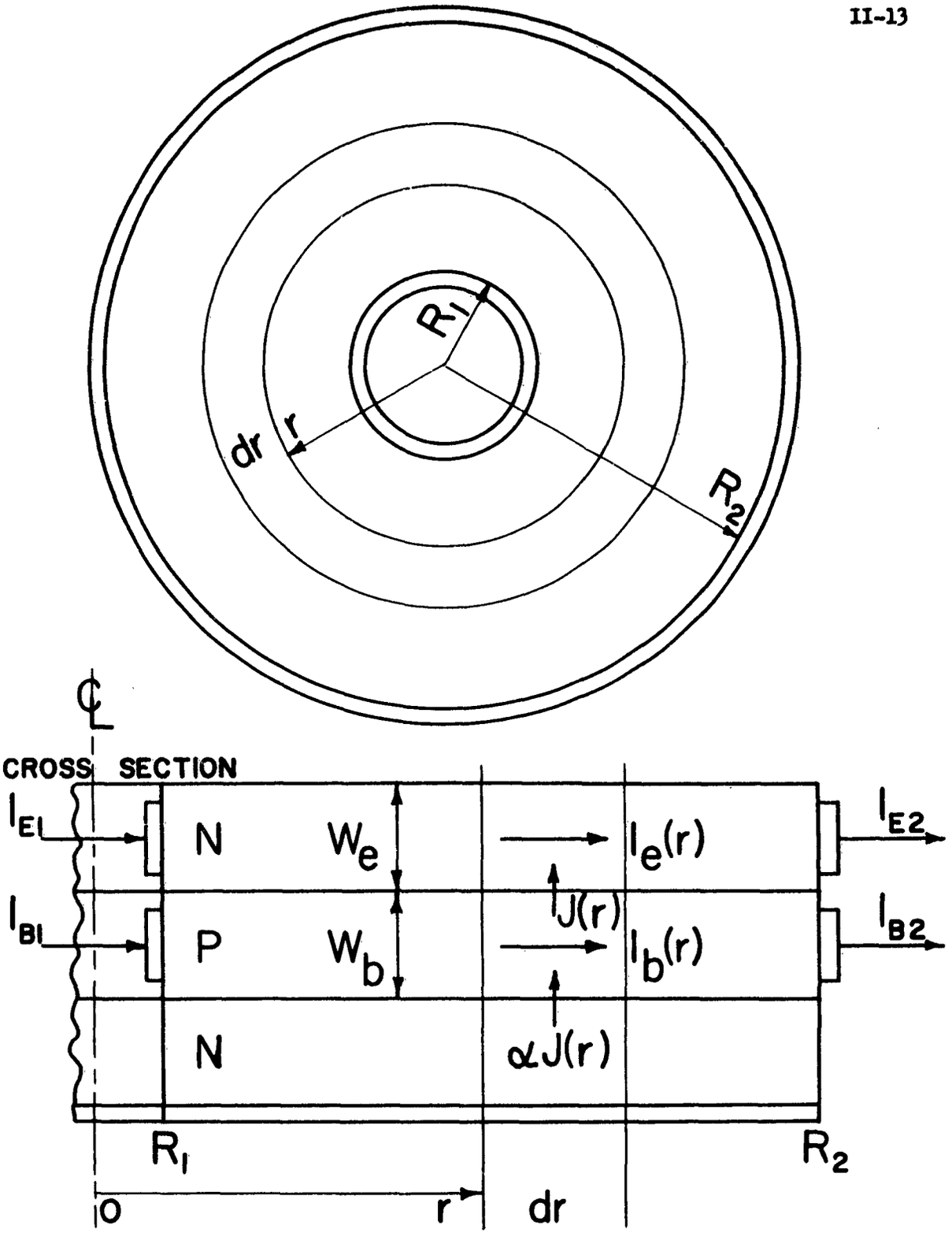

Fig. 4. Cylindrical transistor.

$$V_b(f) - V_{bm} = \frac{-\rho_b(1-\alpha)}{AW_b}\left[\ln(\cos bf - \frac{1}{b}\sin bf) + \left(1 + \frac{Al_{bm}}{2\pi(1-\alpha)}\right)f\right]$$

(2) $Ar_m^2 J_m = 1$.

$$J(f) = \frac{J_m}{(\exp 2f)(1-f)^2}$$

$$I_e(f) - I_{em} = \frac{-[I_b(f) - I_{bm}]}{(1-\alpha)} = 2\pi r_m^2 J_m\left[\frac{f}{1-f}\right]$$

$$V_e(f) - V_{em} = \frac{\rho_e}{AW_e}\left[\ln(1-f) + \left(1 - \frac{Al_{em}}{2\pi}\right)f\right]$$

$$V_b(f) - V_{bm} = \frac{\rho_b}{AW_b}\left[\ln(1-f) + \left(1 + \frac{Al_{bm}}{2\pi(1-\alpha)}\right)f\right]$$

(3) $Ar_m^2 J_m < 1$. Let $c = \sqrt{1 - Ar_m^2 J_m}$

$$J(f) = \frac{J_m}{(\exp 2f)(\cosh cf - \frac{1}{c}\sinh cf)^2}$$

$$I_e(f) - I_{em} = \frac{-[I_b(f) - I_{bm}]}{(1-\alpha)} = 2\pi r_m^2 J_m\left[\frac{\tanh cf}{c - \tanh cf}\right]$$

$$V_e(f) - V_{em} = \frac{\rho_e}{AW_e}\left[\ln(\cosh cf - \frac{1}{c}\sinh cf) + \left(1 - \frac{Al_{em}}{2\pi}\right)f\right]$$

$$V_b(f) - V_{bm} = \frac{-\rho_b(1-\alpha)}{AW_b}\left[\ln(\cosh cf - \frac{1}{c}\sinh cf) + \left(1 + \frac{Al_{bm}}{2\pi(1-\alpha)}\right)f\right]$$

A plot of J(f) is shown in Fig. 5 with $Ar_m^2 J_m$ as a parameter.

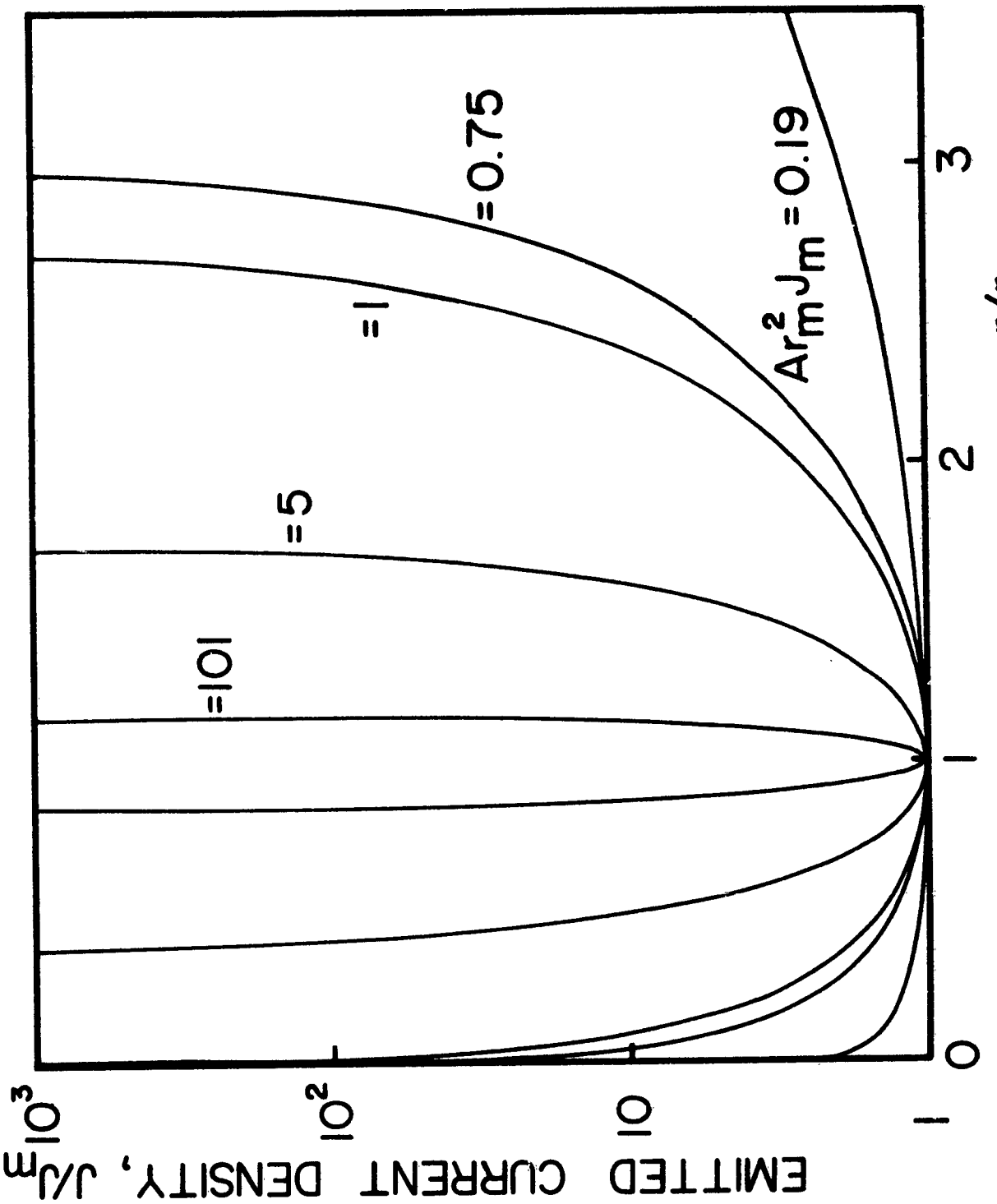

Fig. 5. A plot of the emitted current density $J(r/r_m)$ for the cylindrical transistor with $Ar_m^2 J_m$ as a parameter.

3. DISCUSSION

The equations in this paper have been written in terms of the two arbitrary constants J_m and either x_m or r_m. In a given situation these two constants will be determined by the boundary conditions. If g_1 and g_2 (or f_1 and f_2) are the two boundaries of the transistor, some possible pairs of boundary conditions are $\Theta(g_1)$ and $\Theta(g_2)$, or $J(g_1)$ and $J(g_2)$, or $\left[I_e(g_1) - I_e(g_2)\right]$ and $\left[I_b(g_1) - I_b(g_2)\right]$. Any one of these three pairs of boundary conditions will yield two equations sufficient for determining the two arbitrary constants. In some cases x_m or r_m may lie outside of the physical bounds of the model, but the equations are, of course, still valid.

An estimate of the minimum emitted current density J_m and its location x_m could be obtained by constructing a transistor with small isolated sections in the collector layer. If the reverse-bias current of these isolated sections was observed, the location of the minimum injected current density could be determined and, if a value of α is assumed, an estimate of J_m could be made. This technique would provide an independent check upon the values calculated from the analysis with given boundary conditions.

It is helpful to note that in the rectangular model only one curve is necessary to completely describe the distribution of $J(g)$, $I_e(g)$ or $I_b(g)$. The emitted current distribution $J(g)$, for example, is described by the curve of Fig. 3(a). In a given transistor with a fixed set of boundary conditions a segment of this curve will describe

the emitted current distribution. If the boundary conditions are changed by going to a higher injection level, for example, a different segment, but of the same curve, will now describe the new emitted current distribution. A family of curves for different operation levels is, then, segments of the one curve of Fig. 3(a). The situation in the cylindrical model is not as fortunate, however, since, as Fig. 5 shows, $Ar_m^2 J_m$ must be used as a parameter when drawing the distribution of $J(f)$ or other functions.

Since the analysis has been for two rather general transistor models, the results will apply to many specific cases, some of which have been considered in the literature. One specific case, for example, is a rectangular transistor with no lateral voltage drop in the emitter layer and only one base connection at $x=0$ in Fig. 2. In order to have no lateral voltage in the emitter layer a contact can be applied over the emitter surface so that the average resistivity of the emitter layer is zero. Then $\rho_e = 0$ and by eqn. (12)

$$\frac{\rho_b}{W_b} I_b(x_m) = 0 \quad .$$

But since there is no base connection at $x = L$ we know that $I_{B2} = 0$. Consequently, $x_m = L$ in this case. Equation (15) becomes

$$J(x) = J_m \sec^2 a\left(\frac{x}{L} - 1\right) \quad .$$

J_m can be written in terms of $J(0)$, the injected current density at the edge $x = 0$.

$$J(x) = J(0)\left[\frac{\sec^2 a\left(\frac{x}{L} - 1\right)}{\sec^2 a}\right] \quad .$$

This equation is identical to eqn. (17) in reference (5) for the same specific case. Another case considered in the literature is a rectangular transistor with no lateral voltage drop in the base layer and only one emitter connection at $x = 0$. In this case if we let either $\rho_b = 0$ or $\alpha = 1$ no lateral voltage will exist in the base layer and the equations can be reduced to those derived in reference (3) for this model.

The application of the equations in this paper to actual devices is limited by the assumptions in the derivation. Sometimes the analysis will apply only to certain parts of specific devices. For example, it is possible to pass sufficient lateral current through the base of a transistor to cause part of the emitter junction to be reverse-biased. Here the analysis applies only to the forward-biased part of the junction where $\exp \theta \gg 1$. At sufficiently high injection the base resistivity near the edges may change with injection level, in which case the analysis would apply to the remainder of the device where ρ is constant.

Although α has been assumed constant, in an actual transistor α will decrease at low current levels. This decrease in α means that a larger fraction of the total emitted current will recombine and increase the lateral base current. This increased lateral base current will cause a larger lateral voltage drop in the base layer, thereby making the crowding more severe than expected when α is assumed constant.

When applying the results of this analysis in a quantitative manner some additions will certainly be necessary to account for the edge and surface effects. Many authors have shown that the surface and edge

effects probably account for most of the α drop off at low current levels[2,10,11] and also for the α drop off at high current levels.[12,13] Essentially the boundary currents in our models would have to have additional components for the surface and edge recombination currents.

Although our analysis has been for transistor models, the results can be applied with very little modification to other multijunction devices or at least to parts of other devices. In a later paper we shall use part of this analysis to explain some switching phenomenon we have observed in specially constructed PNPN devices.

Note: In a recent paper, "Bidirectional Triode P-N-P-N Switches," Proc. IEEE, 53, 355-369, (April 1965), F. E. Gentry, R. I. Space, and J. K. Flowers have also analyzed the effect of lateral currents in both the emitter and base layers of a linear model. Their results can be obtained from the results of this paper since the assumptions in both papers are essentially identical although their approach is somewhat different. They have not obtained the expressions for the lateral emitter and base currents or voltages nor have they considered the cylindrical model.

REFERENCES

1. R. A. Gudmundsen. "The Emitter Tetrode." IRE Trans. on Electron Devices, ED-5, 223-225. (Oct. 1958).

2. J. E. Iwersen, A. R. Bray, and J. J. Kleimack. "Low-Current Alpha in Silicon Transistors." IRE Trans. on Electron Devices, ED-9, 474-478. (Nov. 1962).

3. K. J. S. Cave and J. A. Barnes. "Optimum Length of Emitter Stripes in 'Comb' Structure Transistors." IEEE Trans. on Electron Devices, ED-12, 84-85. (Feb. 1965).

4. N. H. Fletcher. "Some Aspects of the Design of Power Transistors." Proc. IRE, 43, 551-559. (May, 1955).

5. J. R. Hauser. "The Effects of Distributed Base Potential on Emitter-Current Injection Density and Effective Base Resistance for Stripe Transistor Geometries." IEEE Trans. on Electron Devices, ED-11, 238-242. (May, 1964).

6. N. H. Fletcher. "Self-Bias Cutoff Effect in Power Transistors." Proc. IRE, 43, 1669. (Nov. 1955).

7. R. Emeis and A. Herlet. "Die effektive Emitterflache von Leistungstransistoren." Z. Naturforschung, 12a, 1016-1018. (Dec. 1957).

8. R. Emeis, A. Herlet, and E. Spenke. "The Effective Emitter Area of Power Transistors." Proc. IRE, 46, 1220-1229. (June, 1958).

9. R. L. Pritchard. "Two-Dimensional Current Flow in Junction Transistors at High Frequencies." Proc. IRE, 46, 1152-1160. (June, 1958).

10. P. J. Coppen and W. T. Matzen. "Distribution of Recombination Current in Emitter-Base Junctions of Silicon Transistors." IRE Trans. on Electron Devices, ED-9, 75-81. (Jan. 1962).

11. C. T. Sah. "Effect of Surface Recombination and Channel on P-N Junction and Transistor Characteristics." IRE Trans. on Electron Devices, ED-9, 94-108. (Jan. 1962).

12. S. Wang and T. T. Wu. "On the Theory of DC Amplification Factor of Junction Transistors." IRE Trans. on Electron Devices, ED-6, 162-169. (April, 1959).

13. C. A. Mead. "The Operation of Junction Transistors at High Currents and in Saturation." Solid State Electronics, 1, 211-224. (, 1960).

APPENDIX

Solution to eqn. (20).

$$\frac{d^2\Theta}{dr^2} + \frac{1}{r}\frac{d\Theta}{dr} = 2Aj\exp\Theta \quad . \tag{A1}$$

In order to solve eqn. (A1) first change the variables to $u(z)=r\frac{d\Theta}{dr}$ and $z(r,\Theta) = r^2\exp\Theta$.

$$(2+u)\frac{du}{dz} = 2Aj \tag{A2}$$

Integrating eqn. (A2) and imposing the conditions

$$\left.\frac{d\Theta}{dr}\right|_{r=r_m} = 0 \quad \text{and} \quad \Theta(r_m) = \Theta_m \tag{A3}$$

yields

$$u^2 + 4u - 4Ajz + 4Ajz_m = 0$$

or $$r^2\left(\frac{d\Theta}{dr}\right)^2 + 4r\frac{d\Theta}{dr} - 4Ar^2j\exp\Theta + 4Ar_m^2j\exp\Theta_m = 0 \, . \tag{A4}$$

Eqns. (A1) and (A4) can be combined to eliminate the $\exp\Theta$ term.

$$2r^2\frac{d^2\Theta}{dr^2} - r^2\left(\frac{d\Theta}{dr}\right)^2 - 2r\frac{d\Theta}{dr} - 4Ar_m^2J_m = 0 \quad . \tag{A5}$$

Substituting

$$\phi^{-2}(f) = \exp\Theta(r) \qquad \text{where} \quad f = \ln\frac{r}{r_m}$$

eqn. (A5) becomes

$$\frac{d^2\phi}{df^2} - 2\frac{d\phi}{df} + Ar_m^2J_m\phi = 0 \quad . \tag{A6}$$

Eqn. (A6) is a linear differential equation whose solution may be

written in three forms according to whether $Ar_m^2 J_m > 1$, $Ar_m^2 J_m = 1$, or $Ar_m^2 J_m < 1$.

$Ar_m^2 J_m > 1$: Let $b = \sqrt{Ar_m^2 J_m - 1}$, then $\phi = C_1 (\exp f) \cos(bf + C_2)$

and $\Theta(f) - \Theta_m = -2f - 2\ln(\cos bf - \frac{1}{b}\sin bf)$.

$Ar_m^2 J_m = 1$: $\phi = (\exp f)(C_3 + C_4 f)$,

and $\Theta(f) - \Theta_m = -2f - 2\ln(1 - f)$.

$Ar_m^2 J_m < 1$: Let $c = \sqrt{1 - Ar_m^2 J_m}$, then $\phi = C_5 (\exp f) \cosh(cf + C_6)$

and $\Theta(f) - \Theta_m = -2f - 2\ln(\cosh cf - \frac{1}{c}\sinh cf)$.

In each of the three cases above the arbitrary constants C_1 through C_6 have been written in terms of r_m and J_m by applying the conditions of (A3).

CHAPTER THREE

SKIP TURN-ON OF SILICON CONTROLLED RECTIFIERS

ABSTRACT

A lateral current in an emitter layer of a silicon controlled rectifier (SCR) is shown to vary the lateral field in the base layers and also to change the distribution of the current density injected from the emitter to the base. A method of using lateral emitter layer currents in an SCR to increase the spreading velocity of the on-region and, at higher currents, to turn on quickly areas of the SCR remote from the gate contact is demonstrated experimentally.

1. INTRODUCTION

When a silicon controlled rectifier (SCR) is triggered by a gate current, initially only a small region next to the gate contact turns on. This initial on-region then spreads laterally throughout the device until the entire area of the SCR is conducting. Although a large area SCR is capable of carrying very high currents after the entire area is on, the initial current must be limited since only the small initial on-region is conducting. Frequently it is desirable for the SCR to carry a large current immediately after turn-on. On such occasions either a large initial area must be turned on or the spreading velocity of the on-region must be made to be very high.

An earlier paper[1] described experiments which permitted the measurement of the spread of the on-region in specially constructed SCRs. This paper describes similar experiments on devices constructed so that after the initial turn-on a lateral current exists in the N emitter layer. The effects of emitter crowding in transistors, caused by the lateral current in the base layer, is well known. It is also well known that a lateral current in the emitter layer of a transistor can vary the injected emitter current distribution.[2,3] In the experiment to be described, a lateral emitter current is used in an SCR to increase the spreading velocity of the on-region after gate turn-on. Regions of the SCR remote from the gate contact can also be turned on with this same lateral emitter current.

First, the effect of a lateral emitter current upon the switching action of an SCR will be shown with the aid of a transistor analogue. Experimental results which substantiate the theory are then presented.

2. THEORY OF OPERATION

The effect of a lateral current in the emitter layer, and its value as a rapid turn-on aid, can be explained by first considering the transistor of Fig. 1. It will be shown that the transistor structure to be considered is an analogue to the SCR fast turn-on device in the pre-turn-on condition. The transistor of Fig. 1 has lateral currents in both the emitter and base layers. The lateral emitter current, in the direction assumed in Fig. 1, tends to make the N emitter layer more negative at $x = L$ than at $x = 0$. This would make the injected emitter current density increase as x increases but the lateral base current counters this tendency to some extent. The net result is that the emitted current is crowded towards both ends of the device and the minimum emitted current density occurs inside the device.

An earlier analysis[4] showed that the distribution of the injected emitter current density in a transistor with lateral currents in both the emitter and base layers is described by the relation

$$J(x) = J_m \sec^2 \left\{ x_m \sqrt{AJ_m} \left[(x/x_m) - 1 \right] \right\} \qquad (1)$$

where J_m is the minimum emitted current density which occurs at x_m and A is constant of material and configuration. The emitted current density is sketched in Fig. 1 for two values of the lateral voltage V_2. The emitted current density at $x = 0$ is dependent only on the emitter bias voltage V_1 and so is constant if V_1 is constant.

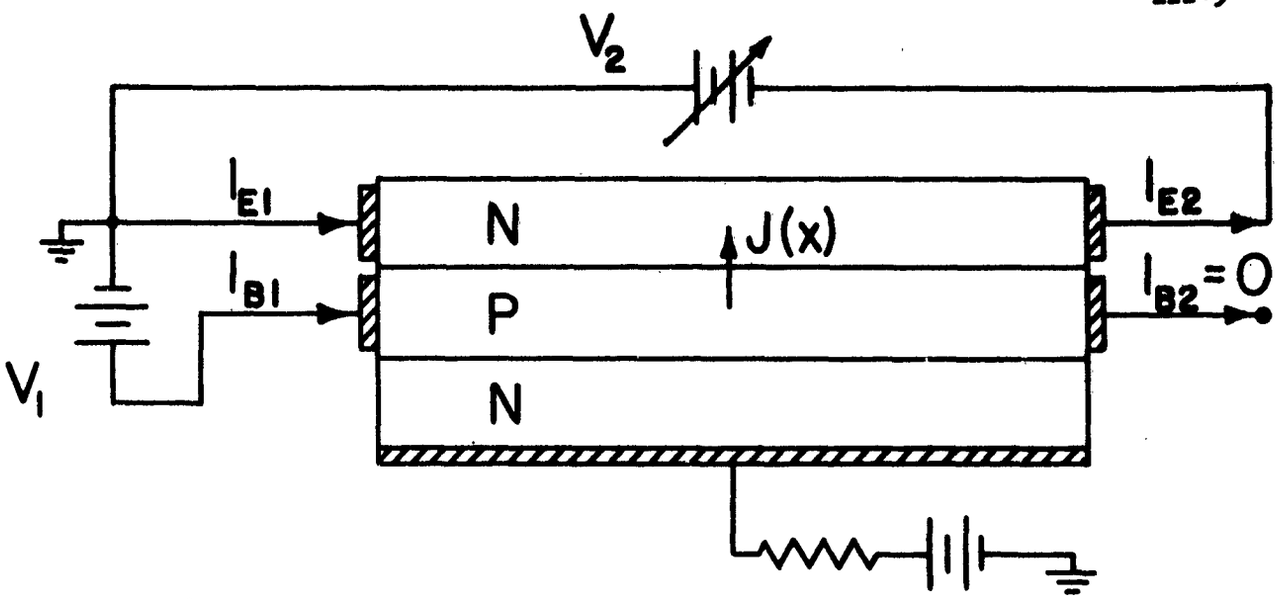

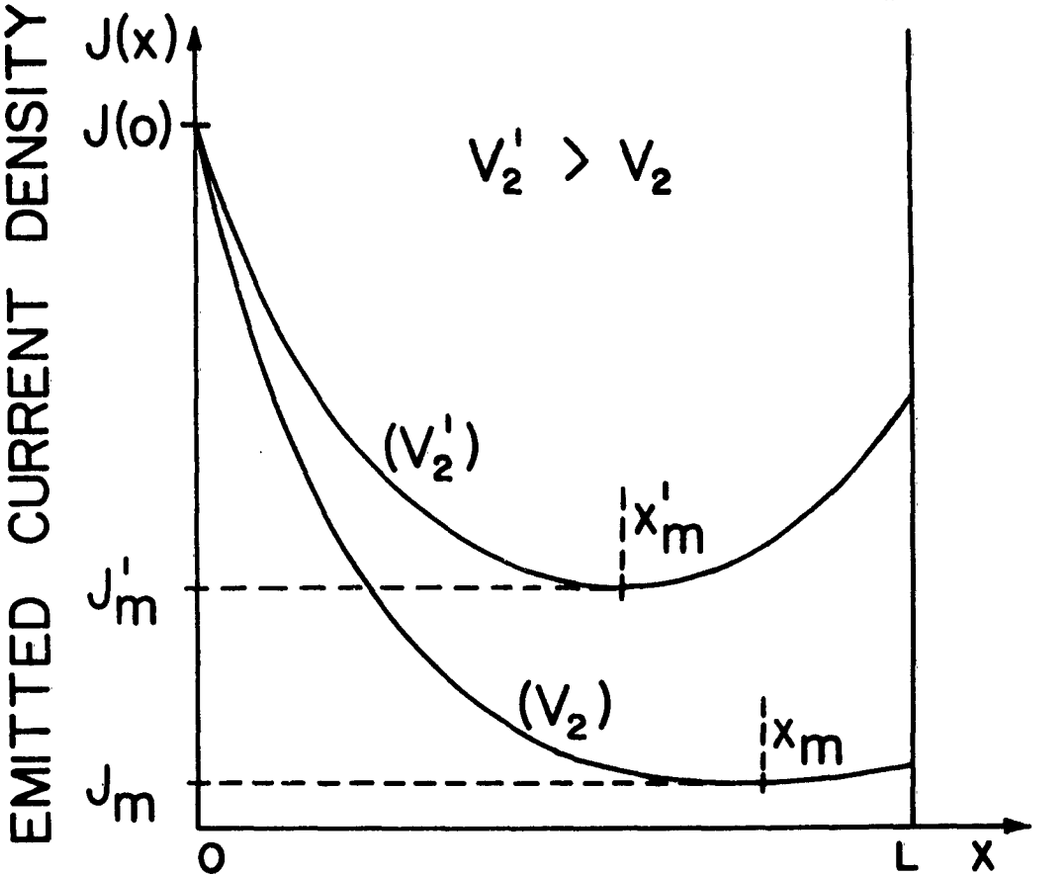

$$J(x) = J_m \sec^2 \left[x_m \sqrt{A J_m} \left(1 - \frac{x}{x_m}\right) \right]$$

Fig. 1. Transistor with lateral currents in both the emitter and base layers. The emitted current density is drawn for two values of the lateral voltage V_2.

That is,

$$J(0) = J_m \sec^2(x_m \sqrt{\lambda J_m}) = \text{constant.} \qquad (2)$$

If V_2 is increased to a value V_2', the emitted current density must increase since the emitter layer will be more negative at $x = L$. This will cause J_m to increase and, by eq. (2), x_m to decrease. The shift in x_m can be seen by examining the two curves of emitted current.

The lateral current in the emitter layer has caused the emitted current density at $x = L$ to increase. In a transistor with no lateral current in the emitter layer, the point x_m occurs at $x = L$ when the base is connected at $x = 0$. The addition of a lateral current in the emitter layer as in Fig. 1 causes the point x_m to move to the interior of the transistor and the emitted current density at $x = L$ to increase.

The total emitted current is

$$H \int_0^L J(x)\, dx = (I_{E2} - I_{E1})$$

and will increase when the lateral emitter current increases. H is the width of the transistor. If α is assumed constant, then

$$I_{E2} - I_{E1} = -(1-\alpha)(I_{B2} - I_{B1}) = (1-\alpha)I_{B1}$$

since $I_{B2} = 0$ in Fig. 1. Since increasing the lateral emitter current

causes $(I_{E2}-I_{E1})$ to increase, the base current I_{B1} must also increase. The increase in I_{B1} implies that the lateral field in the base of the transistor at the region near $x = 0$ also increases since the lateral currents are primarily drift currents carried by majority carriers.

Physically, the increased emitted current increases the number of carriers recombining in the base. The additional majority carriers necessary for this increased recombination is supplied by the base current, I_{B1}, causing I_{B1} to increase, since I_{B2} is fixed at zero.

A lateral current in the emitter layer of an SCR can be obtained without additional external leads if the SCR is constructed as shown in Fig. 2. In this configuration the cathode contact is placed some distance away from the gate contact. When the SCR is triggered with a gate current, initially only the region next to the gate contact turns on. After triggering, the load current builds up through the on-region and passes laterally through the emitter layer as shown by the arrows in Fig. 2. The on-region is continually spreading across the device and, during this time, the off-portion of the device is analogous to the transistor structure of Fig. 1. At the boundary between the on- and off-regions the emitted current density is nearly constant and corresponds to $x = 0$ in Fig. 1. The load current through the on-region makes up the lateral current which was supplied by V_2 in Fig. 1.

As in the case of the transistor of Fig. 1, the lateral current in the emitter layer of the SCR produces two effects. First, the

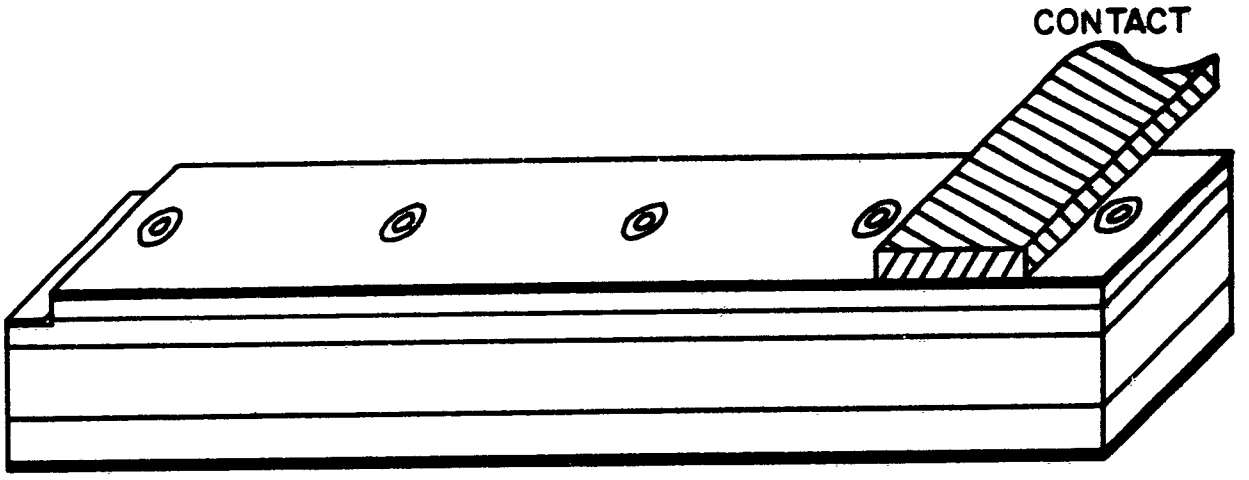

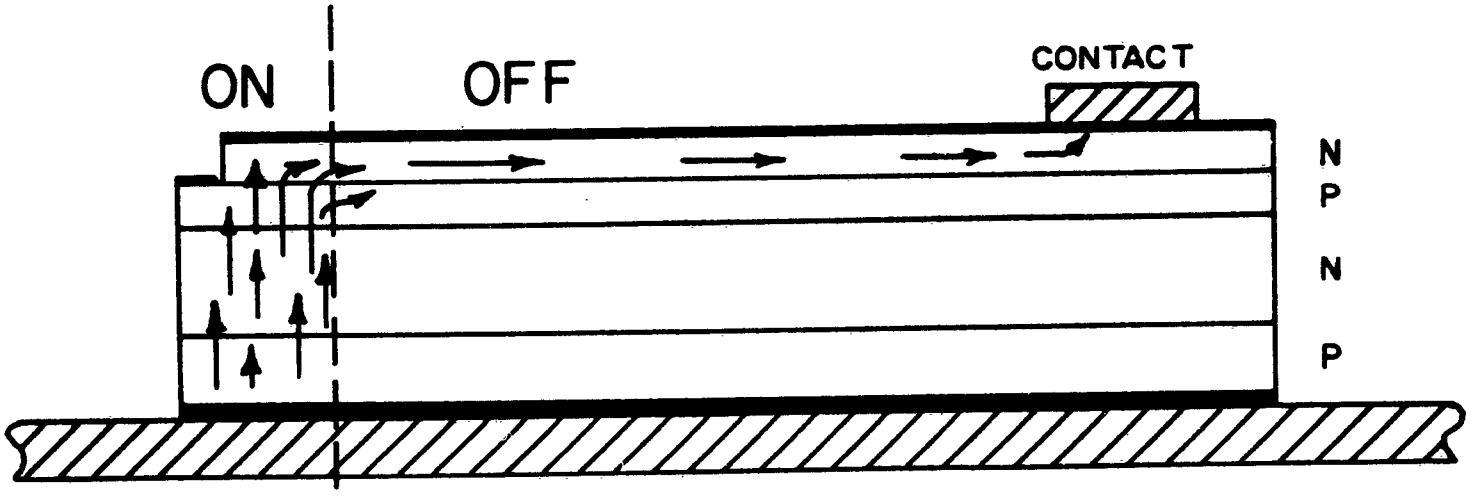

Fig. 2. Configuration of silicon controlled rectifiers used in this experiment. After initiation of turn-on at the gate the anode-cathode current passed laterally through the N emitter layer as shown by the arrows while the on-state spread from the gate towards the contact.

lateral field in the P-base layer is increased in the off-region near the boundary between the on-and off-regions. This field increases the gate current being supplied to the off-region by the on-region and thereby causes the off-region adjacent to the on-region to turn on faster. The final result is that the spreading velocity is increased.

The second effect of the lateral emitter current is that the current density injected from the emitter to the base is increased in the off-region near the cathode contact. This effectively supplies a gate current to this off-region and if the effective gate current is large enough, the off-region near the cathode contact will be turned on. Two on-regions will then exist -- one spreading from the gate contact and the other spreading from the cathode contact.

3. EXPERIMENTAL PROCEDURE

The SCRs used in this experiment were the same as or similar to those used in the earlier experiment to investigate the spread of the on-state.[1] Each SCR was bar shaped with 5 or 6 islands spaced along the length of the bar. The propagation of the on-state after gate triggering was measured by observing the reverse-bias current of the islands.

In the earlier experiment[1] contact to the nickel plated cathode was made by bringing phosphor-bronze spring fingers down upon the cathode between the islands. A gallium-indium eutectic was smeared over the nickel to insure good electrical contact between the fingers and the nickel surface. In this experiment all the fingers except for the finger farthest from the gate contact were insulated from the cathode layer by placing mica strips between the fingers and the device. The current through the SCR therefore had to pass laterally through the cathode emitter layer to the contact at the end of the bar. The devices then approximated the configuration shown in Fig. 2.

The testing procedure of this experiment was identical to that of the earlier experiment. Basically, a d.c. supply voltage and a resistive load were connected in series with the SCR. The SCR was triggered repetitively at 2.5 cps and the reverse-bias current of each of the islands was observed on an oscilloscope. When the on-region reaches one of the islands the reverse-bias current increases. This permitted the measurement of the spread of the on-state.

4. RESULTS AND DISCUSSION

In Fig. 3 the time for the on-region to reach the individual islands of device C1 is plotted as a function of the final load current. Zero time on this graph is the time when the gate pulse was applied. Device C1 had a gate on each end of the bar but, as indicated in Fig. 3, only the first gate was triggered. Contact to the cathode emitter layer was made only between islands 4 and 5 at the end of the bar farthest from the first gate.

At load currents below about 0.5 amperes the spreading velocity was indeed increased from that when no lateral emitter current was present. For comparison purposes a dashed line has been drawn in Fig. 3 to indicate the time of arrival of the on-region at island 5 when all the spring fingers contacted the emitter layer and no large lateral emitter currents were present. It can be seen that the arrival time of the on-region has been reduced by about one-third at low load currents.

Although the lateral currents were purposely produced in the emitter layer in this experiment, similar currents may exist in normal SCRs because of variations in junction depths, resistivities or other inhomogeneities. Under such conditions the velocity of spreading would not be a monotonic function of time. These nonuniformities in the structure of the SCR may partly explain the variations in the spreading velocities that were observed in the earlier paper.[1]

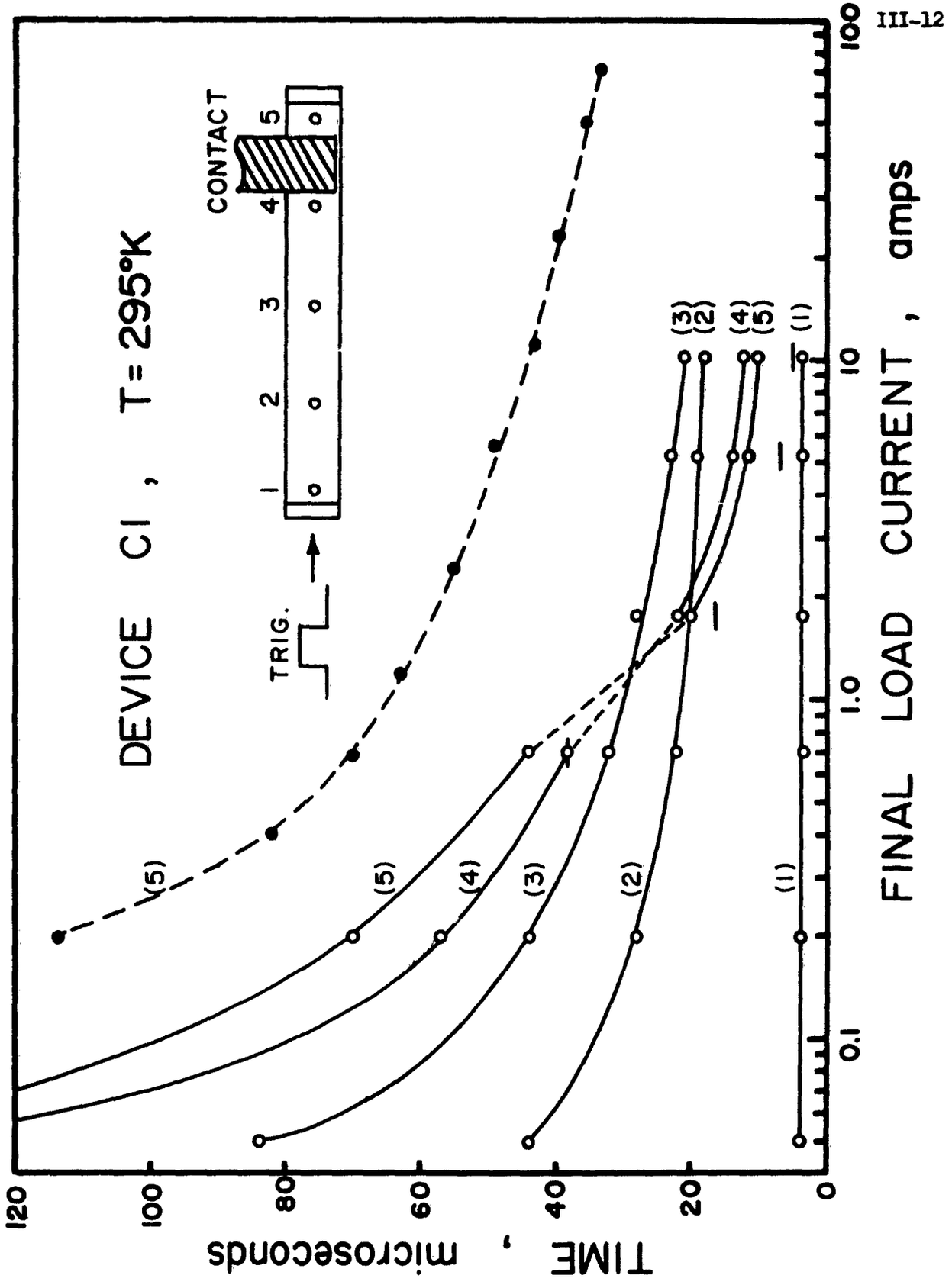

Fig. 3. The arrival time of the on-state at the individual islands of device C1 vs the final load current when only the first gate was triggered.

At load currents above about 0.5 amperes a second on-region begins spreading from the cathode emitter layer contact after the first on-region near the gate has begun to spread. There are two indications that a second on-region begins spreading. First, examination of Fig. 3 shows that the order of the arrival of the on-region to the individual islands changes at high load currents. At low load currents the on-region reaches the islands in the logical order 1, 2, 3, 4, 5 when the first gate is triggered. At high load currents, however, the on-regions reach the islands in the order 1, 5, 4, 2, 3.

This order of arrival of the on-regions can be explained if we remember that after the gate turns on the initial region, this on-region spreads to island 1 first. During this time the load current builds up and passes laterally through the emitter layer. As explained in section 2, this lateral emitter current causes the emitter to inject carriers into the base beneath the contact to the emitter layer. If this injected emitter current is sufficiently great and continues for a sufficient period of time it will turn on the SCR beneath the contact. When this second on-region begins spreading, the data in Fig. 3 indicates that it reaches island 5 first and then island 4. While the second on-region is beginning to spread the first on-region continues to spread down the bar and reaches island 2. Still later in time an on-region reaches island 3 and the entire device is conducting.

The second indication that a second on-region begins spreading is obtained by observing the load current through the SCR and the voltage

across the SCR after triggering. Fig. 4(a) shows an example of the voltage and current traces of device C3. After the device is triggered the voltage across the device falls rapidly from a high value out of the range of the figure to a low value of about 3 volts. During this same time the load current through the device rises rapidly to about 1.6 amperes. About 17 microseconds later, however, the voltage makes a second rapid fall to about 1 volt and the current makes a second rapid rise to about 1.75 amperes. This second voltage fall and current rise may be explained in terms of a second on-region starting.

After triggering, the on-region near the gate carries the entire load current. This load current passes laterally through the emitter layer, however, and the additional lateral resistance of the emitter layer is in series with the active on-region of the device. Because of this additional series resistance the voltage across the device is higher and the load current is somewhat less -- how much less depends upon the external load resistance -- than if no additional lateral series resistance were present. When the second on-region turns on beneath the contact to the emitter layer, the lateral emitter layer resistance in series with the first on-region is shunted by the second on-region. The voltage across the device therefore falls an additional amount and the load current through the device rises an additional amount to their final steady state values when the second on-region starts.

At high load currents the voltage across the SCR may rise slightly after the first rapid fall and before the second fall occurs as

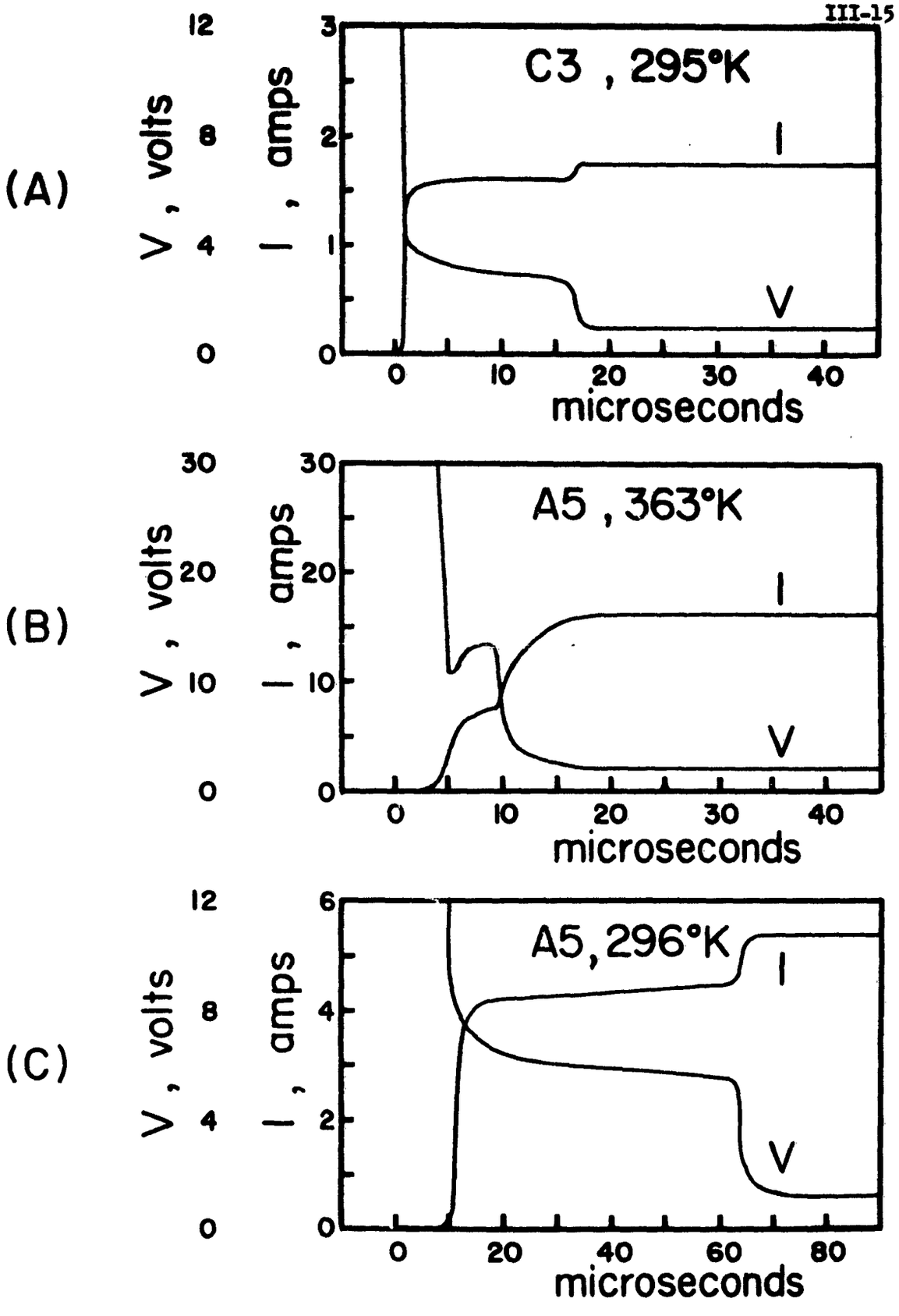

Fig. 4. Examples of the load current through and the voltage across the SCR when remote triggering occurs.

shown in Fig. 4(b). Because of the distributed inductance of the load circuit the load current rise time is a few microseconds at high load currents. As a result the load current is still rising after the initial voltage fall and the voltage across the series lateral emitter resistance will also rise, causing the voltage across the device to increase.

Occasionally the time between the first voltage fall and the second voltage fall (or current rises) was quite long. An example is shown in Fig. 4(c) where a delay of about 55 microseconds exists between the first and the second voltage falls.

Since the second voltage fall and the second current rise occur when the second on-region turns on, the time when the second on-region begins to spread is easy to measure. The times when the second on-region turns on are indicated in Fig. 3 and in subsequent figures by a short horizontal bar drawn for each of the load currents tested.

In Fig. 3 the delay between the turn-on of the first on-region and the turn-on of the second on-region decreases as the load current increases. At high load currents the second on-region turns on in just a few microseconds after the start of load current build-up. The current injected from the N emitter to the P base increases as the lateral emitter current (i.e., the load current) increases as shown in section 2. The injected emitter current density is highest beneath the emitter layer contact and will effectively gate the device on in this region. Just as the delay time between the application of an external gate current and the turn-on of an SCR decreases as the gate

current increases, the delay between the beginning of injection from the emitter to the base (i.e., the start of load current build-up) and the turn-on of the second on-region will decrease as the injected emitter current increases and therefore as the load current increases.

Since device C3 had a gate connection on each end of the bar, this permitted contacting the emitter layer between islands 1 and 2 only and triggering only the second gate to observe the effect of the lateral emitter current when the first on-region spreads from the second gate towards the first gate. Fig. 5 shows the results of this experiment. In general the phenomenon is the same as observed in Fig. 3 although some of the details are slightly different, such as the order in which the on-regions reach the islands.

A dashed line has been drawn in Fig. 5, to indicate the time when the on-region reached island 1 when all the spring fingers contacted the emitter layer and the second gate was triggered. This permits comparing the spread of the on-regions when a large lateral emitter current was present and when it was not, just as in Fig. 3. Examination of Figs. 3 and 5 show that if the load current was large enough to cause a second on-region to begin spreading, the on-regions reached all the individual islands in about one-half the time it took when no lateral emitter current was present. As a consequence the entire area of the SCR became conducting in about one-half the time when a second on-region was remotely triggered.

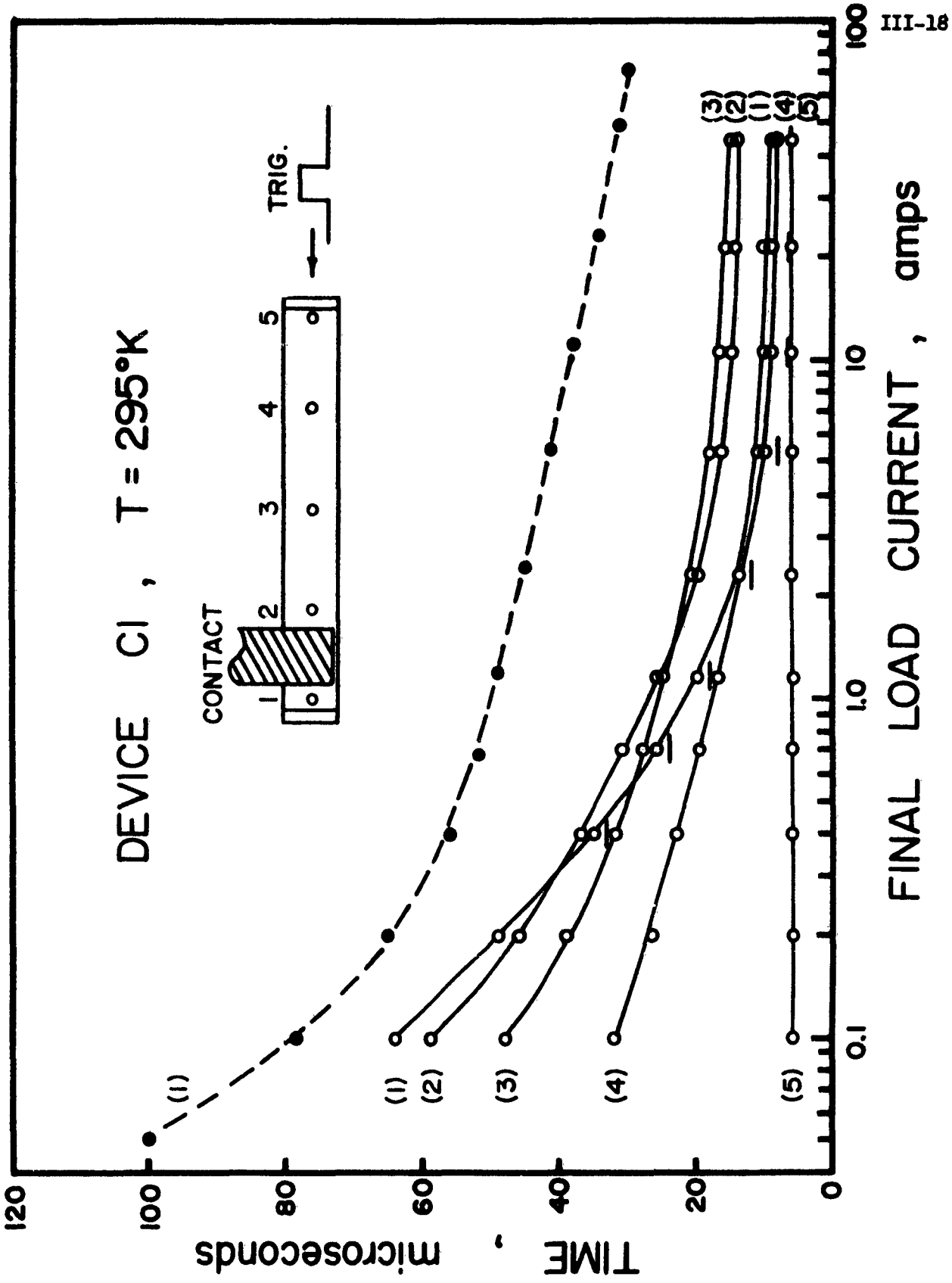

Fig. 5. The arrival time of the on-state at the individual islands of device C1 vs the final load current when only the second gate was triggered.

Although the total area of the SCR may be turned on faster when constructed as in Fig. 2, there is one obvious disadvantage to this type of operation -- the current density is no longer uniform throughout the device after complete turn-on. This nonuniform current density arises from the lateral flow of current in the emitter layer which creates a self-bias effect analogous to the self-bias in a transistor arising from the lateral flow of the base current. This self-bias causes the current density in the SCR to decrease away from the contact to the emitter layer. In fact, if the decrease in the internal current density is sufficient, regions of the SCR remote from the emitter layer contact may not stay on, depending upon the SCR.

In order to see if the on-region would spread the entire length of the SCR when the spreading starts just from the region adjacent to the emitter layer contact, the second gate of device C3 was triggered when only the spring finger between islands 4 and 5 contacted the emitter layer. In this case the gate triggered the region near the emitter contact and the on-region had to spread away from the contact. The results are shown in Fig. 6. The on-region did indeed spread across the entire device. A dashed line has again been drawn in Fig. 6 to show the time when the on-region reached island 1 when all the spring fingers contacted the emitter layer. The velocity of spreading was somewhat less when the on-region spread away from the single contact. Here the lateral emitter current was in the opposite direction to that necessary to increase the spreading velocity as discussed in section 2.

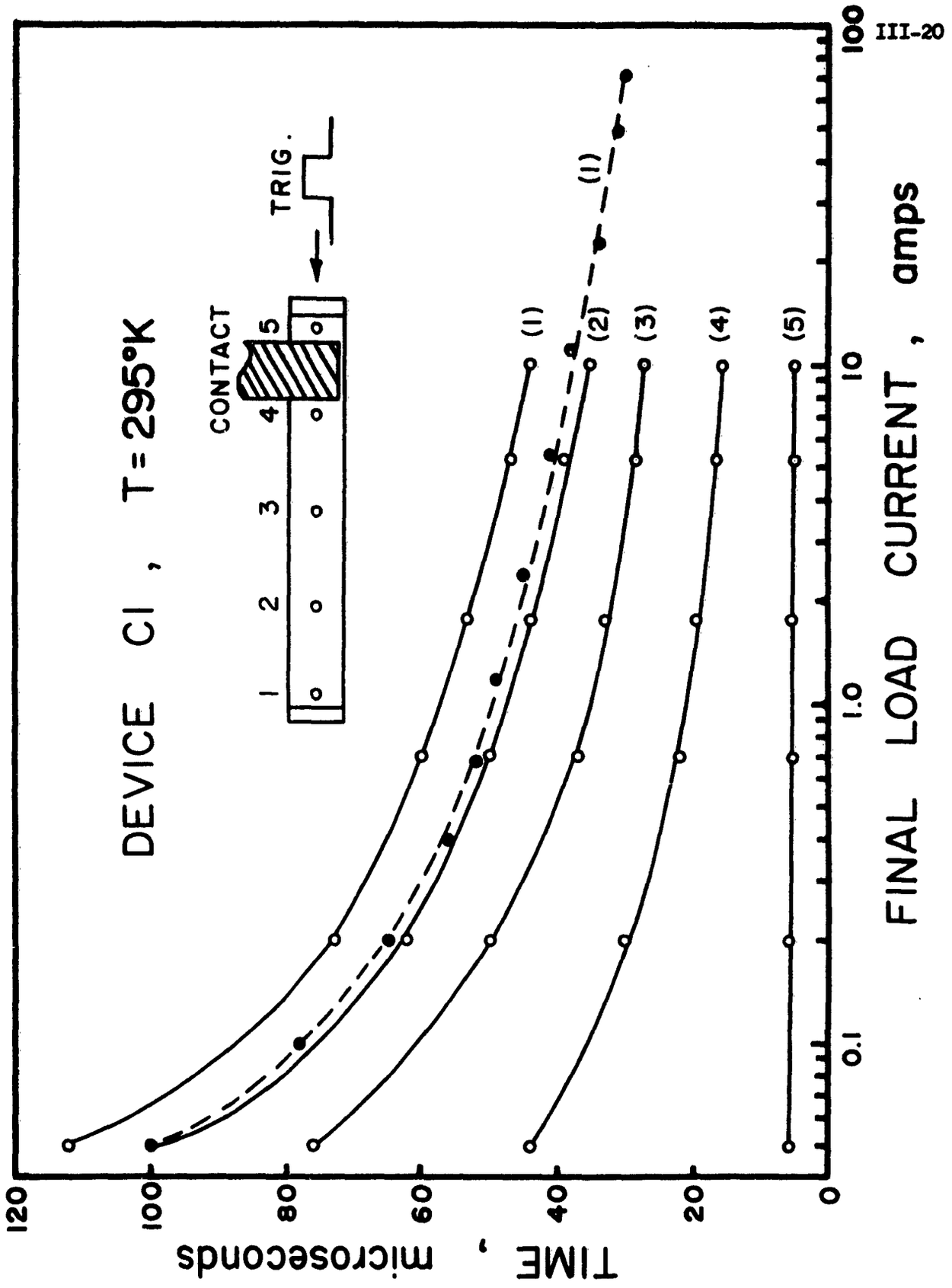

Fig. 6. The arrival time of the on-state at the individual islands vs the final load current when the gate next to the contact was triggered.

In some other devices not all of the area stayed on after the region beneath the emitter layer contact became on. Device A5 whose data is shown in Fig. 7 is an example. The SCR first turned on near the gate as was evidenced by the presence of injected carriers at island 1. At load currents less than about 5 amperes the on-region would spread from the gate to the emitter contact. When the on-region reached the region beneath the contact injected carriers at islands 1 and 2 and sometimes island 3 were no longer detected indicating that this part of the SCR did not stay on. When the load current was greater than about 5 amperes a second on-region started spreading from the single emitter contact. This second on-region was first detected at island 5, then at island 4, and somewhat later at island 3. No on-region was ever detected at island 2, however. After the second on-region turned on, the first on-region turned off and the second on-region did not spread across the entire device because of the drop-off of the current density away from the emitter contact.

The reason the on-region spread entirely across device C1 but not A5 is probably because the two devices had different α s and not because of a difference in the drop-off of the current density away from the emitter contact. Both devices were made during the same diffusion and from identical material so they should have the same emitter sheet resistance. Since the drop-off of current density depends upon the load current and the sheet resistance of the emitter layer, devices C1 and A5 should have the same drop-off profile. The main difference between the devices was in the width of the N-type base. Device C1

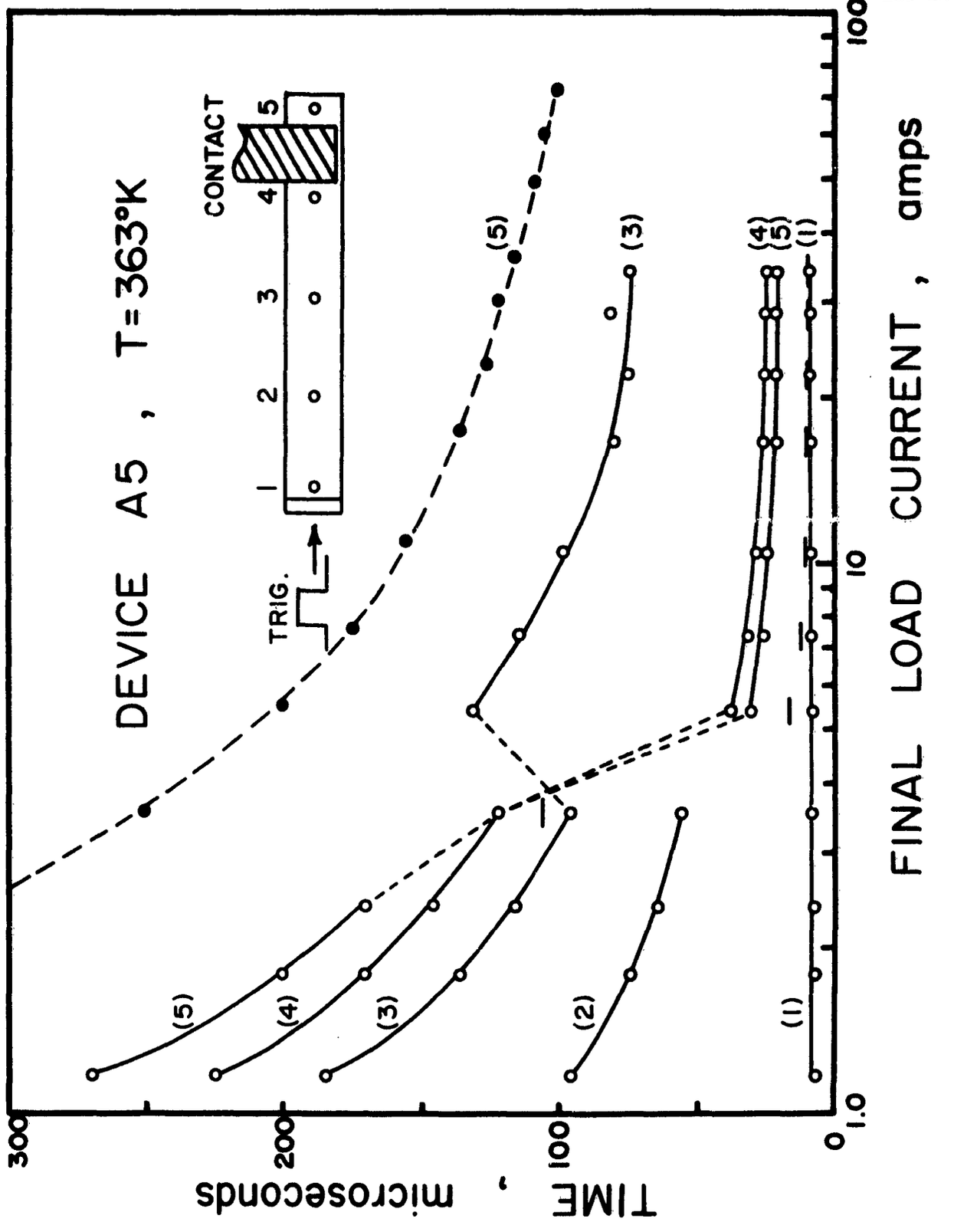

Fig. 7. The arrival time of the on-state at the individual islands of device A5 vs the final load current at 363°K.

had a narrower N base and therefore a higher α_{pnp} than device A5. Because of the higher α in device C1, this device will stay on at a lower current density than device A5 as indeed was indicated by the lower holding current of C1. The on-region will therefore spread farther along the bar of C1 even though both C1 and A5 may have had nearly the same current density drop-off profile away from the emitter contact.

The data of Fig. 7 were taken at 363°K. At lower temperatures (Fig. 8) the second on-region spread even less distance away from the emitter layer contact. In Fig. 8 the second on-region did not even spread to island 3 until the load current was greater than about 20 amperes. This temperature dependence is probably due to the change in the αs arising from the change in lifetime with temperature. For comparison purposes a dashed line has been drawn in Figs. 7 and 8 to indicate the time when the on-region reached island 5 when all the spring fingers contacted the emitter layer.

Examination of Figs. 3 or 5 and Fig. 8 reveals that the second on-region started at a lower current in device C1 than in device A5. Again this is probably due to the higher α and therefore more sensitive gate action of C1 as compared to A5.

The merit of using a lateral current in the emitter layer when switching on an SCR may not lie in the ability to increase the velocity of spreading but rather in the ability to turn on areas of the SCR remote from the gate connection. If two or more remote areas can be

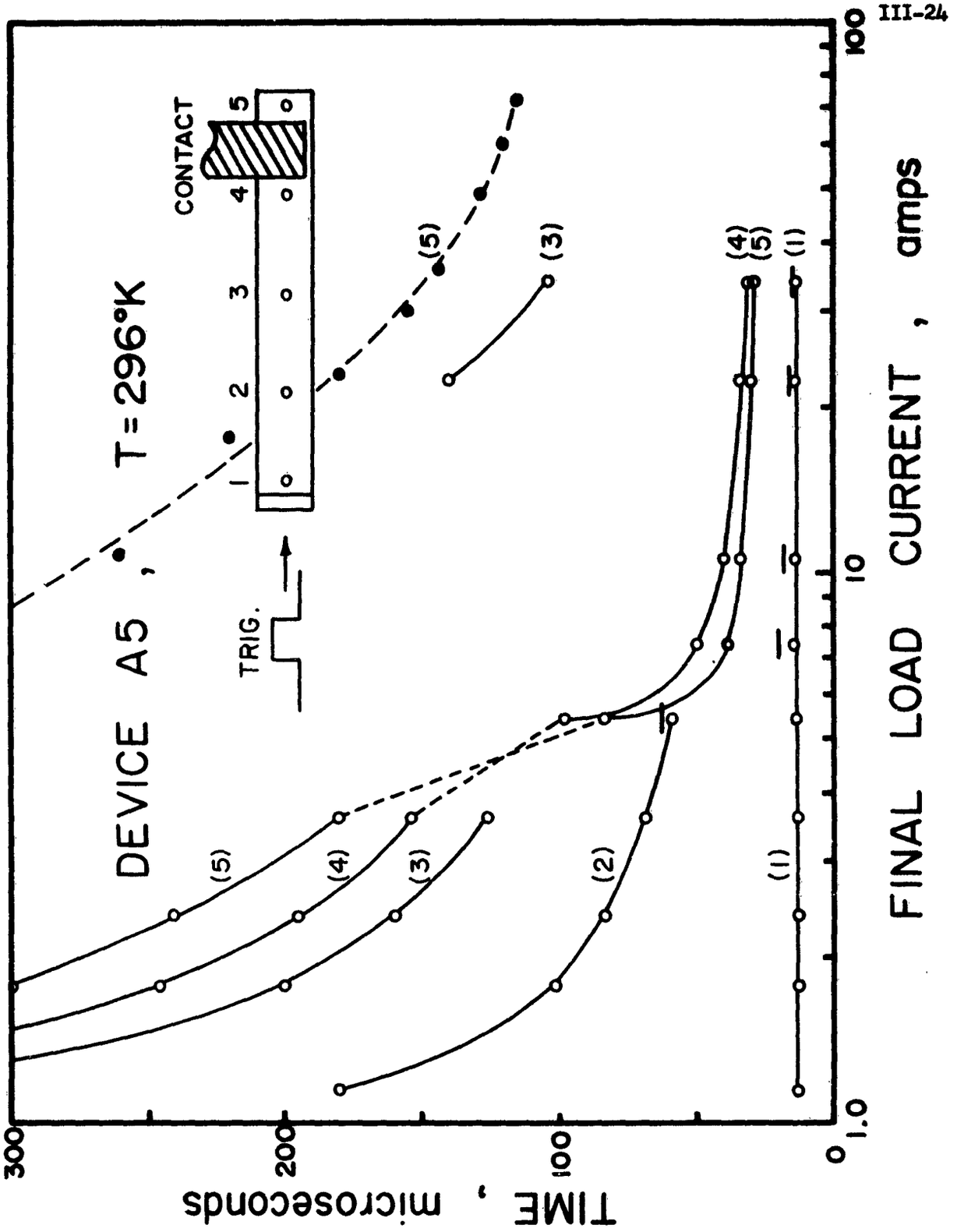

Fig. 8. The arrival time of the on-state at the individual islands of device A5 vs the final load current at 296°K.

turned on very quickly, the load current can be allowed to increase more rapidly, thereby increase the di/dt rating of the SCR.

In order to see if more than one remote area of the SCR could be triggered with a single gate, a center gate device was used which had contacts to the cathode emitter layer only at the two ends of the bar. In this device the gate first turned on the region at the center and the load current passed laterally through the emitter layer in both directions to each end of the bar. Each half of the bar from the center out then approximated the structure shown in Fig. 2. As a result each end of the bar was expected to turn on remotely.

Fig. 9 shows the results of this experiment performed on center-gate device A7. The dashed lines in Fig. 9 show the time for the on-region to reach islands 1 and 6 -- the outermost islands at the ends of the bar -- when all the spring fingers contacted the emitter layer and no large lateral emitter layer currents existed. At high load currents the on-region spread to the end of the device in about one-half the time when lateral emitter currents were present as compared to when they were not.

Although there is good evidence for additional on-regions starting in device A7 it is not as explicit as in the previous devices. Fig. 9 shows that the order of arrival of the on-regions to the individual islands does not change at high load currents as in Figs. 3, 5, 7, and 8. However, this does not necessarily mean that additional on-regions did not start spreading. The distance between the center gate of device A7

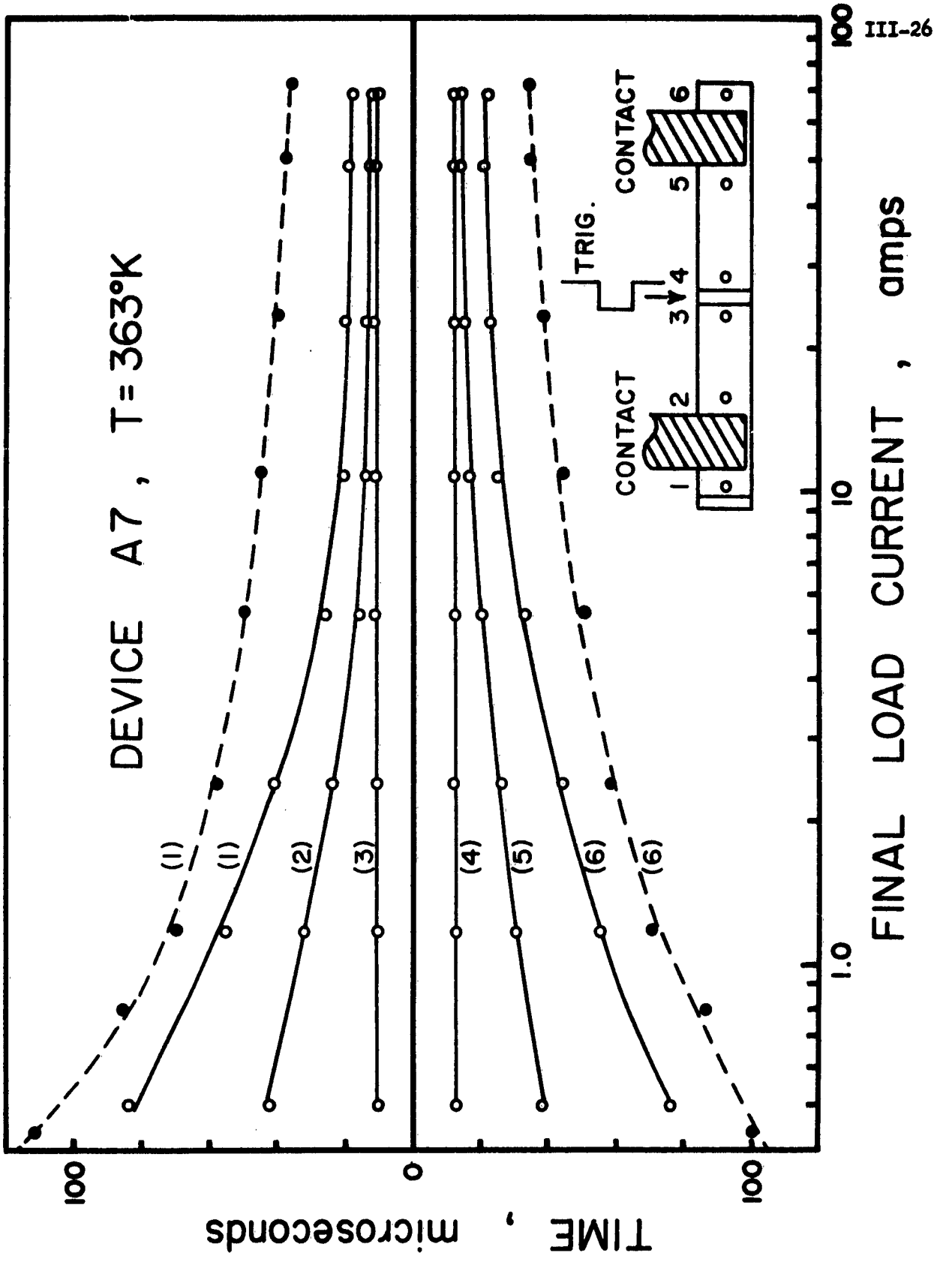

Fig. 9. The arrival time of the on-state at the individual islands of device A7 when triggered at the center gate.

and either of the emitter contacts was about one-third the distance between the gate and the emitter contact in devices C1 and A5. Furthermore, there were only two islands along this distance in A7 as compared to four for C1 and A5. It is quite possible that additional on-regions started spreading from the emitter contacts and reached islands 2 and 5 before the first on-region reached them. The shorter distance and fewer islands between the gate and the emitter contacts did not permit a sure observation of this.

Observation of the voltage across and the current through device A7 did not reveal as striking a second fall or rise as exhibited in Fig. 4. After the first on-region starts, the total lateral emitter layer resistance in series with the load in device A7 is only about one-sixth that of devices C1 and A5 because of the center gate geometry. Much less effect on the external voltage and current characteristics of the device is expected if additional on-regions turn on remotely from the gate. In this experiment a second voltage fall was just noticeable at the highest load currents whereas the rise of the load current seemed to be nearly a smooth exponential without the second break as in Fig. 4.

Some evidence which indicates that additional on-regions turned on remotely in device A7 is obtained from a plot of the velocity of spreading. In the earlier paper[1] measurements of the velocity of spreading were obtained by measuring the time for the on-region to spread from one island to the next and dividing the distance by this time. The velocities were calculated in this manner for device A7 (Fig. 10). In

Fig. 10, below about 5 amperes, the velocity plot is rather normal when compared to similar plots in the earlier paper[1]. Above about 5 amperes, however, the velocity points seem to split into two groups. This splitting of the points can be explained in terms of additional on-regions turning on beneath the two emitter contacts.

In device A7 the first on-region is initiated at the center of the device by the gate signal and first spreads to island 3 and 4. If conditions are correct two additional on-regions start spreading shortly thereafter from the emitter layer contacts. These two additional on-regions may first reach islands 2 and 5 and somewhat later islands 1 and 6. Here if the time from when an on-region reaches island 3 to when an on-region reaches island 2 is measured, the velocity calculations based on this measurement will be erroneous. Most likely the "velocity" calculated from island 3 to 2 will be higher than if the first on-region had actually spread from island 3 to 2. The same argument applies to islands 4 and 5. In Fig. 10 the calculated velocities V_{32} and V_{45} did go much higher for load currents greater than 5 amperes. This then is evidence that the on-region did not merely spread from the center out to the ends of the bar but instead two additional on-regions turned on remotely at the ends of the bar when the load current exceeded 5 amperes. If this is the case then all the velocities in Fig. 10 at currents above 5 amperes are not actual velocities of spreading.

The data of Figs. 9 and 10 were taken at 363°K. At 296°K a similar phenomenon was observed in device A7.

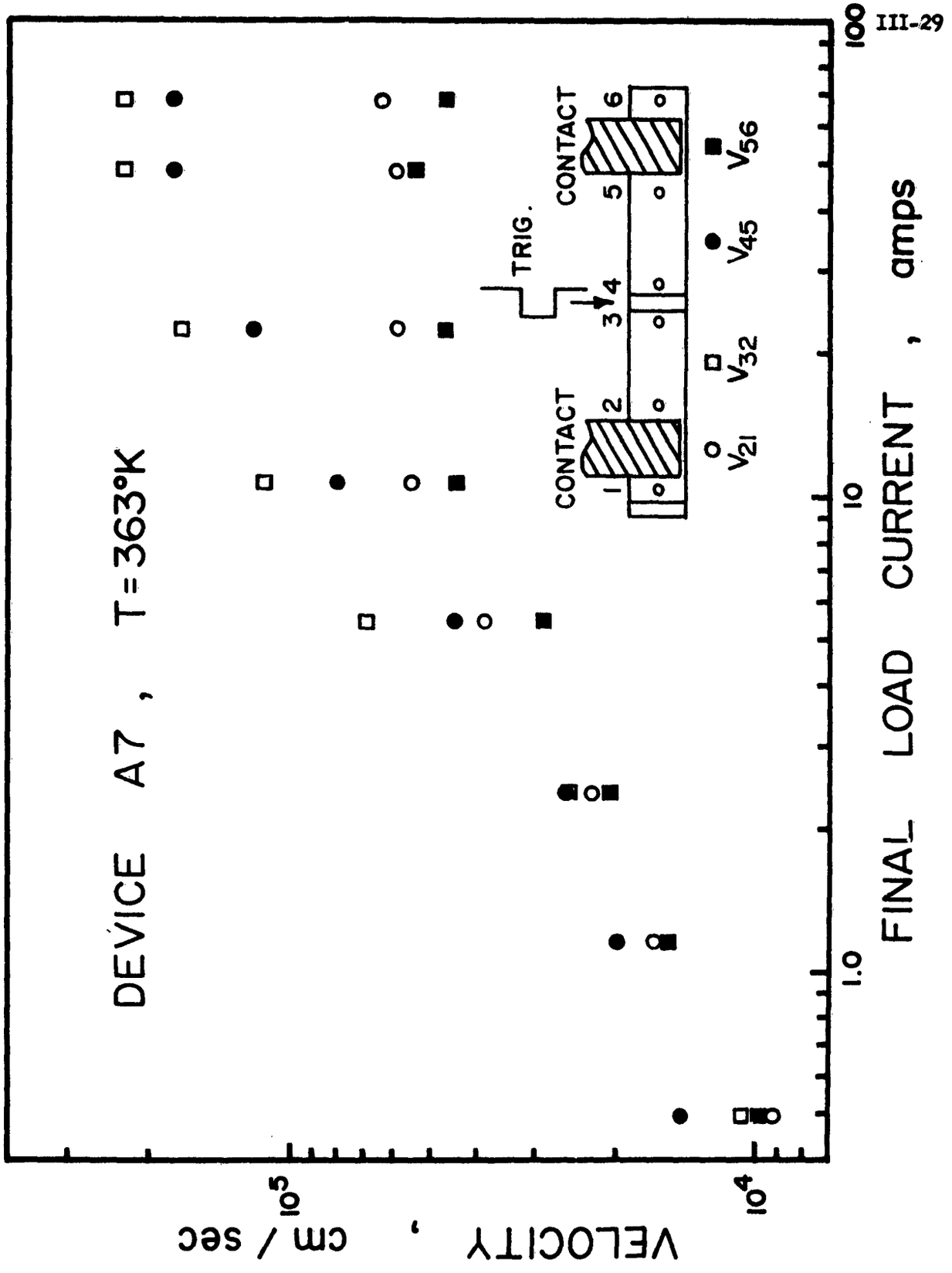

Fig. 10. The velocity of propagation of the on-state of device A7 when triggered at the center gate vs the final load current. As explained in the text, the velocities at load currents greater than about 5 amperes are probably not true velocities.

Although the evidence is less direct, it is fairly certain that two additional on-regions were triggered on remotely by the use of lateral emitter layer currents in device A7. In order to obtain lateral currents in the emitter layer some of the area of the SCR was sacrificed. In Fig. 9, under worst case assumptions, the total effect area was reduced by one-half in order to bring the total effective area on in one-half the time. Therefore no advantage was gained. However, the linear geometry of device A7 was not optimum and a little reflection shows that a smaller fraction of the total area need be sacrificed in a circular geometry in order to obtain similar lateral currents.

The question arises whether the use of lateral emitter layer currents in a circular geometry would have any advantage over the use of a distributed gate to turn on large areas initially. This work did not investigate this question and it remains to be answered.

5. CONCLUSIONS

Lateral currents in an emitter layer of a silicon controlled rectifier can affect the spreading velocity of the on-region. Lateral currents, which may exist in standard SCRs because of nonuniformities of structure, may partly explain observed variations in the spreading velocity.

Lateral emitter currents can cause areas of the SCR remote from the gate contact to turn on shortly after gate triggering. This technique of turning on areas of the SCR remote from the gate contact may possibly be used to increase the di/dt rating of large area SCRs.

REFERENCES

1. W. H. Dodson and R. L. Longini. "Probed Determination of Turn-on Spread of Large Area Gated Silicon Controlled Rectifiers." (Paper no. 1 of this series)

2. R. A. Gudmundsen. "The Emitter Tetrode." IRE Trans. on Electron Devices, ED-5, 223-225. (Oct., 1958).

3. J. E. Iwersen, A. R. Bray, and J. J. Kleimack. "Low-Current Alpha in Silicon Transistors." IRE Trans. on Electron Devices, ED-9, 474-478. (Nov., 1962).

4. W. H. Dodson and R. L. Longini. "Base and Emitter Lateral Current Analysis Applicable to Multijunction Devices." (Paper no. 2 of this series)

APPENDIX A

Device Fabrication.

The procedure for constructing the SCRs used in this investigation is described in some detail in this appendkx. The procedure consisted of five main operations: (1) preparing the wafers, (2) diffusing the junctions, (3) applying the contacts, (4) making the bars, and (5) making the islands.

(1) Preparing the wafers.

The rectifiers were made from 15 ohm-cm N type silicon. After orientation on the optical goniometer, 20 mil slices were cut from the ingot with the diamond saw so that the sides of the wafers were (111) faces. This orientation was chosen primarily because the (111) face is most desirable for any subsequent alloying. Both sides of the wafers were lapped flat and parallel with successively finer grits to a final lap with 3 micron grit (Al_2O_3, Geoscience Instruments Corporation). The pressure on the full size wafers (1 inch diam.) was about 70 gm/cm^2 during lapping. The rate of material removal varied greatly with pressure, grit size, freshness of grit, and technique of lapping but was usually about 5 mils/hour or less. The final wafers ranged in thickness from 5 to 10 mils.

Some care was necessary to obtain wafers with flat and parallel sides. After one side of the wafer was finish lapped, the wafer was cleaned of excess wax and placed lapped side down upon a hot, clean

lapping block. Mounting wax (LOC-WAX-10, Geoscience Instruments Corporation) was applied to the edges of the wafer. The surface tension of the melted wax caused the wax to flow beneath the wafer. Another hot, clean lapping block was coated with mineral oil on one side and the oiled side placed down against the mounted wafer. The oil prevented the wax from sticking the top block. Additional lead weights were placed on top of the oiled lapping block so that the wafer was firmly pressed against the bottom lapping block. After the lapping blocks had cooled the oiled block and weights were removed, leaving the wafer mounted to the bottom block, and with the wafer's lapped side pressed flat against the lapping block. During the lapping it was necessary to frequently renew the grit in order to insure a flat surface. The thickness of the final wafers were usually uniform to within 0.5 mil or less over the entire area (1 inch diam. wafers).

After the final lap the wafers were removed from the block by placing the block wafer-side down upon a filter paper placed on a hot plate and sliding the block off the wafer after the wax had softened. This technique minimized wafer breakage.

Cleaning the wafers was one of the most important steps prior to diffusion. The wax was removed from the wafers by refluxing in trichloroethylene in an extraction apparatus. Following this the wafers were agitated in hot nitric acid for a few minutes, rinsed in distilled demineralized water, agitated in hydrofluoric acid, again rinsed in water, and then placed in methyl alcohol. Each wafer was removed from the alcohol, placed on a filter paper, and swabbed with

a cotton swab saturated with methyl alcohol. Normally a brownish stain came off on the swab and swabbing was continued with new swabs until the swab remained clean. The wafers were then placed in methyl alcohol until diffusion. The brownish stain was probably very fine grit that was loosened from the surface during the oxidation in the nitric acid.

The wafers were not etched prior to diffusion since it was desirable that the surfaces be as flat and parallel as possible over a large area and the deep diffusions to follow did not warrant a finish smoother than the fine lapped surface.

(2) Diffusing the junctions.

The P layers were obtained by diffusing boron in an open tube set up.[1,2,3] With the main zone of the furnace at 1000°C and with 2 liters per minute (lpm) of nitrogen flowing (inside tube diameter was 4.5 cm), the source, B_2O_3, was placed in a quartz boat in the upstream end of the hot zone. After equilibrium was obtained in the furnace, the wafers were removed from the alcohol, dried thoroughly on hard-surfaced filter paper, and set upright in a slotted quartz boat. The boat was then placed in the middle zone of the furnace, two or three inches downstream from the B_2O_3 source.

After 30 minutes predeposit the B_2O_3 source was slid out the upstream end of the furnace. The carrier gas was switched from nitrogen to 1/2 lpm of dry oxygen and the furnace temperature at the samples raised to 1250°C. The predeposit of boron at the lower

temperature is necessary since if the B_2O_3 is left in the furnace any appreciable length of time at temperatures greater than about 1000°C, a glassy, sticky mess results. After 50 hours at 1250°C the samples were slid slowly out of the furnace.

One side of the diffused wafers was waxed down on glass slides and the oxide removed from the unwaxed side with HF. The sheet resistivity of the diffused layer was measured with a four point probe [4,5] and the junction depth (around 30 microns) determined by angle lapping and staining one of the wafers. Surface concentrations as determined from the graphs in Irvin [6] were usually around 10^{17} to 10^{18} cm^{-3} after the boron diffusion. The junction staining techniques [1,2] used were essentially those described in the literature except that straight HF was usually used without the addition of a trace of HNO_3. The addition of HNO_3 seems to hasten the staining process but in the staining technique the most important ingredient seems to be experience.

After the resistivity measurements the unoxidized side of the wafer was sometimes hand lapped with 3 micron grit to remove any hard glaze. After cleaning the wafer by refluxing in solvents and swabbing in alcohol the wafers were stored in alcohol.

The N layer was obtained by diffusing phosphorus in an open tube, two temperature zone system. The main zone of the furnace was set to 1250°C and the source zone set to about 230°C, with the temperature increasing monotonically from source to main zone. The source, P_2O_5,

was placed in a quartz boat at the 230°C zone and a gas flow of 3 lpm of nitrogen adjusted. Precaution must be taken to keep the P_2O_5 as dry as possible since moisture in the system usually results in splotchy surfaces with uneven surface concentration. Rapid loading of the P_2O_5 and allowing the nitrogen to flow for 30 minutes or so before loading the samples usually resulted in a sufficiently dry system. The wafers and a P type test sample were set upright in a slotted quartz boat and placed in the 1250°C zone of the furnace. After 15 minutes the gas flow was switched to 1 lpm of dry O_2 since nitrogen tends to corrode the surfaces at high temperatures. The samples were slowly slid out of the furnace 1 hour and 45 minutes later so that the total diffusion time was 2 hours.

The N layer in the wafers was usually around 8 microns deep. Sheet resistivity and junction depth measurements on the test sample showed the surface concentration to be around 10^{20} to 10^{21} cm^{-3}.

(3) Applying the contacts.

Preliminary experiments indicated that the best contacts for this investigation were evaporated and alloyed aluminum to the P layer and electroless plated and annealed nickel to the N layer. These two contacts were chosen because of their low resistance and ease of applying. The nickel contact is probably the least satisfactory of the two because of uncontrollable variations in the results.

The most important step in applying the contacts is the preparation of the surface to be contacted. After the phosphorus diffusion the oxide was removed from all surfaces with HF. In order to make a gate

connection, part of the N layer was removed from the wafer by masking with apiezon W wax and etching. Thermal probing between short etches showed when the N layer was removed and the inner P layer reached. The outer P and N layers were lapped with 3 micron grit just long enough to remove any glaze and to leave a freshly roughened surface for contacting. The outer P layer sometimes had thin outer N regions since the oxide did not always completely mask the phosphorus. These N regions were removed by the lapping as determined by the thermal probe. The wafers were then cleaned using the hot nitric acid and swabbing techniques described in the first section, "preparing the wafers." The wafers were stored in methyl alcohol until time for evaporation.

The aluminum was evaporated to the outer P layer and the gate region by standard techniques as described in references (7) and (8). Those areas to be nickel plated later were masked with glass cover slides during the evaporation. After evaporation the aluminum was alloyed by placing the wafers on a flat carbon strip inside the bell jar. Alloying was done under a vacuum at about 700 to 800°C.

After alloying the wafers were waxed to glass slides and the gate masked with apiezon W wax. The N layer was electroless nickel plated by the technique described in reference (9). Approximately 5 minutes plating time was used. After plating the wafers were cleaned of wax by refluxing in solvents and annealed at about 600 to 700°C on the carbon strip in vacuum.

(4) Making the bars.

The SCRs used for this investigation were obtained by cutting the wafers into long bar shaped devices. The wafers were mounted on ceramic blocks and coated with glycol thiolate wax before cutting to minimize chipping at the edges. A diamond saw was the only available tool for cutting the wafers and was not entirely satisfactory because of the chipping. Lapping through the wafers with a thin wire may be a better technique for dicing the wafers.

After cutting, the bars were cleaned of wax and rewaxed on glass slides and covered with apiezon W wax. The wax was removed from the edges by scraping with a razor blade. The edges of the bars were then etched to remove the saw damage. This step was important for obtaining a high breakover voltage in the SCR.

After etching and cleaning, the bars were checked on a curve tracer to select the good from the bad. The breakover voltage was highly dependent on the conditions of the surface at the edges and sometimes re-etching was necessary to make a device satisfactory. Moisture or other contaminants on the surface had to be removed, usually with solvents.

(5) Making the islands.

In order to etch the islands it was necessary to mask part of the device. Masking with a thin layer of wax and scribing the wax was the technique selected for this purpose. The devices were mounted with the N layer up on glass slides with apiezon W wax and dipped in a

solution of toluene and apiezon W wax to put a thin film of wax over the surface. Toluene is a better solvent for this purpose than trichloroethylene since toluene does not cause any bubbling or blistering upon subsequent heating. The slides were held upon a hot plate to soften the wax and remove all of the toluene for good adherence.

For scribing the wax, very fine tungsten probes were made by shape etching tungsten wire in a 4 per cent KOH solution.[10] Although this technique can yield extremely fine points (less than 0.05 mil diameter tip), points with about 1 mil tip diameter were used for the scribing.

The glass slide with the device waxed down was mounted on a cold thermocompression bonder heat column and the normal thermocompression bonding point replaced with a fine tungsten point. All extra weights were removed from the tungsten point holder. The islands were scribed by bringing the point down upon the waxed surface of the device and moving the chessman in a circle with the help of a circular template attached to the base platform.

After scribing the wax, the islands were etched (5 parts HNO_3, 3 parts HF, 3 parts $HC_2H_3O_2$) for about 5 seconds and then rinsed. The slide was then placed on a hot plate and, while observing the islands with a microscope, the wax was softened slightly for good wax adherance. They were etched for about 10 seconds more, rinsed, and heated again. This alternate etching and heating prevented the wax from peeling off of the island. After the groove was etched nearly through the N layer, as estimated from the known etch rate (about 1 mil/minute) and the

known junction depth, the island was tested for isolation by making contact to the island and the adjacent N layer with fine tungsten probes mounted on micromanipulators. The probes easily penetrated the wax layer. Testing on the curve tracer revealed when an island was isolated since the islands had a sharp reverse bias breakdown voltage and a very low (less than 1 microampere) leakage current when completely isolated. If the island was not isolated, heating closed the pin holes in the wax from the micromanipulator probes and permitted further etching.

After the islands were formed the wax was removed and the devices cleaned by refluxing in solvents. The devices were stored in a dry atmosphere until needed for testing.

REFERENCES

1. C. S. Fuller and J. A. Ditzenberger. "Diffusion of Donor and Acceptor Elements in Silicon." J. of Applied Physics, 27, 544-553. (May 1956).

2. C. J. Frosch and L. Derick. "Surface Protection and Selective Masking during Diffusion in Silicon." J. of Electrochemical Society, 104, 547-552. (Sept. 1957).

3. F. M. Smits. "Formation of Junction Structures by Solid-state Diffusion." Proc. IRE, 46, 1049-1061. (June 1958).

4. F. M. Smits. "Measurement of Sheet Resistivities with the Four-Point Probe." B.S.T.J., 37, 711-718. (May 1958).

5. M. A. Logan. "An AC Bridge for Semiconductor Resistivity Measurement Using a Four-Point Probe." B.S.T.J., 40, 885-919. (May 1961).

6. J. C. Irvin. "Resistivity of Bulk Silicon and of Diffused Layers in Silicon." B.S.T.J., 41, 387-410. (March 1962).

7. L. Holland. Vacuum Deposition of Thin Films. John Wiley and Sons Inc., New York, 1956.

8. J. Strong, et. al. Procedures in Experimental Physics. Prentice-Hall Inc., Englewood Cliffs, N. J., 1938.

9. M. V. Sullivan and J. H. Eigler. "Electroless Nickel Plating for Making Ohmic Contacts to Silicon." J. of Electrochemical Society, 104, 226-230. (April 1957).

10. F. G. Pany. "Tungsten Needles for Semiconductor Tests." Electronics, May 18, 1962, pp. 102-104.

APPENDIX B

Measuring circuitry.

This appendix gives a brief description of the circuitry used for this investigation.

The sequence in the measurement cycle consisted of the following: The oscilloscope trace was triggered, then after a fixed delay time, the gate of the SCR was triggered. The necessary observations were made while the on-region spread across the SCR and, after turn-on was complete, the SCR was turned off. The voltage across the SCR was reset so that the SCR was returned to the high voltage forward blocking state (off-state). The cycle was then repeated. The circuitry which performed these operations is shown in Fig. B1.

In the circuit of Fig. B1 suppose the SCR is in the forward blocking state. V_3 supplies any leakage current through the SCR. The voltage across the SCR is clamped by V_2 and is very nearly equal to V_2. Pulse generator no. 1 is free running and determines the period of triggering. A square pulse from generator no. 1 closes relay no. 1 which in turn closes relay no. 2. Two relays were used since the pulse generator was not large enough to drive the high amperage relay no. 2. The closing of relay no. 2 does not affect the voltage across the SCR since $V_3 \gg V_2 \gg V_1$ and diode D1 is reverse biased. Diode D3 prevents any change across the forward biased diode D2 when relay no. 2 closes.

At the same time that a square pulse leaves generator no. 1 to close the relays, a sync pulse from generator no. 1 goes to the external drive of generator no. 2 and triggers it. A delayed sync pulse from generator no. 2 triggers the oscilloscope sweep. The purpose of this delay will be explained subsequently. Another delayed trigger is obtained from the oscilloscope to trigger generator no. 3 after the oscilloscope sweep has started. Pulse generator no. 3 drives the gate trigger generator which triggers the SCR. The length of the gate pulse is adjusted by generator no. 3 and the magnitude by the gate trigger generator.

The voltage across the SCR falls after triggering. The high load current is supplied by V_1 and is limited by the load resistor. Flat strips of nichrome were chosen for the load resistor since they are very cheap and have little self-inductance. The leads connecting V_1, the load resistor, and the SCR were kept as short as possible to minimize circuit inductance.

Relay no. 2 opens at the end of the pulse from generator no. 1 and the SCR turns off. V_2 cannot supply any current to the SCR after relay no. 2 opens because diode D2 is blocking. V_3 still supplies current to the SCR but if the resistors in series with V_3 are large enough the current V_3 supplies will be less than the holding current and the SCR returns to the forward blocking state. The voltage across the SCR will return to nearly the value of V_2. The system is now ready to repeat the cycle.

The trigger signal from generator no. 1 must be delayed by generator no. 2 so the SCR can be triggered just a few hundred microseconds before relay no. 2 opens. A means of delaying the SCR triggering signal is necessary because of the inertia lag of relay no. 2.

The load current was measured by measuring the voltage across the current measuring resistor in series with the SCR.

The circuit used to reverse bias the islands consisted of a battery and resistor in series. The voltage across a series resistor gave a measure of the reverse-bias current. The critical part of this circuit was the shielding. The battery and all leads including the probe for contacting the islands had to be shielded and the shield grounded to eliminate spurious pickup.

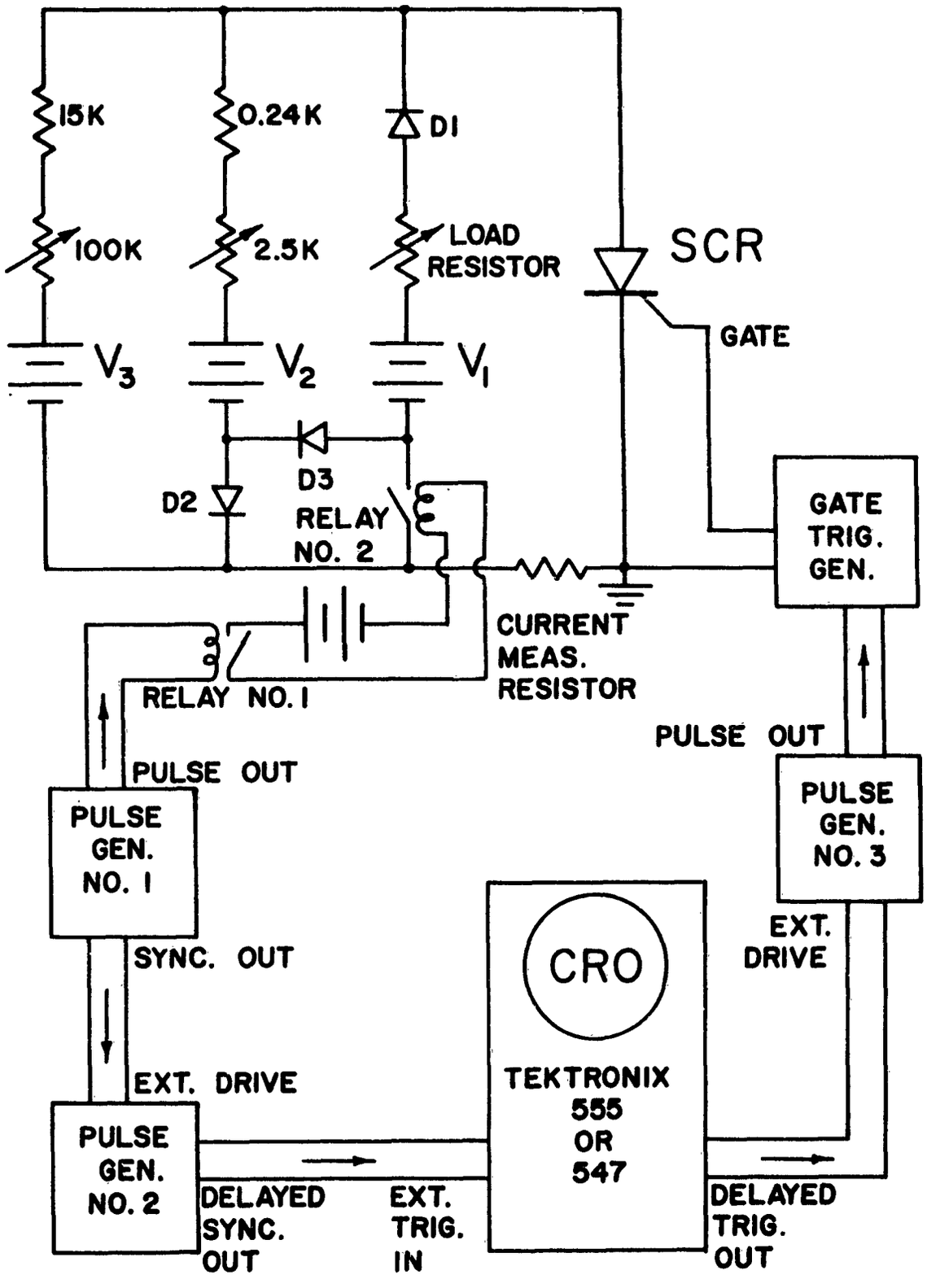

Fig. B1. Basic measuring circuit.

Unclassified

Security Classification

DOCUMENT CONTROL DATA - R&D

(Security classification of title, body of abstract and indexing annotation must be entered when the overall report is classified)

1. ORIGINATING ACTIVITY *(Corporate author)*
Carnegie Institute of Technology
Pittsburgh, Pennsylvania 15213

2a. REPORT SECURITY CLASSIFICATION
Unclassified

2b. GROUP

3. REPORT TITLE
Silicon controlled rectifiers: Lateral turn-on velocity, lateral field distribution, and lateral skip phenomenon.

4. DESCRIPTIVE NOTES *(Type of report and inclusive dates)*
Final report September 1, 1964 - June 30, 1965

5. AUTHOR(S) *(Last name, first name, initial)*
Dodson, William H.

6. REPORT DATE	7a. TOTAL NO. OF PAGES	7b. NO. OF REFS
June, 1965	124	31

8a. CONTRACT OR GRANT NO.	9a. ORIGINATOR'S REPORT NUMBER(S)
Nonr - 760	~~375-272/11-12-64~~
b. PROJECT NO. 09	
c.	9b. OTHER REPORT NO(S) *(Any other numbers that may be assigned this report)*
d.	

10. AVAILABILITY/LIMITATION NOTICES
Qualified requesters may obtain copies of this report from DDC

11. SUPPLEMENTARY NOTES	12. SPONSORING MILITARY ACTIVITY
	Office of Naval Research Department of the Navy Washington, D. C.

13. ABSTRACT

The silicon controlled rectifier (SCR) is essentially an "area" device whereas the transistor is a "periphery" device. In the application of SCRs some trouble arises in making use of this large area because of the slow spreading of turn-on from the gate region. SCRs were specially constructed to permit the direct observation of the lateral spread of turn-on within the device. The effects on the spread of turn-on of load current, base widths, temperature, anode-cathode voltage, the gate signal, and a large inhomogeneity were observed. ~~(U)~~

An analysis of a linear and of a cylindrical transistor with lateral currents in both the emitter and the base layers is included. The results are written in a general form and can be applied to many specific cases including those that have a lateral current only in the base layer or only in the emitter layer. A lateral current in an emitter layer of an SCR is shown to vary the lateral field in the base layers and also to change the distribution of the current density injected from the emitter to the base. A method of using lateral emitter layer currents in an SCR to increase the spreading velocity of the on-region and, at higher currents, to turn on quickly areas of the SCR remote from the gate contact is demonstrated experimentally. (U)

DD FORM 1 JAN 64 1473

Security Classification

14. KEY WORDS	LINK A		LINK B		LINK C	
	ROLE	WT	ROLE	WT	ROLE	WT
Semiconductor device						
Silicon controlled rectifier						
PNPN						
Gated switching						
Lateral turn-on						

INSTRUCTIONS

1. ORIGINATING ACTIVITY: Enter the name and address of the contractor, subcontractor, grantee, Department of Defense activity or other organization *(corporate author)* issuing the report.

2a. REPORT SECURITY CLASSIFICATION: Enter the overall security classification of the report. Indicate whether "Restricted Data" is included. Marking is to be in accordance with appropriate security regulations.

2b. GROUP: Automatic downgrading is specified in DoD Directive 5200.10 and Armed Forces Industrial Manual. Enter the group number. Also, when applicable, show that optional markings have been used for Group 3 and Group 4 as authorized.

3. REPORT TITLE: Enter the complete report title in all capital letters. Titles in all cases should be unclassified. If a meaningful title cannot be selected without classification, show title classification in all capitals in parenthesis immediately following the title.

4. DESCRIPTIVE NOTES: If appropriate, enter the type of report, e.g., interim, progress, summary, annual, or final. Give the inclusive dates when a specific reporting period is covered.

5. AUTHOR(S): Enter the name(s) of author(s) as shown on or in the report. Enter last name, first name, middle initial. If military, show rank and branch of service. The name of the principal author is an absolute minimum requirement.

6. REPORT DATE: Enter the date of the report as day, month, year; or month, year. If more than one date appears on the report, use date of publication.

7a. TOTAL NUMBER OF PAGES: The total page count should follow normal pagination procedures, i.e., enter the number of pages containing information.

7b. NUMBER OF REFERENCES: Enter the total number of references cited in the report.

8a. CONTRACT OR GRANT NUMBER: If appropriate, enter the applicable number of the contract or grant under which the report was written.

8b, 8c, & 8d. PROJECT NUMBER: Enter the appropriate military department identification, such as project number, subproject number, system numbers, task number, etc.

9a. ORIGINATOR'S REPORT NUMBER(S): Enter the official report number by which the document will be identified and controlled by the originating activity. This number must be unique to this report.

9b. OTHER REPORT NUMBER(S): If the report has been assigned any other report numbers *(either by the originator or by the sponsor)*, also enter this number(s).

10. AVAILABILITY/LIMITATION NOTICES: Enter any limitations on further dissemination of the report, other than those imposed by security classification, using standard statements such as:

(1) "Qualified requesters may obtain copies of this report from DDC."

(2) "Foreign announcement and dissemination of this report by DDC is not authorized."

(3) "U. S. Government agencies may obtain copies of this report directly from DDC. Other qualified DDC users shall request through _____."

(4) "U. S. military agencies may obtain copies of this report directly from DDC. Other qualified users shall request through _____."

(5) "All distribution of this report is controlled. Qualified DDC users shall request through _____."

If the report has been furnished to the Office of Technical Services, Department of Commerce, for sale to the public, indicate this fact and enter the price, if known.

11. SUPPLEMENTARY NOTES: Use for additional explanatory notes.

12. SPONSORING MILITARY ACTIVITY: Enter the name of the departmental project office or laboratory sponsoring *(paying for)* the research and development. Include address.

13. ABSTRACT: Enter an abstract giving a brief and factual summary of the document indicative of the report, even though it may also appear elsewhere in the body of the technical report. If additional space is required, a continuation sheet shall be attached.

It is highly desirable that the abstract of classified reports be unclassified. Each paragraph of the abstract shall end with an indication of the military security classification of the information in the paragraph, represented as *(TS), (S), (C), or (U)*.

There is no limitation on the length of the abstract. However, the suggested length is from 150 to 225 words.

14. KEY WORDS: Key words are technically meaningful terms or short phrases that characterize a report and may be used as index entries for cataloging the report. Key words must be selected so that no security classification is required. Identifiers, such as equipment model designation, trade name, military project code name, geographic location, may be used as key words but will be followed by an indication of technical context. The assignment of links, rules, and weights is optional.